THE ROLE OF APOPTOSIS AND NECROSIS IN AGE-DEPENDENT ENZYMATIC MITOCHONDRIAL ABNORMALITIES IN INDIVIDUAL SKELETAL MUSCLE FIBERS

by

Nashwa J. Cheema

A thesis submitted in partial fulfillment of the requirements for the degree of

Doctor of Philosophy

in

Physiology, Cell and Developmental Biology

Department of Biological Sciences
UNIVERSITY OF ALBERTA

THE ROLE OF APOPTOSIS AND NECROSIS IN AGE-DEPENDENT ENZYMATIC MITOCHONDRIAL ABNORMALITIES IN INDIVIDUAL SKELETAL MUSCLE FIBERS

Nashwa J. Cheema
Under the supervision of Associate Professor Deborah McKenzie
At the University of Alberta - Edmonton

I. ABSTRACT

Aging is associated with the functional decline of cells, tissues and organs affecting the lifespan of all organisms. Age-associated changes to the skeletal muscle such as decline in muscle mass and function is termed as sarcopenia. Sarcopenia results from fiber atrophy and loss of myofibers. We have previously characterized sarcopenia in Fischer Brown Norway (FBN) rats, documenting age-dependent declines in muscle mass and fiber number in quadriceps muscles. The sarcopenic changes in the muscle is concomitant with increased abundance of mitochondrial DNA deletion mutations and electron transport chain abnormalities. We have previously established the physiological impact of mtDNA deletions in aged fibers in rats, monkeys and humans. mtDNA deletions accumulate in aged myofibers via mitochondrial biogenesis to a level of 95-98% of mitochondrial genomes in the cell. The deletions in the mitochondrial genome span the major arc region of the genome and are 2-10 kbp in length which results in the disruption of protein complexes in the electron transport chain (ETC). Fibers with an abnormal ETC, do not have a functional complex IV, cytochrome c oxidase (COX) and have a hyperactive complex II, succinate dehydrogenase (SDH). ETC abnormal fibers are more prone to intra-fiber atrophy and fiber breakage suggesting that they may play a significant role in fiber loss through unknown molecular pathways.

In this study, we used immunohistological and histochemical approaches to define cell death pathways involved in sarcopenia. Activation of muscle cell death pathways was age-dependent with most apoptotic and necrotic muscle fibers exhibiting electron transport chain abnormalities. Although activation of apoptosis was a prominent feature of electron transport abnormal muscle fibers, necrosis was predominant in atrophic and broken ETC abnormal fibers. These data suggest that mitochondrial dysfunction is a major contributor to the activation of cell death processes in aged muscle fibers. The link between electron transport chain abnormalities, apoptosis, fiber atrophy and necrosis supports the hypothesis that mitochondrial DNA deletion mutations are causal in myofiber loss. To test the causal relationship of ETC abnormal fibers in myofiber loss in aged tissue, we pharmacologically induced ETC abnormal fibers via latent mtDNA deletion accumulation. We observed a 1,200% increase in electron transport chain abnormal muscle fibers, an 18% decrease in muscle fiber number, 22% loss of muscle mass, increased deposition of fibrosis and increased abundance of apoptotic myofibers. These studies suggest a progression of events beginning with the generation and accumulation of a mtDNA deletion mutation, the concomitant development of ETC abnormalities, a subsequent triggering of apoptotic and, ultimately, necrotic events resulting in muscle fiber atrophy, breakage and fiber loss. These data affirm the hypothesized role for mitochondrial dysfunction in the etiology of muscle fiber loss at old age.

II. PREFACE

This research project was carried out in accordance with the recommendations in the NIH Guide for Care and Use of Laboratory Animals and the guidelines of the Canadian Council on Animal Care. The protocols used were approved by the Institutional Animal Care and Use Committees at the University of Alberta.

Chapter 2 has been published as Nashwa Cheema, Allen Herbst, Debbie McKenzie and Judd M. Aiken (2015), "Apoptosis and Necrosis Mediate Skeletal Muscle Fiber Loss in Age-Induced Mitochondrial Enzymatic Abnormalities," *Aging Cell* 14(6): 1085-1093. I performed all the experiments, data analysis and composed the manuscript. Allen Herbst, Debbie McKenzie and Judd M. Aiken contributed to manuscript edits.

Chapter 3 has been published as Allen Herbst, Jonathan Wanagat, Nashwa Cheema, Kevin Widjaja, Debbie McKenzie, Judd M. Aiken (2016), "Latent mitochondrial DNA deletion mutations drive muscle fiber loss at old age," *Aging Cell*, pp1-8. This project was in collaboration with Professor. Jonathan Wanagat at the University of California. Allen Herbst, Dr. Wanagat and I contributed equally to this work. I performed all the histological experiments. mtDNA analysis was performed by Allen Herbst using equipment provided by Dr. Wanagat.

III. ACKNOWLEDGMENTS

I would like to express my utmost gratitude and thanks to my supervisor, Dr. Debbie McKenzie, for her understanding, patience, guidance and support throughout my graduate career and for making it an enjoyable experience. A very special thanks to my co-supervisor, Dr. Judd Aiken, for his continuous support, guidance, suggestions and comments. I would like to express my gratitude to Dr. Frank Nargang for his encouragement towards my research, Drs. Martin Srayko and Satyabrata Kar for serving on my candidacy committee and Dr. Kar and Dr. Greg Cartee for serving on my thesis defense committee.

I thank the past and present members of the McKenzie lab for making the past years full of science and fun. I would like to acknowledge the companionship of the ladies in the student office, Pam Banser, Chiye Kim, Katrina Ellestad, Elizabeth Triscott and Danielle Gushue. And I would like to thank my fellow senior graduate student, Camilo, to introducing me to cookies and waffles. I would especially like to thank Dr. Allen Herbst for teaching me techniques in histology, discussing new ideas and introducing me to the rat.

I thank my friends for being there when it was sorely needed. I thank my father and mother, Baba and Ammi, and my brothers, Ararat and Wafi, for supporting me during this period of my life. Achieving my goals would not have been possible without their love and support.

IV. TABLE OF CONTENTS **PAGE**

V. LIST OF ABBREVIATIONS

8-OH-dG	8-oxo-7,8-dihydro-2'deoxyguanosine
AIF	Apoptosis inducing factor
AMPK	5' adenosine monophosphate-activated protein Kinase
APAF-1	Apoptotic protease activating factor 1
ATP	Adenosine triphosphate
BN	Brown Norway
CAD	Caspase activated DNase
cl-Cas3	Cleaved caspase 3
COX	Cytochrome c oxidase
COX-/SDH++	ETC abnormal fibers
CR	Calorie restriction
CSAR	Cross-sectional area ratios
CuZnSOD	Copper/zinc-dependent superoxide dismutase
DNA	Deoxyribonucleic acid
Endo G	Endonuclease g
ETC	Electron transport chain
F344	Fischer 344
FADD	Fas-associated death domain
FBN	Fischer 344 x Brown Norway
GH	Growth hormone
GPA	guanidinopropionic acid
H&E	Haematoxylin and Eosin staining
IMF	intermyofibrillar
MAC	Membrane attack complex
MiRNA	Micro ribonucleic acid
MMP	Mitochondrial membrane permeabilization
mtDNA	Mitochondrial DNA
mtPTP	Mitochondrial permeability transition pore
NADPH	Nicotinamide adenine dinucleotide phosphate
PUMA	p53 upregulated mediator of apoptosis
RF	Rectus femoris
ROS	Reactive oxygen species
RRF	Ragged red fibers
rRNA	Ribosomal RNA
SDH	Succinate dehydrogenase
SSBP	Single-strand binding proteins
SS	subsarcolemmal
tBid	Truncated Bid
TNFα	Tumor necrosis factor alpha
TOR	Target of rapamycin
tRNA	Transfer RNA
TUNEL	Terminal deoxynucleotidyl transferase dUTP nick end labeling
VI	Vastus intermedius
VL	Vastus lateralis
VM	Vastus medialis

VI. LIST OF TABLES **PAGE**

TABLE

VII. LIST OF FIGURES **PAGE**

FIGURE

VII. LIST OF FIGURES **PAGE**

FIGURE

Chapter 1: Introduction

Aging

Aging can be defined as the accumulation of change over the lifespan of an organism. The aging process entails the progressive decline in functional capacity of cells and increases the risk of mortality. Aging negatively impacts organelle, cellular and tissue function and is associated with a decline in physical, psychological and cognitive function (Passarino *et al.*, 2007). Phenotypes of aging commonly observed are alopecia, kyphosis, hearing loss, cataracts, immune dysfunction, neoplasia, neurodegeneration, osteoporosis and sarcopenia.

Aging and age-associated diseases are among the greatest challenges and financial burdens faced by developed countries (Christensen *et al.*, 2009). In Canada, the aging population is increasing as the "baby boom" cohort of 1945-1965 turn 65. In 2015, 16.1 % (5.8 million) of the Canadian population was >65 years old. By 2024, it is projected that this will increase to 20% of the population (Statistics Canada, 2015). Currently, the senior population consumes 45% of the total government health expenditure. In 2012, 60 billion dollars were spent on government health care for >65 years old (National Health Expenditure Trends, 2014). This cost will exponentially increase as elderly individuals continue to increase in number.

The rapid increase in life expectancy has been one of the greatest achievements of human history. In the 1900s, a Canadian's average life span was 60 years. Due to the advances in medical practices, life expectancy in 2010 was 81 years (Statistics Canada, 2012). As we live longer, the leading causes of death have shifted from infectious, parasitic and acute conditions to chronic disease. Age is one of the strongest risk factors for chronic diseases such as

cardiovascular disease, cancer, diabetes, hypertension, atherosclerosis, osteoarthritis and neurodegenerative disorders (Rocca *et al.,* 2014; Christensen *et al.*, 2009). The prevalence of dementia is very low at young ages, however, after 65 years, it doubles every 5 years. By 85 years, the prevalence of dementia in the elderly population is 30% (WHO, 2011). Cardiovascular diseases and cancer increase in incidence between the ages of 40 and 80 years (Driver, 2008). Similarly, the elderly population have increased prevalence of age-related macular degeneration, AMD, the leading cause for vision loss with age (Akpek and Smith, 2013) and nephrosclerosis, an age-related kidney disease (Rule *et al.,* 2010) which is often co-diagnosed with hypertension and diabetes. A new dilemma in geriatrics is the diagnosis of co-morbidities occurring at higher rates in the elderly. In U.S, approximately 80% of patients older than 65 had 2 or more morbidities (Rocca *et al.,* 2014). As the elderly population increases in future years, age-related disease and multi-morbidities pose a huge burden to the public health and financial system.

Theories of Aging

Aging is a complex process and affects several molecular, cellular and organellar systems. A number of theories have been proposed to understand the biological mechanisms underlying the aging process. The theories can be divided into two categories: (i) programmed aging and (ii) stochastic events resulting in accumulation of damage. The proposed theories are not mutually exclusive as there is cross-talk between programmed and accumulation of damage theories.

The programmed longevity theory states that the aging process is dictated by genetic components such as changes in gene expression of systems responsible for maintenance, repair and defense. Programmed aging was initially theorized by August Weismann in his evolutionary theory of aging where he states that death is a mechanism designed by natural selection to eliminate the old members of a population, therefore, allowing the younger generation free access to resources (Weismann, 1889). This theory was later expanded by Medawar (Medawar, 1952), stating that aging is a by-product of natural selection. Genes are selected for reproductive success and any beneficial/deleterious mutations that occur in later stages of life after the reproductive period are not selected and, therefore, accumulate. In 1957, George Williams stated that natural selection was biased towards the young. He hypothesized the antagonistic pleiotropy theory of aging where certain genes have pleiotropic effects. These genes are advantageous in development and early stages of life and ensure for successful reproduction, however, in later stages, the same genes become deleterious to the organism (Williams, 1957). Many debilitating genetic diseases should have been selected against by nature, however, due to antagonistic pleiotropy these genetic disorders exist e.g. the HTT allele for Huntington's Diseases (HD). Patients with HD, a neurological disorder which manifests after puberty, have increased fecundity and a reduced risk to cancer due to the increased activity of a tumor suppressor gene, p53 (Carter and Nguyen, 2011).

A number of theories have incorporated genetic programming e.g. the endocrine, Hayflick limit and DNA methylation theories. The endocrine theory postulates that aging mechanisms are dictated by a biological clock in the brain. The endocrine glands in the body secrete hormones

and neurotransmitters, which decline with increasing age (Everitt, 1980). In support of the endocrine theory, alterations to the hormonal signalling pathway have been associated with longevity studies in worms and flies (reviewed in van Heemst, 2010). To explain programmed aging at a biological level, Weismann proposed the theory of cell division limit; somatic cells have limited capacity to divide. Following the discovery that mammalian cells divide approximately 50 times and then undergo senescence, this theory is now known as the Hayflick limit theory of aging (Hayflick and Moorhead, 1961). Senescent cells cannot proliferate but remain metabolically active by releasing pro-inflammatory cytokines, growth factors, proteases and chemokines (Campisi, 2013). Cellular senescence may also be considered an example of antagonistic pleiotropic mechanism, as in early stages of life, senescent growth arrest suppresses the development of cancer, but later in life, the pro-inflammatory secretome from senescent cells contributes to the development of cancer (reviewed in Campisi, 2013). Craig Cooney hypothesized that cellular functional decline in senescence is the result of the accumulation of incomplete methylation of DNA upon cell division (Cooney, 1993). In support of this DNA methylation theory, a global decline in DNA methylation is observed with increasing age (Mugatroyd *et al.,* 2010), however, hyper-methylation may play a role in the aging process as age-associated increase in methylation was observed in a genetic loci regulating cell proliferation (Koch *et al.,* 2011).

Damage accumulation theories state that random events from the environment result in accumulation of damage and decline in cellular and biological functions. A traditional theory of aging is the wear and tear theory proposed by August Weismann (Weismann, 1889). This

theory states that, over time, cell and tissues in an organism wear out due to repeated use similar to the mechanical use of an inanimate object. Organs are considered analogous to parts of an automobile where the accumulation of damage resulting from abuse results in decline in function. Weismann proposed that somatic cells play an integral role as they succumb to environmental damage and are unable to proliferate as the organism ages.

Many theories have focused on damage induced by wear and tear e.g. DNA mutation accumulation (Franceschi*,* 1989), disposable soma (Kirkwood, 1993) and oxidative damage (Harman, 1972). The somatic mutation theory, initially proposed by Failla (Failla, 1958), states that cellular function declines with age due to the accumulation of DNA mutations in somatic cells. In support of this theory, age-dependent increases in nuclear mutations have been reported in tissues such as lung, blood, stomach and thyroid (Yadev *et al.,* 2016). This theory is further supported by transgenic mouse models where short-lived strains have higher mutational burden and long-lived strains have a lower mutational burden (reviewed in Kennedy *et al.,* 2013). Another classical theory is the disposable soma theory involves a cross-talk between the evolutionary and damage accumulation theories. This theory was proposed by Thomas Kirkwood in 1977 and hypothesizes that organisms have a limited amount of energy that is allocated between cellular maintenance and reproduction (Kirkwood, 1993). As energy levels are budgeted, repair and maintenance processes are compromised and result in accumulation of damage in the absence of external environmental hazards (i.e. predators, accidents, pathogens). The theory predicts that there is a trade-off between survival and reproduction of organisms. In 1993, Steven Austad tested this theory in two distinct

populations of opossums (Austad, 1993). The population with the least predation rate had the least pups per litter and longer lifespan than the mainland group with the higher predation rate, therefore, with shorter lifespans. However, these opossums had the most pups per litter. This study suggests that in the mainland possums, biological mechanisms exist to ensure the survival of the species.

The Mitochondrial Free Radical Theory of Aging

The free radical theory of aging was proposed by Harman and postulates that aging results from a gradual accumulation of mitochondrial damage from mutagenic oxygen radicals and reactive oxygen species (ROS) which are by-products of metabolism (Harman, 1972). Oxygen radicals have been shown to damage nuclear (Fano *et al.,* 2001) and mitochondrial DNA (Linnane *et al.,* 1998) as well as induce lipid peroxidation (Pansarasa *et al.,* 2000) and protein carbonylation (Rousset *et al.,* 2004). In support of this theory, increase in ROS production has been detected in multiple tissues with increasing age (Donato *et al.*, 2007; Moon *et al.*, 2001; Chen *et al.*, 2001).

The free radical theory was later modified to the oxidative stress theory, stating that with age there is a decline in antioxidant defense and that ROS are not eliminated efficiently (Sies *et al.,* 1985). However, the role of ROS in aging has been questioned due to studies in transgenic mice expressing antioxidant enzymes; altering the expression of antioxidant enzymes had no effect on the life span (Perez *et al.,* 2009). These studies suggest that increasing the rate of ROS

elimination does not affect longevity. However, the rate of production of ROS seems to be more relevant to longevity than the rate of ROS elimination. Species with a longer life span have a slower rate of ROS production than short-lived organisms. The rate of superoxide production is lower in brain homogenates from humans than rodents that have a lifespan of 2-3 years (Kudin *et al.,* 2004).

ROS, besides its toxic effects, also play an important role in regulating cellular functions and are essential for cell survival. ROS signalling is mediated through altering catalytic activities of proteins. Activities of specific proteins are regulated by redox, reduction and oxidation, reactions of cysteinyl thiols. Deprotonated cysteine residues act as redox-sensitive switches that modulate the activity of the protein by either oxidation via hydrogen peroxide or reduction by thioredoxin or glutathione systems (Brandes *et al.,* 2009). An alternate notion to the oxidative stress, is the redox stress theory of aging which postulates that the age-dependent increase in ROS production shifts the cell's redox state to pro-oxidizing. This results in increased oxidation of cysteines of redox-sensitive proteins and a decline in reduction potential, ultimately disrupting the redox signalling pathways (Sohal and Orr, 2012).

Reactive oxygen species are produced in cellular sites such as microsomes, peroxisomes or at membrane-bound NADPH-oxidases (Boveris *et al.,* 1972). The site of ROS production most critical to longevity is, however, the inner mitochondrial membrane. Median and maximal life span was extended in transgenic mice overexpressing catalase targeted to the mitochondria (Schriner *et al.,* 2005). The free radical theory became known as the mitochondrial theory following the discovery that majority of the ROS were produced in the mitochondria at complex

I (Herrero and Barja, 1998) and complex III (Muller *et al.,* 2004). The mitochondrial theory of aging states that there is an age-dependent increase in mitochondrial dysfunction which results in a decline in energy levels and increase in cell death. The theory focuses on the susceptibility of mitochondrial damage as the mtDNA lacks histones, an efficient DNA repair system and has increased proximity to ROS. A vicious cycle of events is proposed where ROS induces genetic alterations and protein defects to the subunits in the electron transport chain (ETC) resulting in enhanced ROS production from faulty complexes in the ETC (reviewed in Johnston *et al.,* 2008).

There is an age-related increase in ROS levels which correlates with increase in mtDNA damage (Gianni *et al.,* 2004). A measure of oxidative damage to the DNA is performed by analyzing the levels of 8-oxo-7,8-dihydro-2'deoxyguanosine (8-OH-dG) and it was found that levels of mtDNA damage negatively correlated with longevity (Kudin *et al.,* 2008). The oxidative damage in heart and brain mtDNA was determined in 8 mammalian species which greatly differed in longevity, i.e. mouse, rat, guinea pig, rabbit, sheep, pig, cow and horse. The least amount of oxidative damage was observed in the horse species that have a maximum lifespan of 46 years whereas mice that live up to 3.5 years had a fourfold increase in mtDNA damage in heart (Barja and Herrero, 2000).

Cellular Death Mechanisms in Aging

Age-dependent loss of of myofibers in skeletal muscle have been observed in rats (Bua *et al.*, 2008), monkeys (McKiernan *et al.*, 2009) and humans (Lexell *et al.,* 1988; Lexell *et al.* 1986).

Similarly in aged heart, 35% decline in cardiac myocytes was detected between the ventricles of young and elderly individuals (Olivetti *et al.,* 1991). In 24 month old male Fischer 344 rats, both apoptosis and necrosis occur with increasing age in the left ventricular wall (Kajstura *et al.*, 1996). Along with heart, upregulation of apoptosis in an age-dependent manner has been suggested in a variety of tissues e.g. kidney (Lee *et al.,* 2004), stomach (Tarnawski *et al.,* 2014) and skeletal muscle (Alway *et al.,* 2011). These studies suggest that age-related decline in organ function might be attributed to increase in cell death mechanisms.

Necrosis and apoptosis are the primary cell death pathways. Necrosis is initiated upon physical and chemical injuries e.g. membrane damage, toxin exposure and cellular energy depletion. Distinct morphological changes associated with necrosis is the swelling of the cell, loss of membrane integrity, organelle swelling and extensive DNA damage (Henriquez *et al.*, 2008). The necrosis pathway results in the swelling of the cell due to changes in membrane ion transport. Increase in cytosolic influx of Ca^{2+} and Na^{+} and the disruption of K^{-} and Cl^{-} efflux results in cell swelling and membrane disruption (Henriquez *et al.*, 2008). Rupturing of the cell results in the release of intracellular cytoplasmic contents into the extracellular space. This triggers the infiltration of immune cells into the necrotic site (Kharraz *et al.*, 2013). Eventually the surrounding area becomes inflamed (Scaffidi *et al.*, 2002) **(Figure 1.1)**.

Necrotic cell death has been implicated in age-related cardiovascular diseases and neurodegenerative disorders (Syntichaki *et al.*, 2002; Tavernarakis, 2007; Artal-Sanz and Tavernarakis, 2005). Elderly are more susceptible to cardiovascular diseases such as coronary heart disease, heart failure and stroke. In stroke, necrotic cell death of cardiomyocytes is a

major contributor (Tavernarakis, 2007). In neurodegenerative disorders such as Alzheimer's, Huntington's and Parkinson's, necrotic cell death contributes to disease progression (reviewed in Artal-Sanz and Tavernarakis, 2005). The inflammatory response triggered by necrosis, may also damage normal tissue. The combinative effect of leakage of reactive oxygen species (ROS) from necrotic cells and the activation of macrophages contribute to increased oxidative stress (Rock and Kone, 2008). This can further exacerbate the aging process by triggering ROS induced cellular death. Exogenously produced ROS affects cellular death mechanisms by oxidatively damaging proteins, lipids and DNA. Necrotic cell death was induced in the presence of very high levels of exogenous ROS (Panieri *et al.,* 2013). The cytotoxic effect observed in cells was due to extensive DNA damage, energy depletion and the activation of a Serine/Threonine kinase, RIP1, which is a key mediator of caspase-independent necrosis.

Apoptosis is a programmed cell death pathway where the cell undergoes distinctive molecular, biochemical and morphological changes. The apoptotic cell shrinks and the nucleus and chromatin condense. Fragmentation of the chromatin precedes membrane blebbing and budding of the cell into "apoptotic bodies" which are engulfed by macrophages via phagocytosis. The molecular mechanism of apoptosis involves activation of cysteine proteases known as caspases. Caspases are zymogens, activated by proteolytic cleavage under appropriate conditions. Initiator caspases, e.g. caspase 9, cleave downstream caspases known as effectors, e.g. caspase 3. Effector caspases cleave cytoskeleton proteins and indirectly activate DNA cleaving enzymes. Apoptosis can be triggered in a cell by either external or internal stimuli. Mitochondria have an important role in the intrinsic pathway of apoptosis,

however, there is significant crosstalk between the two distinct pathways. Once a cell death stimulus is received, proteins belonging to the Bcl-2 family translocate to the mitochondria and initiate outer mitochondrial membrane permeabilisation. Translocation of cytochrome c from the mitochondria to the cytosol activates the apoptotic machinery by the cleavage of procaspase 9 (Johnson and Jarvis, 2004).The caspase cascade is initiated resulting in DNA fragmentation and apoptotic cell death. Mitochondria release other pro-apoptotic proteins such as Smac/ Diablo, endonuclease g (Endo G) and apoptosis inducing factor (AIF). In the extrinsic pathway, transmembrane death receptors bind to a death ligand. This triggers the binding of caspase 8 to the death domain. Activated caspase 8 can activate caspase 3 and induce apoptotic cell death independent of mitochondria. However, caspase 8 can also cleave a pro-apoptotic Bcl-2 family member, Bid. Truncated Bid (tBid) can interact with Bax, a Bcl-2 family member that permeabilises the mitochondrial membrane (Grinberg *et al.,* 2005) initiating the mitochondrial pathway **(Figure 1.2)**.

Sarcopenia

Sarcopenia is defined as the age-related decline in skeletal muscle mass, quality and function (Rosenberg, 1997). The word is derived from the Greek language where Sarco- means flesh and penia- means poverty. Sarcopenia is a ubiquitous hallmark of aging. It has been observed in nematodes (Herndon *et al.,* 2002), flies (reviewed in Demontis *et al.,* 2013), rats (Bua *et al.*, 2008), monkeys (McKiernan *et al.*, 2009) and humans (Lexell *et al.,* 1988; Lexell *et al.* 1986: Klein *et al.,* 2003; Lee *et al.,* 2006). The prevalence of sarcopenia in humans, was determined to

be greater than 50% after the age of 80 years (Baumgartner *et al.,* 1998). Thus, muscle wasting is an important aspect of aging as it is highly prevalent in old animals and highly conserved in a wide range of organisms.

The decline in muscle mass is accompanied by a loss in muscle cross-sectional area. In measurements of human cadaver samples, there was a 40% decline in cross-sectional area from whole muscle by 80 years of age (Lexell *et al.,* 1988). Studies employing different assays *in vivo,* i.e. ultrasound and computed tomographic scanning, observed similar average reductions. Ultrasonographic imaging detected a 25% reduction in quadriceps CSA from elderly men (Young *et al.,* 1985). Similarly, computed tomographic scanning showed that quadriceps muscles from elderly men had a 26% decline in muscle area (Overend *et a.,* 1992), 36% and 35% reduction of muscle area in bicep brachii and gastrocnemius muscle (Rice *et al.,* 1989).

Accompanying the loss in muscle mass and cross-sectional area, there is age-related increase in fat and connective tissue in muscle which contributes to decline in muscle quality. Non-muscle tissue was found to increase 27% in bicep brachii, 81% in gastrocnemius muscle of elderly men (Rice *et al.,* 1989), 66% in quadricep muscles and 127% in hamstrings of men (Overend *et al.,* 1992). Age-dependent fatty infiltration in muscle is due to lipid accumulation within myofibers and increase in adipocyte deposition (reviewed in Hamrick *et al.,* 2016). Additionally, muscle quality is further compromised by an increase in fibrotic tissue which increases the stiffness of muscle (Wood *et al.,* 1985). This increase in non-muscle tissues contributes to the age-related loss in muscle function.

The relationship of sarcopenia and disability was established in a longitudinal study which examined body composition and self-reported disability in 68-78 year old men and women. A decline in skeletal muscle mass was associated with a 2.5 increased risk of disability (Fantin *et al.*, 2007). The elderly exhibit a 2-3 fold increase in functional disability (Baumgartner *et al.*, 1998) and the prevalence of mobility impairments is as high as 80-90% (Newman *et al.*, 2003). The major consequences of increased disabilities in the elderly are falls, injuries and fractures (Baumgartner *et al.*, 1998; Szulc *et al.*, 2005) and increases the need of personal assistance (Janssen *et al.,* 2002). Furthermore, sarcopenia increases mortality risk. Loss of muscle mass in elderly was associated with a 14% mortality rate (Szulc *et al.*, 2010). Similar findings were found in 65 years and older with a poor grip strength (Metter *et al.*, 2002).

Fiber Loss in Sarcopenia

The decline in muscle mass is due to a decrease in fiber number and an increase in fiber atrophy (Wanagat *et al.,* 2001; Lexell *et al.,* 1988; Klein *et al.,* 2003; McKiernan *et al.,* 2009). In humans, the average decline in fiber number from quadriceps biopsies was 40% between 20 to 80 years (Lexell *et al.,* 1988) and it was estimated that humans lose ~25 muscle fibers per day at age 80 (Lexell *et al.*, 1986). Muscles from aged humans have smaller fiber cross sectional area compared to 20 year olds (Klein *et al.,* 2003). Similar observations have been made in rhesus monkeys and FBN rats. In a 12 year longitudinal study, the decline in muscle mass and increase in fiber atrophy has been observed in old rhesus monkeys (McKiernan *et al.,* 2009). The oldest monkey in the study exhibited a 44% decline in muscle mass and a 20% decline in fiber CSA

over the course of 6 years. In 33-months old FBN rats, significant decline in muscle mass is observed in three of the quadriceps muscles, rectus femoris, vastus lateralis and vastus medialis. By 36 months, fiber number declined by 46%, 31%, and 32% in rectus femoris, vastus lateralis, and vastus medialis. Along with decline in muscle mass and fiber number, there was an age-dependent decline in muscle cross sectional areas and fiber size. By 36 months, fiber CSA in RF and VL muscle declined by 40% (Bua *et al.,* 2008).

Additionally, there are muscle groups that do not exhibit significant changes in muscle mass and fiber number (Alnaqeeb and Goldspink, 1987; Holloszy *et al.*, 1991; Bua *et al.,* 2002). The muscles susceptibility to sarcopenia is attributed to differences in fiber type composition. Muscles have been characterized based on color and contraction speed. There are two primary types of muscle fibers, type I and type II (reviewed in Schiaffino and Reggiani, 2011). Type I fibers are smaller, appear red in color and have very slow contraction speeds. They have very high oxidative capacity with higher levels of oxidative enzymes, myoglobin content, mitochondria and increased resistance to fatigue. A lower ATPase level result in slower contraction times and minimum force production. Type II fibers have a larger cross sectional area, appear white in color and have very fast contraction speeds. They rely on a glycolytic metabolism, therefore, type II fibers fatigue faster. Due to these characteristics, type I fibers are also known as “slow twitch oxidative” fibers whereas type II are known as “fast twitch” fibers. Fast twitch fibers can be further characterised into type IIa, fast oxidative glycolytic, and IIb, fast glycolytic fibers. Type IIa fibers have a higher oxidative capacity, increased resistance to fatigue and are less glycolytic than type IIb fibers. Type IIa fiber are primarily needed in exercises such

as running and heavy weight training whereas type IIb fibers are suited for short bursts of power e.g. sprinting. Type 1 fibers are used for slower activities e.g. walking and cycling (reviewed in Schiaffino and Reggiani, 2011).

Muscles contain a mixture of both fast and slow fiber types and depending on the activity, can be enriched in type I or type II fibers. Slow muscles are composed of type I fibers and can endure longer muscle contractions. Fast muscles are predominantly type II and produce short bursts of force but have a shorter endurance. Muscle atrophy in aged tissue is most evident in fast muscles whereas type I-enriched muscles are sarcopenia-resistant. Significant decline in muscle mass in aged rats was observed in two different fast muscles, rectus femoris (Wanagat *et al.*, 2001) and vastus lateralis (Bua *et al.,* 2008; McKiernan *et al.,* 2004) whereas there is minimal loss observed in slow muscles e.g. adductor longus (Holloszy *et al.*, 1991) and extensor digitorum longus (Alnaqeeb and Goldspink, 1987). Additionally, type II muscle fibers are predominantly lost in elderly (Lee *et al.,* 2006), have higher levels of oxidative stress (Siu *et al.*, 2008), increased susceptibility to apoptosis (Pistilli *et al.*, 2006) and are more prone to atrophy (Lee *et al.,* 2006) than type I fibers. Mitochondrial abnormalities are abundant in fast muscles (Bua *et al.*, 2002) and occur primarily in type II fibers (Wanagat *et al.*, 2001). Moreover, apoptosis is activated in predominantly fast muscles of aged rodents (reviewed in Alway *et al.*, 2011) suggesting a role for apoptosis in muscles that exhibit atrophy and fiber loss.

Mechanisms of Sarcopenia

Sarcopenia is a complex process and many factors contribute to its aetiology. Hormonal changes (Visser *et al.*, 2003), alteration in muscle architecture (Hamrick *et al.,* 2016), mitochondrial dysfunction are a few of the proposed contributing factors. Other factors that might play a role in sarcopenia are decline in physical activity (Baumgartner *et al.*, 1998), vitamin D deficiency (Visser *et al.,* 2003), decline in muscle regeneration (reviewed in Jones and Rando, 2011), satellite cell dysfunction (Gallegly *et al.*, 2004), muscle fiber denervation (Jang *et al.,* 2010), and loss of motor unit number (Roos *et al.*, 1997).

Hormonal imbalance is prominent in the elderly and is thought to be an important factor of sarcopenia. Declining levels of growth hormone (GH), insulin, estrogen, testosterone and other steroid factors result in a lower anabolic potential. The age-related decline in estrogen and testosterone is associated with loss of muscle mass and bone density. This decline predisposes the elderly to fractures and further health complications. Testosterone regulates the levels of myostatin, a protein that negatively regulates muscle cell differentiation and proliferation. Aged muscle have increased levels of myostatin which is suppressed upon testosterone supplementation. In mice, it was determined that testosterone treatment suppressed age-specific increases in oxidative stress, myostatin levels and prevented muscle mass decline in aged muscles (Kovacheva *et al.,* 2010). Lower levels of circulating growth hormone, IGF-1, is concomitant with declining muscle strength (Cappola *et al.*, 2001). In 70 year old women, low levels of IGF was associated with poor knee extensor strength, a slower gait and difficulty in mobility (Cappola *et al.,* 2001). Both GH and IGF-1 have important anabolic effects on skeletal

muscle tissue. IGF1 stimulates muscle cell proliferation and differentiation, facilitates muscle protein synthesis, and inhibits muscle atrophy (reviewed in Woodhouse *et al.,* 2006).

Senescent cells, which release inflammatory cytokines, also secrete proteases which cleave ligands on their cell surface and ligand receptors on natural killer cells (Campisi, 2013). Along with the age-dependent decline in immune function, this results in senescent cell accumulation and increase in circulating inflammatory cytokines. In the elderly, increases in pro-inflammatory cytokines such as interleukin-6 and tumor necrosis factor (TNF-alpha) trigger muscle mass loss and decline in muscle strength (Schaap *et al.,* 2009). In transgenic mice deficient for IL-10, an anti-inflammatory cytokine, mice had increased levels of IL-6 and exhibited acceleration in muscle wasting and weakness as observed in sarcopenia (Walston *et al.,* 2008). These cytokines have a catabolic effect as they can inhibit protein synthesis and increase proteolytic pathways, resulting in the decline in muscle mass and function. TNF-alpha can trigger myofibrillar protein degradation via the ubiquitin-proteasome pathway, inhibit protein synthesis by inactivating eukaryotic initiation factors, eIF, and regulate expression of additional cytokines (Zoico *et al.,* 2002). Additionally, TNF alpha can induce apoptotic cell death in skeletal muscle and contribute to fiber loss (Pistilli *et al.,* 2006).

Animal Models of Sarcopenia

Aging research has focused on several rodent strains including Wistar (Roth *et al.,* 1993), Sprague-Dawley (Cohen *et al.,* 1978), Brown Norway (Cohen *et al.,* 1978) and Fischer 344 rats

(Masoro, 1990). F344 rats have been used as a model system for studying mammalian aging due to their mild temperament and high fertility rate. Male F344 rats have a median life span of 24 months with a maximum life span of 30 months (Holmes, 2003). The strain, however, is prone to extreme nephropathy, renal failure and high rates of Leydig cell adenoma (Weindruch and Masoro, 1991). Old F344 rats also do not show significant decline in muscle mass or function indicating that a rat strain with a longer life span is required to understand muscle atrophy (Rice *et al.,* 2005). Brown Norway (BN) rats have a longer life span of 29 months (Holmes, 2004a). The pathologies present in the F344 are absent in BN rats and in the outcrossed hybrid strain, Fischer 344 x Brown Norway (FBN). FBN rats have lower lesion incidences in their tissues than the parental strains and a longer mean life span of 31 months with a maximum of 42 months (Holmes, 2004b). Thus, the FBN rat, a model with increased longevity and lower rate of disease, is an excellent rodent strain to study age-related effects in the muscle. FBN rats exhibit an age-dependent decline in muscle mass (Bua *et al.,* 2008) and function (Olfert *et al.,* 2004).

The Mitochondria

Mitochondria are double-membrane organelles present in eukaryotic cells. The engulfment of an alpha proteobacterium two billion years ago by a precursor eukaryotic cell evolved into the modern mitochondria (Lane and Martin, 2010). During evolution, most of the ancestral proteobacterium genome was transferred to the eukaryotic cell's nuclear genome (Gabaldon and Huynen, 2004) leaving behind a smaller mitochondrial genome. The mammalian

mitochondrial genome is circular and comprised of approximately 16,000 bp encoding 37 genes, 13 of which encode for core subunits of the mitochondrial electron transport chain, ETC (Anderson *et al.,* 1981). The ETC contains respiratory complexes I - IV present in the inner mitochondrial membrane and is the site of oxidative phosphorylation and ATP production (Figure 1.3). Intermediates from the Krebs cycle donate electrons to the ETC. The transfer of electrons to the ETC respiratory complexes coupled with the transfer of protons to the mitochondrial intermembrane space generates an electrochemical gradient. The proton gradient is utilised by ATP synthase, complex V, to generate adenosine triphosphate (ATP). Most of the cell's ATP is generated in the mitochondria. The glycolytic pathway in the cell produces 2 molecules of ATP per glucose molecule metabolised whereas the mitochondria can generate up to 30 molecules of ATP (Rich, 2003).

There are approximately 1,000 mitochondrial proteins (Forner *et al.*, 2006). The mitochondrial proteome is primarily nuclear-encoded (Gabaldon and Huynen, 2004). Cytosolic ribosomes translate nuclear-encoded mRNA to proteins which are then imported into the mitochondria by outer and inner mitochondrial membrane translocase machinery (Neupert *et al.*, 2007; Schmidt *et al.*, 2010). The complexes in the ETC are composed of several subunits. Complex IV, Cytochrome c oxidase, consists of 13 subunits. The core of the complex, containing the three largest subunits, is encoded by the mitochondrial genome. The remaining 10 subunits are nuclear-encoded (Tsukihahra *et al.*, 1996). Interestingly, succinate dehydrogenase (SDH), complex II of the ETC, is entirely encoded by the nuclear genome (Boore, 1999).

Aside from the 13 polypeptides, mtDNA also encodes for 22 transfer RNA (tRNA) and 2 ribosomal RNA (rRNA) molecules. As in prokaryotes, mitochondrial transcription occurs from the double-stranded mtDNA as a continuous polycistronic RNA molecule. Transcription and replication of the mtDNA depend heavily upon nuclear-encoded factors. Enzymes that charge tRNAs with the proper amino acid, aminoacyl tRNA synthases, are encoded by the nuclear genome. Similarly, replication of the mitochondrial genome occurs by nuclear encoded DNA polymerase (Polg), single-strand binding proteins (SSBP) (Taanman, 1999) and a helicase (Jemt *et al.,* 2011).

Aside from their role in ATP production, mitochondria have several other important functions including intracellular calcium regulation (Khodorov *et al.,* 1996), regulation of the membrane potential (Saraste, 1999), steroid synthesis (Rossier, 2006), hormone signalling (McBride *et al.*, 2006) and apoptosis (Primeau *et al.,* 2002).

Mitochondrial Dysfunction in Sarcopenia

Skeletal muscle is a metabolic tissue with high energy demands and is enriched with mitochondria (D'Erchia *et al.,* 2014). Studies suggest mitochondrial dysfunction as one of the factors of sarcopenia as there are various age-related changes in the mitochondrial morphology and function.

Swollen mitochondria and age-dependent fragmentation of mitochondria have been observed in nematodes (Regmi *et al.,* 2014), mice (Leduc-Gaudet *et al.,* 2015), rats (Iqbal *et al.,* 2013) and

humans (Beregi and Regius, 1987). Skeletal muscle biopsies from aged humans showed in electron microscopy that mitochondria existed in an interconnected network and there was an age dependent increase in swollen mitochondria with ultrastructural abnormalities (Beregi and Regius, 1987). Recently, age-dependent alterations in mitochondrial morphology were detected from skeletal muscle of old mice (Leduc-Gaudet *et al.,* 2015). There are two distinct subpopulations of mitochondria in the muscle. Subsarcolemmal mitochondria (SS) are located under the sarcolemmal membrane of the muscle and intermyofibrillar mitochondria (IMF) are located between myofibrils. In aged atrophied muscle, SS mitochondria are enlarged and less circular compared to young muscle and IMF mitochondria are elongated and exhibit more branching in their 3D spatial distribution. Abnormalities in mitochondrial structure have been associated with impaired function. They produce lower ATP levels, have a lower membrane potential and are susceptible to apoptosis (Chabi *et al.,* 2008).

In skeletal muscle, age related decline is observed in mtDNA copy number, mitochondrial protein expression, enzymatic activity and respiration rate in old humans (Herbert *et al.,* 2015). The correlation of decline in mtDNA and function has been observed in other tissues. There is age related decline in mtDNA copy number in human pancreatic beta cells which results in decline in cell function (Cree *et al.,* 2008). Alterations in the ETC result in an increase in reactive oxygen species (ROS) generation (Capel *et al.* 2005; Mansouri *et al.,* 2006; Chabi *et al.,* 2008) and diminished capacity for ATP production (Conley *et al.,* 2000; Drew *et al.,* 2003; Tonkonogi *et al.,* 2003). This drastically increases the susceptibility of mitochondria to cell death (Honda *et al.,* 2003 and Izyumov *et al.,* 2004). Other factors that contribute to the decline in mitochondrial

function in aged muscle are the increase in mitochondrial permeability (Figueiredo *et al.,* 2009), reduced biogenesis of mitochondria (Chabi *et al.* 2008), slower mitochondrial enzyme activities (Coggan *et al.,* 1993*),* declines in mitochondrial protein synthesis (Rooyackers *et al.* 1996), impaired removal of oxidatively damaged mitochondrial proteins (Bota *et al.* 2002), reduced mitochondrial autophagy (Terman and Brunk, 2004) and mtDNA damage (Wanagat *et al.,* 2001).

Mitochondrial DNA Mutations Accumulate with Age

The first mitochondrial DNA mutation detected in aged human tissues was a large scale deletion of 4977bp in length, frequently found in genetic neuromuscular disorders (Cortopassi and Arnheim, 1990). Age-dependent accumulation of this specific mtDNA deletion mutation was detected in 21-53 year old human hearts. A pattern of tissue specificity was observed in the accumulation of mtDNA deletions. Highest levels of this common mtDNA deletion, mtDNA-4977, were detected in post-mitotic tissues, i.e., brain, heart, diaphragm and psoas muscles while no deletions were detected in mitotic tissues such as kidney, lung, spleen, skin and liver (Cortopassi *et al.,* 1992). Several studies have reported the presence of multiple unique mtDNA deletion mutations in aged post mitotic tissues such as brain, heart and skeletal muscle (Van Tuyle *et al.,* 1996; Zhang *et al.,* 1992). These tissues are highly metabolic, consume the most oxygen for energy production and exhibit the most decline in mitochondrial activity with age (Melov *et al.,* 1999). In sarcopenic elderly individuals, mtDNA deletion products were prevalent in skeletal muscle samples and correlated with a decline in mitochondrial activity (Shah *et al.,*

2009). Initial studies identified an increase in abundance (Linnane *et al.*, 1990) and frequency (Zhang *et al.,* 1992) in mtDNA deletion products in aged muscle tissue. The abundance of mtDNA deletions in these tissue homogenate studies was very low (1-0.1%) (Simonetti *et al.,* 1992; Edris *et al.,* 1994). When the muscle was separated into smaller fiber groups, however, the abundance of mtDNA deletions in aged muscle drastically increased (Schwarze *et al.,* 1995) suggesting that mtDNA deletion mutations accumulated in a few fibers. *In situ* hybridization experiments confirmed that mtDNA deletion mutations focally accumulated within a subset of cells that were dysfunctional in mitochondrial activity (Müller-Höcker *et al.,* 1993; Lee *et al.,* 1998; Lopez *et al.,* 2000).

The role of mtDNA point mutations in ageing has been ambiguous due to the lack of reliable methods to detect mutations. Mitotic tissues exhibited an age-dependent accumulation of mtDNA point mutations. Cultured fibroblasts from old humans, demonstrated that mtDNA mutations accumulated in individual >65 year of age and localized to the mtDNA control region of replication, the D-loop (Michikawa *et al.,* 1999). However, no clinical phenotype was observed with age-dependent accumulation of mutations. Most evidence for a role of mtDNA point mutations in aging have been in aged stem cells. Age-dependent accumulations of mtDNA point mutations have been observed in stem cell populations for epithelium (Blackwood *et al.*, 2011), gastric (McDonald *et al.*, 2008), bone marrow (Shin *et al.*, 2004) and granulocytes (Shin *et al.*, 2004). Aged stem cells of colonic crypts have increased mtDNA point mutations which disrupt the respiratory activity of the cell (Taylor *et al.,* 2004). This results in decreased proliferation of colon crypt cells and increased apoptosis in aged human tissue (Nooteboom *et*

al., 2010). There is, however, a substantial lack of evidence on the pathogenic role of mtDNA point mutations in aging.

The first causative association of mtDNA damage and sarcopenia was delineated by Trifunovic *et al.* (2004) in transgenic mice expressing a proof-reading deficient mtDNA polymerase. They showed that somatic mtDNA mutations in transgenic mutator mice resulted in premature aging phenotypes such as shortened life span, accelerated osteoporosis, alopecia, weight loss, kyphosis, myocardial hypertrophy and sarcopenia (Trifunovic *et al.*, 2004).

mtDNA Deletion Accumulation Disrupts Cellular Function

Mitochondrial DNA deletions have been linked to focal electron transport chain defects observed in aged muscle (Müller-Höcker *et al.*, 1993; Lopez *et al.,* 2000; Lee *et al.*, 1998; Lee *et al.*, 1993). There is an age-associated increase in cells lacking cytochrome c oxidase (COX) activity in multiple tissues such as cardiomyocytes (Wanagat *et al.*, 2002), skeletal muscle (Bua *et al.,* 2006), diaphragm (Müller-Höcker *et al.*, 1990) and extraocular muscles (Müller-Höcker *et al.*, 1992). These COX^- fibers have abnormal mitochondria clustered together (Olson *et al.*, 1972) and are also known as “ragged red fibers” (RRF). RRFs can be identified by histochemical staining for COX and SDH (succinate dehydrogenase) activity; abnormal fibers lack in COX activity but exhibit an increase in SDH activity. Studies have utilized laser capture microdissection to extract individual skeletal muscle fibers and identify mtDNA deletion events in focal regions.

Unique mtDNA deletions have been identified within the focal ETC defect from RRFs studied in rats (Cao *et al.,* 2001; Herbst *et al.*, 2007), monkeys (Gokey *et al.*, 2004) and humans (Bua *et al.*, 2006). The size of the deletion varies from a few hundred base pairs to 12kb. These deletion events generally occur between the origin of replications of the heavy and light strand, known as the major arc region, removing the majority of the genes encoding ETC subunits **(Figure 1.4)**. Furthermore, unique mtDNA deletion events suggest a clonal expansion of the mutated genomes. Ultimately, the ETC function is disrupted when the abundance of the mtDNA deletion mutations reaches ~90% (Herbst *et al.*, 2007) **(Figure 1.5)**. A similar threshold of 60 (Hayashi *et al.,* 1991) -90% (He *et al.,* 2002) mtDNA deletion mutations in RRFs is observed in myopathy patients. The disruption in the ETC phenotype results in oxidative damage within the abnormal segment (Wanagat *et al.*, 2001) and fiber atrophy (Wanagat *et al.*, 2001; Lopez *et al.,* 2000; Bua *et al.*, 2004). The degree of atrophy is positively correlated with the length of the abnormal segment, i.e., a fiber with a longer dysfunctional ETC segment will be atrophic. In cases where the atrophy is extreme, the fiber breaks within the focal ETC defect (Bua *et al.*, 2004).

There is an age-dependent increase in the abundance of ETC abnormal fibers in skeletal muscle. In 38-month old rats, volume density analysis estimated that ~15% of the fibers in the rectus femoris muscle of the quadriceps tissue are to be ETC abnormal (Wanagat *et al.*, 2001). Similarly in rhesus monkeys, extrapolation from 0.16 cm of muscle biopsies estimated that in a 32 year old, 28% and in a 34 years old, 60% of the fibers would be ETC abnormal (Lopez *et al.*, 2000). In humans, post-mortem muscle samples were obtained from different aged individuals. A progressive increase in ETC abnormality abundance was observed with age. The percent

abundance was 6% in a 49 year old, 22% in a 67 year old and 31% in a 92 year old (Bua *et al.*, 2006). The estimates of RRF abundances in the skeletal muscle do not take into account fibers that have been already lost due to the energy deficit. Hence, the load of ETC abnormalities throughout the lifespan is much greater than the percent abundances reported in the above studies and implicate ETC abnormalities in sarcopenia.

Furthermore, muscles that exhibit atrophy and fiber loss have a higher ETC abnormal abundance than muscles that are resistant to sarcopenia. Rectus femoris and vastus lateralis muscles, which are muscles susceptible to sarcopenia and have the most significant decline in mass and fiber number, have a greater abundance of ETC abnormalities. However, sarcopenia resistant muscles, soleus and adductor longus, have the rarest abundance of ETC abnormalities (Bua *et al.*, 2002). Additionally, apoptotic and necrotic cell death occur predominantly in ETC abnormal fibers (Cheema *et al.,* 2015). These studies suggest that increased cell death in ETC abnormal fibers contribute to decline in fiber number observed in sarcopenic muscles.

Activation of Apoptosis and Necrosis in Aged Muscle

In skeletal muscle, there is an age-dependent increase in DNA strand breaks and pro-apoptotic factors such as Bax, procaspase-3, and APAF-1 (reviewed in Alway *et al.*, 2011). The intrinsic pathway of apoptosis can be caspase-independent involving mitochondrial pro-apoptotic factors, AIF and EndoG. There is an age-dependent increase in the levels of AIF (Baker and Hepple, 2006) and EndoG in fast contracting muscle (Marzetti *et al.*, 2008). The extrinsic

apoptotic pathway can be activated by the increase of circulating serum cytokines in aged tissue. Apoptotic extrinsic factors such as caspase 8 (Marzetti *et al.*, 2009; Pistilli *et al.,* 2006a), Bid (Pistilli *et al.*, 2006a) and FADD (Pistilli *et al.*, 2006a) are present in high levels in old rat muscles suggesting that the extrinsic pathway may also be important in sarcopenia. Cross-talk can occur between the extrinsic and intrinsic pathway mediated by the cleavage of Bid. Truncated Bid (tBid) interacts with Bax to initiate mitochondrial apoptotic signalling.

Although several reports suggest an increase in apoptotic factors in aged muscle, there are a few conflicting reports (Alway *et al.,* 2011). In 26 month old F344 rats, age-dependent increase in DNA fragmentation in gastrocnemius muscle was attributed to increase in procaspase 3 and cleaved caspase 3 levels. However, cytosolic extracts from aged rat tissues did not detect any changes in the enzymatic activity of caspase 3 (Dirks & Leeuwenburgh, 2004). Interestingly, in an independent study in 33 month old FBN rats, plantaris muscle had age-dependent increase in DNA fragmentation and cytosolic extracts had significant increase in caspase-3 activity (Pistilli *et al.,* 2006a). The differences observed between the studies may be due to differences in rat strains, ages and muscles studied. Furthermore, in the above mentioned studies, aged muscle tissues were homogenized for the different assays. This may dilute any focal accumulation of apoptosis signalling in individual myofibers.

Simultaneous occurrence of apoptosis and necrosis occur in situations such as nutrition deprivation in culture conditions (Malagelada *et al.*, 2005), upon exposure to toxic chemicals, e.g., mustard gas (Heinrich *et al.*, 2009), excitotoxic neuronal death (Portera-Cailliau *et al.*, 1997), oxidative stress in lymphocytes (Behrens *et al.*, 2011) and ischemia reperfusion injury in

cardiac myocytes (Ray *et al.*, 2001), brain and skeletal muscle. Additionally, the form of cell death varies with different concentration of toxic agent, for example, apoptosis is induced at low concentrations of hydrogen peroxide, whereas with high concentrations, necrosis occurs (McConkey, 1998). Alternatively, blocking one mode of cell death may also activate the other type to ensure cell death (Zhang *et al.*, 2009; Nicotera, 1998). This suggests an existence of a broad interconnected spectrum of cell death modes, "apoptosis necrosis continuum" (Zeiss, 2003) rather than separate distinct pathways. Generally, apoptosis occurs first when a large stress signal is received. If no corrective measure is taken by the cell, the stress levels become lethal and the cell becomes necrotic (Soti *et al.*, 2003). Myofibers that are both apoptotic and necrotic are detected in mouse models for Duchenne muscular dystrophy, an X-linked recessive disorder primarily characterized by progressive muscle weakness and wasting (Abmayr *et al.*, 2003). Mutator mice that exhibit extreme muscle wasting had significant apoptotic signalling, suggesting a role of cell death in myofiber loss (Kujoth *et al.,* 2005). In 11 month old mutator mice, 2 months after the onset of muscle mass decline, gastrocnemius and quadricep muscle tissues had increased DNA fragmentation and caspase 3 activity compared to age matched wild type mice (Hiona *et al.*, 2010). These studies support the hypothesis that in aged muscle tissue, cell death pathways may contribute to fiber loss.

Thesis Objectives

Mitochondrial damage has been proposed to be one of the leading cause of aging, playing a significant role in sarcopenia. This study focuses on aged rat quadriceps tissue to determine the

biological impact of enzymatic mitochondrial abnormalities. This research is based on the hypothesis that mitochondrial abnormalities in the electron transport chain (ETC) are a primary source of age-dependent fiber loss. mtDNA deletion accumulate in focal segments of fibers, disrupting the ETC at a threshold of ~90%. ETC abnormal fibers accumulate in an age-dependent manner and are prone to intra-fiber atrophy and fiber breakage **(Figure 1.6)**. Muscles that exhibit the most decline in muscle mass and fiber number exhibit the most burden in ETC abnormalities suggesting that mitochondrial damage plays a significant role in fiber loss.

In this study, I examined adult (12-month) and old (36-month) FBN rat quadriceps muscle. ETC abnormal fibers were only detected in old rats. As ETC abnormal fibers appear focally and segmentally, a serial cross-sectional histological approach was employed. Immunohistochemical analysis was performed to identify apoptotic and necrotic positive fibers. Individual fibers were followed through multiple serial sections to characterize the ETC phenotype and staining for apoptotic and necrotic markers. We hypothesize that ETC abnormal fibers will have increased abundance of apoptotic and necrotic activation.

In addition, I pharmacologically induced ETC abnormal fibers in aged rats using an AMPK activator, guanidinopropionic acid (GPA), to directly test the causal role of ETC abnormalities in inducing fiber loss. We have previously shown that ETC abnormal fibers upregulate mitochondrial bioenergetic proteins suggesting that the cell is responding to an energy deficit. In low intracellular energy levels, AMPK regulates mitochondrial biogenesis and was detected in ETC abnormal segments. We hypothesize that oral GPA treatment will induce acceleration of fiber loss in rat quadriceps. In this study, FBN rats of 30-month old were fed food chow with 1%

GPA *ad libitum* for 4 months. During the treatment regime, the body weight and survival of rats were monitored. At the end of study, quadriceps muscles were extracted and were divided in half. One half was frozen for homogenate analysis and the other half embedded in media for histological and immunohistochemical analysis.

Our studies will delineate a molecular pathway of fiber loss in sarcopenia where mitochondrial dysfunction is the primary source of cell death. Studying mechanisms induced in ETC dysfunctional cells may allow us to identify certain pathways to delay the occurrence of cell death.

Figure 1.1. Necrotic cell death. A necrotic signal such as energy depletion of cellular damage initiates the complement cascade pathway and mediates the lysis of the cell. Transmembrane protein channels are formed on the necrotic cell surface membrane, known as the membrane attack complex (MAC). The complement protein C5 is cleaved by C5 convertase to C5a and C5b. C5b binds to C6, C7 and C8. This complex inserts in the cell membrane. Oligomerized C9 inserts into the complex and spans through the cell membrane to form the membrane pore and a functional MAC. A necrotic cell contains several copies of MAC on its membrane resulting in severe damage to membrane integrity. Influx of Ca2+ and Na+, alteration in ion transport and ATP depletion cause cellular lysis. The complement system triggers inflammation, through C5a which activates macrophages. Macrophages infiltrate the necrotic site and can be visualised by the glycoprotein, CD68, present in their cytoplasm.

Modified from: Cole and Morgan, 2003. Clinical Sciences, 104: 455-466.

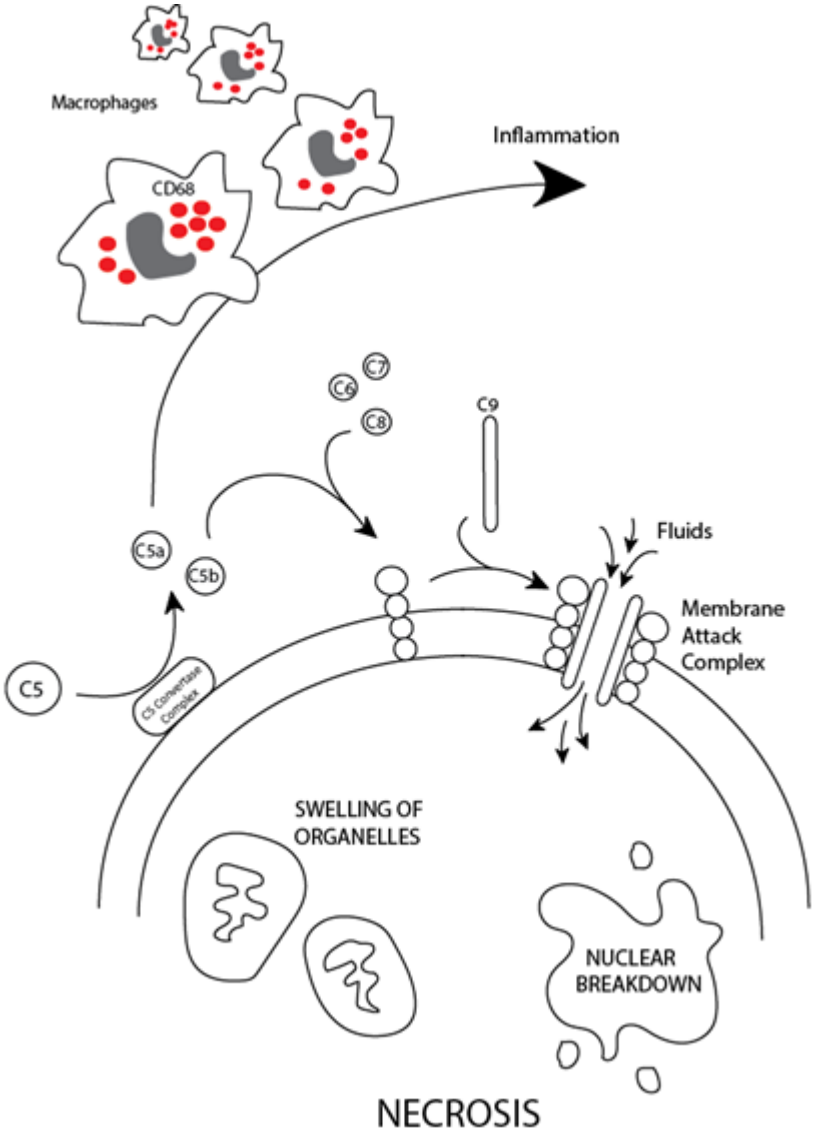
Macrophages
CD68
Inflammation
C6
C7
C8
C9
C5a
C5b
C5
C5 Convertase Complex
Fluids
Membrane Attack Complex
SWELLING OF ORGANELLES
NUCLEAR BREAKDOWN
NECROSIS

Figure 1.2. Molecular pathways of apoptosis. Apoptosis is initiated via intrinsic and extrinsic pathways. The intrinsic pathway is activated upon an intracellular stimuli such as Ca^{2+} overload or an increase in reactive oxygen species (ROS). PUMA (p53 upregulated mediator of apoptosis) is activated resulting in BAX release from Bcl-2. BAX oligomerizes, mediated by truncated Bid, to form the mitochondrial permeability transition pore (mtPTP) resulting in the release of cytochrome c. Cytoplasmic cytochrome c forms the apoptosome activating caspase 9 which activates the effector caspase 3. Caspase 3 activates caspase-dependent DNases (CAD) leading to fragmentation of the nuclear genome. Additionally, caspase 3 cleaves actin binding proteins and actin filaments to ultimately cause disassembly of the cellular structure, membrane blebbing and formation of apoptotic bodies (Porter and Janicke, 1999). The extrinsic apoptotic pathway is initiated at the cell surface membrane by the binding of an extracellular ligand to its specific death receptor. The activated death receptor recruits procaspase 8 via the adaptor protein Fas-associated death domain (FADD). This results in the activation of caspase 8. Activated caspase 8 cleaves full length Bid to mediate Bid-dependent mitochondrial membrane permeabilization (MMP) and directly cleaves procaspase 3 to activate downstream effector caspase 3.

Modified from: Creagh, EM. 2014. Trends in Immunology, 35 (12): 631-640.

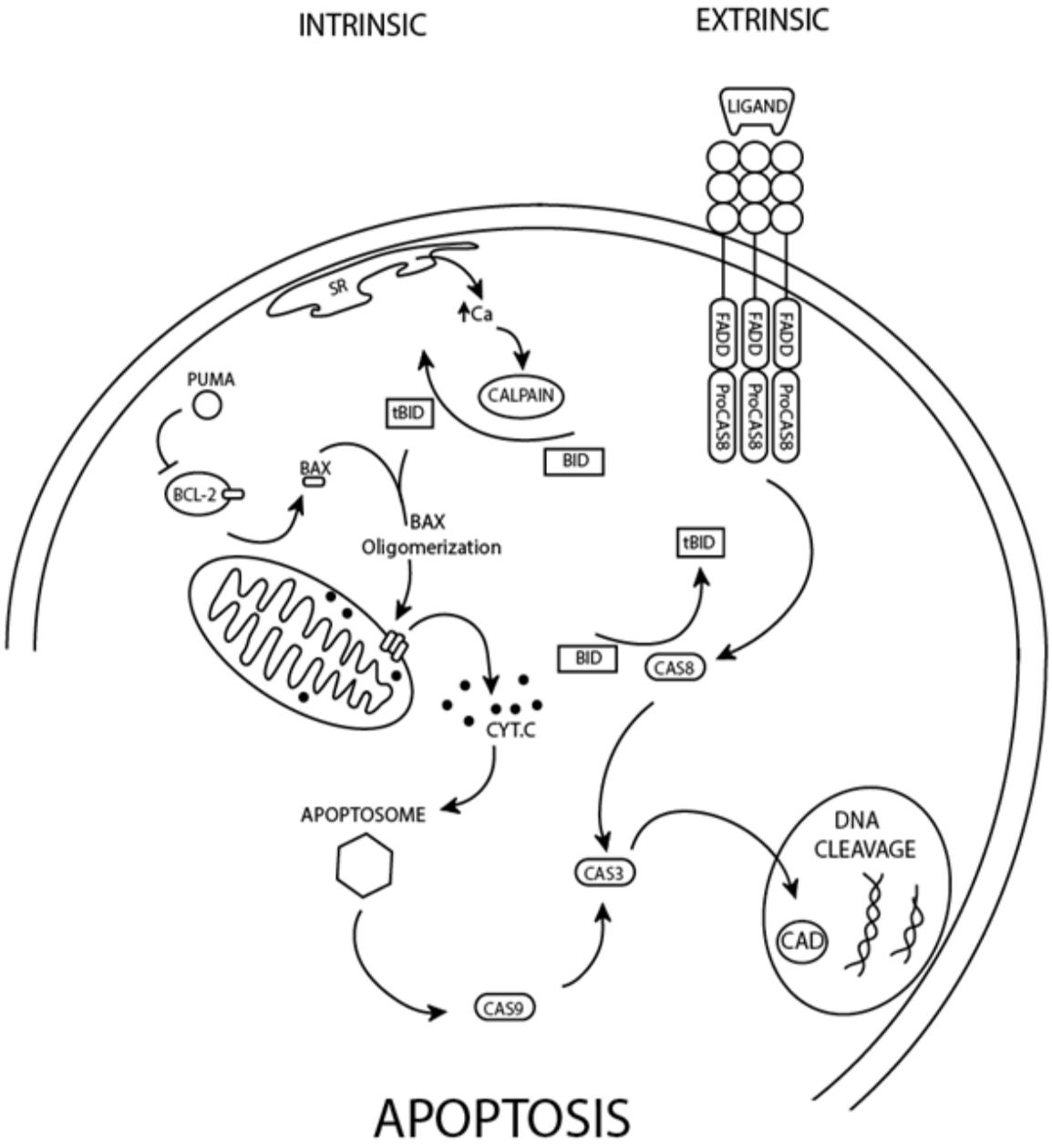
INTRINSIC
EXTRINSIC
LIGAND
FADD
ProCAS8
SR
↑Ca
CALPAIN
PUMA
tBID
BID
BAX
BCL-2
BAX
Oligomerization
tBID
BID
CAS8
CYT.C
APOPTOSOME
DNA
CLEAVAGE
CAS3
CAD
CAS9

APOPTOSIS

Figure 1.3. The electron transport chain. Complex 1: NADH Dehydrogenase, Complex 2: Succinate Dehydrogenase, Complex 3: ubiquinol:cytochrome C Oxidoreductase, Complex 4: Cytochrome C Oxidase (COX), Complex 5: ATP Synthase. NADH donates 2 electrons to Complex 1 which are transferred to an electron carrier, ubiquinone, UQ. Reduced UQ passes electrons from Complex 1 and 2 to Complex 3. Cytochrome c shuttles electrons to complex 4 which reduces oxygen to water. The electron flow is indicated in the dashed black line. The flow of protons is indicated in the solid black line.

Citation: http://www.genome.jp/kegg-bin/show_pathway?map00190

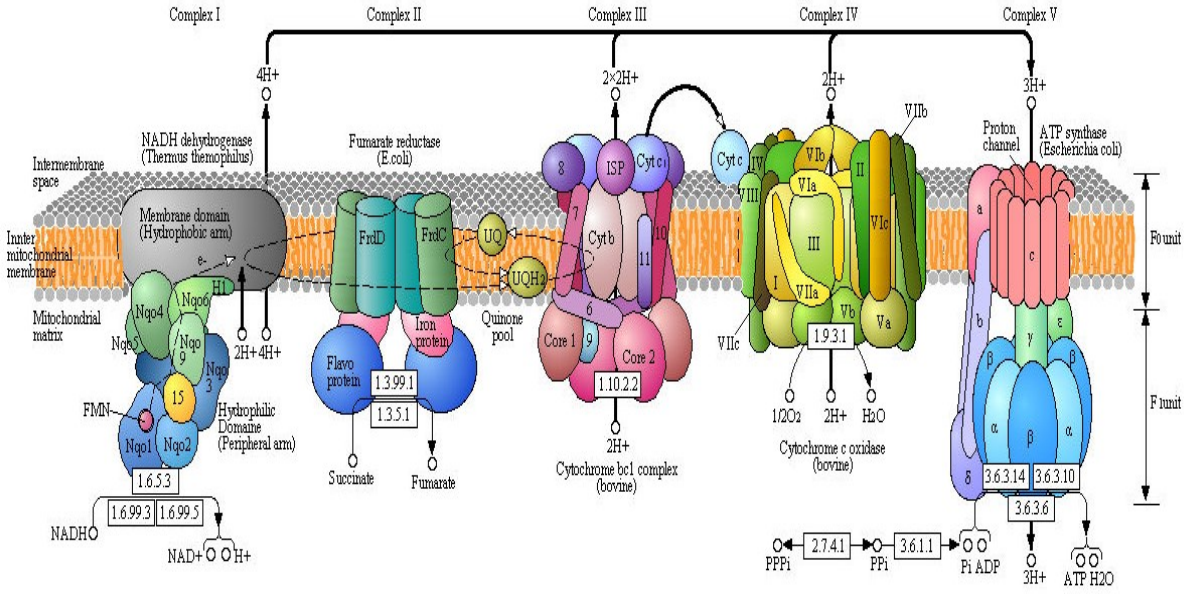
Complex I
Complex II
Complex III
Complex IV
Complex V
4H+
2×2H+
2H+
3H+
NADH dehydrogenase
(Thermus thermophilus)
Fumarate reductase
(E.coli)
Proton
channel
ATP synthase
(Escherichia coli)
Intermembrane
space
Inner
mitochondrial
membrane
Membrane domain
(Hydrophobic arm)
e-
H+
Mitochondrial
matrix
Nqo4
Nqo6
Nqo5
Nqo
9
Nqo
3
1S
FMN
Nqo1
Nqo2
Hydrophilic
Domaine
(Peripheral arm)
2H+ 4H+
1.6.5.3
1.6.99.3
1.6.99.5
NADH
NAD+
H+
FrdD
FrdC
UQ
UQH2
Flavo
protein
Iron
protein
1.3.99.1
1.3.5.1
Succinate
Fumarate
Quinone
pool
8
ISP
Cyt c1
7
Cyt b
10
11
6
9
Core 1
Core 2
1.10.2.2
2H+
Cytochrome bc1 complex
(bovine)
Cyt c
IV
VIIb
VIb
VIa
II
VIII
III
VIc
I
VIIa
Vb
Va
VIIc
1.9.3.1
1/2O2
2H+
H2O
Cytochrome c oxidase
(bovine)
a
c
b
ε
γ
β
α
δ
3.6.3.14
3.6.3.10
3.6.3.6
Fo unit
F1 unit
PPPi
2.7.4.1
PPi
3.6.1.1
Pi ADP
3H+
ATP H2O

Figure 1.4. The rat mitochondrial DNA. The mitochondrial DNA is a double stranded circular genome, 16,300 basepairs in length that encodes 22 transfer RNAs (white bars), 2 ribosomal RNAs (yellow bars) and 13 complex subunits of the electron transport chain (colored bars). D-Loop refers to the non-coding region and is at the site of the origin of replication of the heavy strand (O_H). The light strand origin of replication is located between the ND2 and COX1 genes (O_L). The minor arc in the mitochondrial genome is the regions between the O_H and O_L and spans the 12S rRNA to ND2 region. The major arc in the genome is the region between Cyt b and COX1. The arrows demonstrate the distribution of mtDNA deletion breakpoints in 29 ETC abnormal skeletal muscle fibers. Arrowheads on the inner edge of the circle denote the 5' deletion breakpoints. Arrowheads on the outer edge of the circle represent the 3' deletion breakpoint.

Citation: Cao *et al.,* 2001. Nucl. Acids Res. 29 (21):4502-4508.

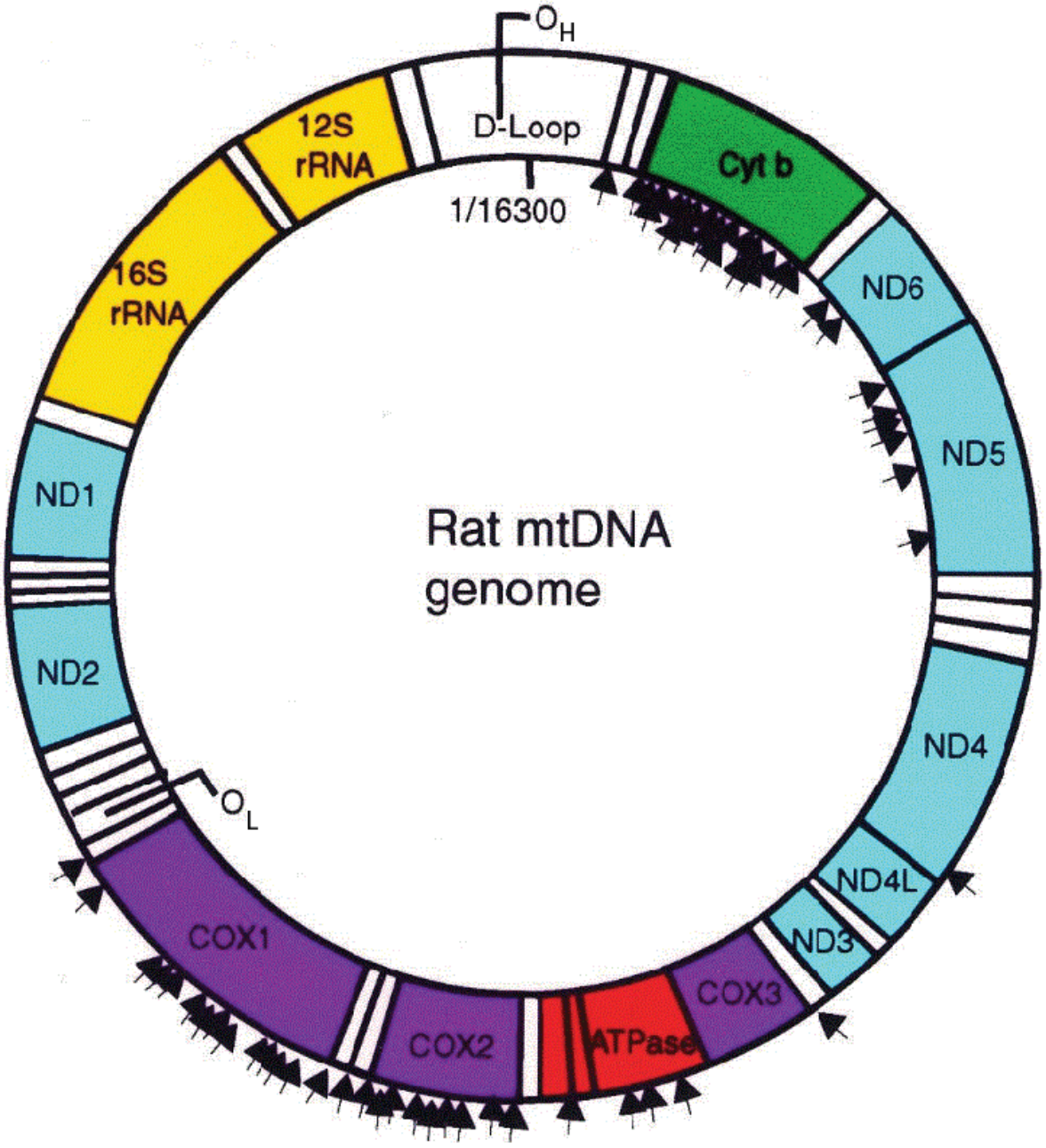
O_H
D-Loop
1/16300
12S rRNA
16S rRNA
Cyt b
ND6
ND5
ND1
Rat mtDNA genome
ND2
ND4
O_L
ND4L
ND3
COX1
COX3
COX2
ATPase

Figure 1.5. Accumulation of unique mtDNA deletion in skeletal muscle fiber disrupts ETC function. (A) Serial micrographs staining for cell morphology with H & E and enzymatic activities for COX and SDH. The ETC abnormal region extends for over 700µm and includes a 250µm region where the fiber has ruptured and cannot be detected. The scale bar is 25µm. (B) Digital reconstruction of fiber where the color denotes the ETC abnormal phenotype, red is COX−/SDH++ and orange is COX−/SDHnormal. (C) Percentage of mtDNA genomes that contain a deletion along the length of the abnormal fiber. The same mtDNA deletion mutation is detected across the broken fiber region and the highest levels (>99%) of mutation are found immediately flanking the fiber break.

Citation: Herbst *et al.,* 2007. J Gerontol A Biol Sci Med Sci. 62(3): 235–245.

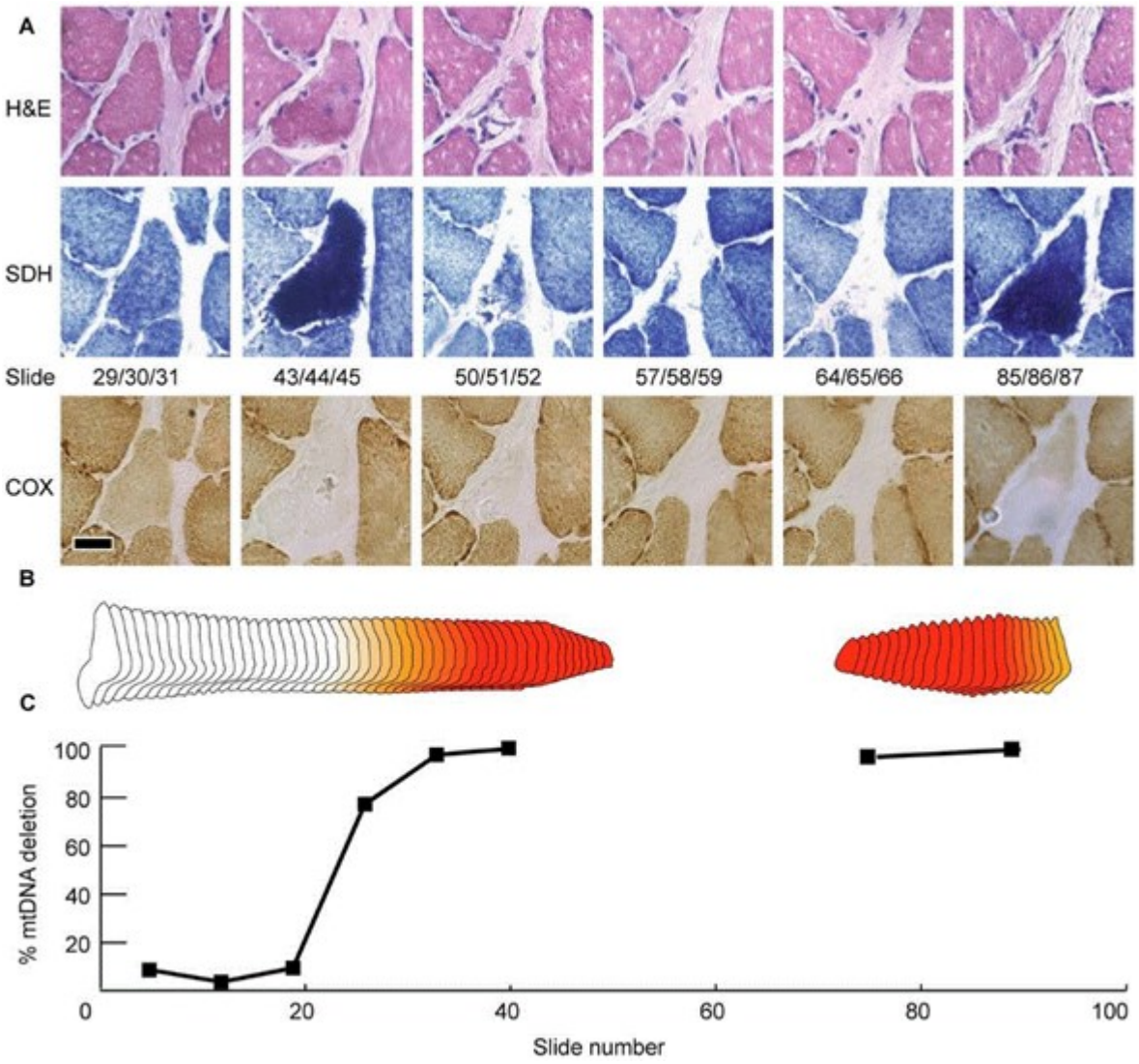
A
H&E
SDH
Slide
29/30/31
43/44/45
50/51/52
57/58/59
64/65/66
85/86/87
COX
B
C
% mtDNA deletion
100
80
60
40
20
0
20
40
60
80
100
Slide number

Figure 1.6. Model of fiber loss in aged skeletal muscle. (A) In young skeletal muscle, fiber bundles are healthy. (B) Age-dependent accumulation of mtDNA deletion occurs and ETC phenotype is disrupted when deleted genomes are >90% of the total mitochondrial genomes. (C) The abnormal segment expands to become (D) atrophic and (E) break.

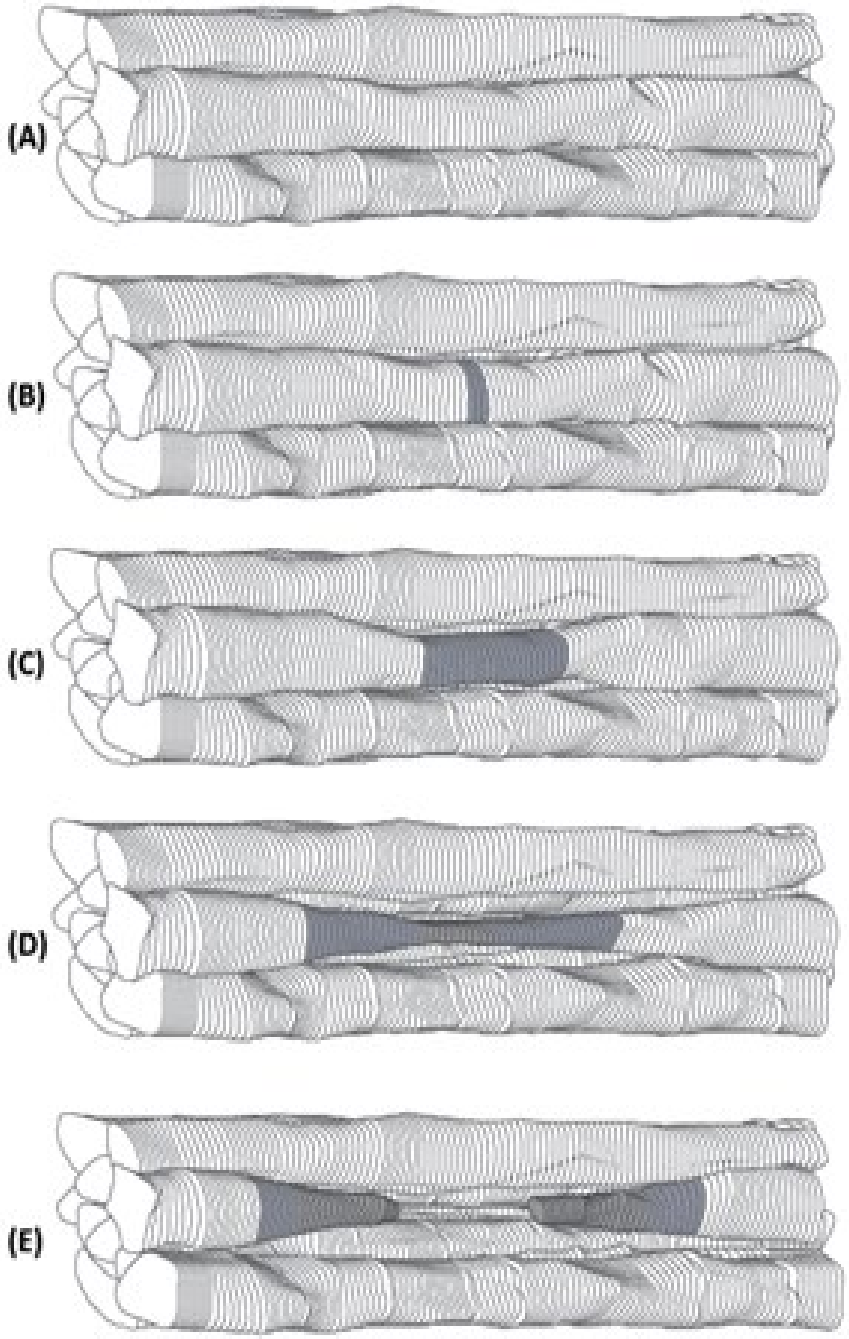
(A)
(B)
(C)
(D)
(E)

Chapter 2

The data in this chapter have been published in:

Nashwa Cheema, Allen Herbst, Debbie McKenzie and Judd M. Aiken (2015) Apoptosis and Necrosis Mediate Skeletal Muscle Fiber Loss in Age-Induced Mitochondrial Enzymatic Abnormalities. *Aging Cell* 14(6): 1085-1093.

Abstract

Sarcopenia, the age-induced loss of skeletal muscle mass and function, results from the contributions of both fiber atrophy and loss of myofibers. We have previously characterized sarcopenia in FBN rats, documenting age-dependent declines in muscle mass and fiber number along with increased fiber atrophy and fibrosis in vastus lateralis and rectus femoris muscles. Concomitant with these sarcopenic changes is an increased abundance of mitochondrial DNA deletion mutations and electron transport chain abnormalities. In this study, we used immunohistological and histochemical approaches to define cell death pathways involved in sarcopenia. Activation of muscle cell death pathways was age-dependent with most apoptotic and necrotic muscle fibers exhibiting electron transport chain abnormalities. Although activation of apoptosis was a prominent feature of electron transport abnormal muscle fibers, necrosis was predominant in atrophic and broken ETC abnormal fibers. These data suggest that mitochondrial dysfunction is a major contributor to the activation of cell death processes in aged muscle fibers. The link between electron transport chain abnormalities, apoptosis, fiber atrophy and necrosis supports the hypothesis that mitochondrial DNA deletion mutations are causal in myofiber loss. These studies suggest a progression of events beginning with the generation and accumulation of a mtDNA deletion mutation, the concomitant development of ETC abnormalities, a subsequent triggering of apoptotic and, ultimately, necrotic events resulting in muscle fiber atrophy, breakage and fiber loss.

Introduction

Sarcopenia, the involuntary loss of skeletal muscle mass and function with age (Rosenberg, 1997), contributes significantly to frailty and causes a decline in quality of life. In humans, 30% of the muscle mass is lost between 20 to 80 years of age (Frontera *et al.*, 2000). The muscle mass decline observed in sarcopenia is due to fiber atrophy and loss (Lexell *et al.*, 1986). There are several proposed mechanisms for the decline of muscle mass including altered satellite cell function (Gallegly *et al.*, 2004), decreases in motor unit number (Roos *et al.*, 1997), changes in hormone levels (Visser *et al.*, 2003), accumulation of mitochondrial DNA deletions (Wanagat *et al.*, 2001) and loss of myocytes via apoptosis (Dupont-Versteegden, 2005).

Myofiber loss is an important component of sarcopenia yet the cell death pathways involved in the process are not known. There are similarities in the apoptotic pathways in post-mitotic multinucleated skeletal muscle and mononuclear mitotic cells, including cellular/nuclear shrinkage and activation of caspase 3 (McArdle *et al.*, 1999). In multinucleated myofibers, however, individual nuclei decay and cellular apoptosis occurs segmentally over an extended period of time (Dupont-Versteegden, 2005). The mitochondrion is an important regulatory centre for cell fate decisions as it sequesters factors that, upon release, lead to initiation of apoptosis. Mitochondrial-mediated apoptosis involves the Bcl-2 family members which mediate release of cytochrome c, AIF and Endo G into the cytosol as well as subsequent caspase activation. PUMA (P53 up-regulated modulator of apoptosis) and Bid are key apoptotic factors of the Bcl-2 family. Caspase 8 cleaves Bid, generating tBid, which is then translocated to the mitochondria to promote release of cytochrome c (Dirks & Leeuwenburgh, 2005). Similarly,

PUMA is translocated to the mitochondria in response to p53 stress where it promotes apoptosis by inhibiting anti-apoptotic proteins (Yee & Vousden, 2008).

Numerous lines of evidence suggest an involvement of apoptosis in myocyte loss. Down-regulation of the apoptotic pathway can reduce the decline in muscle mass and function in aged animals (Dirks & Leeuwenburgh, 2004; Marzetti *et al.*, 2009). Up-regulation of the apoptotic pathway has been identified in premature aging models including mice lacking the antioxidant enzyme copper/zinc-dependent superoxide dismutase (CuZnSOD or Sod1) that exhibit accelerated sarcopenia (Jang *et al.*, 2010), as well as interleukin 10-deficient mice that exhibit extreme frailty (Walston *et al.*, 2008). Increased levels of DNA laddering and caspase 3 activity have been observed in transgenic mice expressing defective mitochondrial polymerase (Hiona *et al.*, 2010).

Apoptosis occurs in muscle myonuclei as evidenced by observation of DNA strand breaks and expression of pro-apoptotic proteins Bax, caspase 3, AIF and APAF-1, reviewed in (Alway *et al.*, 2011). In human muscle biopsies, increased levels of TUNEL positive nuclei have been detected (Strasser *et al.*, 1999; Malmgren *et al.*, 2001; Whitman *et al.*, 2005). An increase in caspase 3 levels was not, however, detected (Whitman *et al.*, 2005). These studies are homogenate-based with only one study, in 26-month F344 rats, (Dirks & Leeuwenburgh, 2004) detecting increased levels of cleaved caspase 3, the active form of the effector caspase.

Cellular necrosis is a second significant mechanism of cell death. Prominent features of necrosis are ATP depletion, loss of ion homeostasis and membrane polarity leading to rapid swelling of the cell, membrane rupture and subsequent release of cellular contents. Necrosis is neither

organized nor executed in a similar manner to apoptosis and cell death is a consequence of irreparable damage (Henriquez *et al.*, 2008). Necrosis, therefore, frequently occurs during pathological conditions including stroke, ischemia and neurodegenerative disorders (Syntichaki *et al.*, 2002; Malhi *et al.*, 2006; Henriquez *et al.*, 2008). Inflammation is associated with necrosis and not with apoptotic cell death (Scaffidi *et al.*, 2002). The complement system, a major component of innate immunity, responds to inflammation (Carroll, 2004). Activation of the complement cascade leads to assembly of terminal components and insertion of the C5b-9 membrane attack complex (MAC) into the lipid bilayer of the plasma membrane. Assembly of MAC complexes results in the formation of transmembrane channels, loss of membrane integrity (Bhakdi & Tranum-Jensen, 1978), leakage of intracellular contents and macrophage infiltration to the site of inflammation (Kharraz *et al.*, 2013).

There is a considerable body of evidence suggesting a mitochondrial involvement in age-dependent muscle fiber loss. Mitochondrial DNA (mtDNA) deletion mutations increase in abundance with age (Müller-Höcker, 1989; Chung *et al.*, 1996; Aspnes *et al.*, 1997). Accumulation of myofibers with deletion mutations in the mitochondrial genome are linked to the decline in muscle mass observed in sarcopenia (Lee *et al.*, 1998; Wanagat *et al.*, 2001; Bua *et al.*, 2008). In line with the segmental decay observed in multinucleated fibers, mtDNA deletions are not distributed homogeneously but accumulate focally in individual cells appearing in a segmental pattern along the length of fibers, resulting in a mosaic distribution between fibers (Wanagat *et al.*, 2001). Focal accumulation of mtDNA deletion mutations, within individual fibers, to a threshold value of ~90% or more results in disruption of the electron

transport chain (ETC) (Bua *et al.*, 2006; Herbst *et al.*, 2007). There is an increase, with age, in accumulation of ETC abnormal fibers in sarcopenic muscles of rhesus macaques, humans and rats (Lee *et al.*, 1998; Pesce *et al.*, 2001; Bua *et al.*, 2002). In 38-month old rats, an estimated 15% of the rectus femoris muscle fibers contained regions of severely compromised mitochondrial function (Wanagat *et al.*, 2001).

To understand the role of apoptosis and necrosis in aged muscles, we used a histological approach to localize cell death event to individual muscle fibers. Five diverse markers of apoptosis and necrosis were examined, each having differential specificity to these processes. Bid truncation is an early event of apoptosis but does not necessarily dictate an apoptotic fate. PUMA, known to be transcriptionally activated in ETC abnormal fibers (Herbst *et al.*, 2013), is a transcriptional response to p53 activation and influences Bid truncation by binding to Bcl-2 and inducing membrane permeability transition pore formation. By contrast, activation of caspase 3 is typically considered a committed step of apoptosis and directs proteolytic cleavage of cellular components. Two markers of necrosis were chosen encapsulating the loss of membrane polarity (C5b-9) as well as the proinflammatory response of macrophages to the necrotized fiber (CD68). Each of these markers of cell death indicates different stimuli, responses and progression which collectively help to define the cell fate decision and outcome.

By localizing the activation, execution and characteristics of cell fate effector pathways to individual muscle fibers, we show that the predominant cause of cell death pathway activation in aged rat muscle is mitochondrial abnormalities. Mitochondrial abnormalities accumulate in

an age-dependent manner, initiate apoptotic and necrotic mechanisms as the dysfunctional region elongates and thus contribute to fiber atrophy and fiber loss in sarcopenia.

Results

Sarcopenic change in aged rats

As previously observed, there is a loss of muscle mass in the quadriceps of aged rats. In this study, 12-month rat quadriceps mass averaged 8.5 $\pm$ 0.15 g while 36-month rat quadriceps weighed 4.6 $\pm$ 0.23 g. As expected, fiber loss was also evident with the rectus femoris of 36-month old rats averaging 6484 $\pm$ 477 fibers compared to 12- month old rats with an average of 9169 $\pm$ 447 fibers.

Activation of cell death pathways is increased in the quadriceps of aged rats

To determine the abundance of individual muscle fibers undergoing cell death, immunohistochemical analysis was performed on adult (12-month) and aged (36-month) rat quadriceps muscles using markers indicative of apoptosis (truncated form of Bid (tBid), PUMA, cleaved caspase 3 (cl-Cas3) and necrosis (C5b-9 and CD68) **(Figure 2.1A).** Fibers that stained positive for any cell death marker at a 100 µm interval were counted, annotated and followed throughout the 1 mm of tissue. In the aged rectus femoris, there is a significant increase in the fraction of fibers positive for cl-Cas3 ($p = 0.03$), C5b-9 ($p = 0.02$) and CD68 ($p = 0.03$) **(Table 2.1).**

In the 36-month old rat quadriceps, there is a significant 8-fold (p =0.047) and 9-fold (p=0.048) increase in the number of fibers staining positive for C5b-9 and CD68, respectively, compared to the 12-month rat. There is also a trend toward an increase in the numbers of myofibers positive for tBid and cl-Cas3 with a 3-fold difference observed in aged rats **(Figure 2.1B).**

Cell death markers localize to ETC abnormal regions

To ascertain the involvement of mitochondrial enzymatic abnormalities in age-induced cell death processes, we stained tissue sections for COX and SDH activities. Mitochondrial enzyme activities were followed at 100µm intervals for 1,000µm to define the mitochondrial ETC phenotype. Within the 1mm of quadriceps sectioned and assayed from the 36 month old rat, 39 ETC abnormal (COX^-/SDH^{+++} phenotype) fibers were identified. No ETC abnormal fibers were observed in the 12-month old rat quadriceps samples **(Figure 2.2A).** We found a strong linkage between the regions of fibers positive for cell death markers and mitochondrial enzymatic abnormalities. 42% of myofibers positive for tBid, 45% of myofibers positive for PUMA, 69% of myofibers positive for cl-Cas3, 86% of myofibers positive for C5b-9 and 78% myofibers positive for CD68 were ETC abnormal **(Figure 2.2B).** This suggests that the significant increases in cl-Cas3, C5b-9 and CD68 positive fibers in aged rectus femoris **(Table 2.1)** are predominantly ETC abnormal fibers. A digital reconstruction of a representative COX^- and SDH^{+++} fiber from an aged rat illustrates the linkage between cell death pathway activation and the ETC abnormal region **(Figure 2.2C, 2.2D).**

Approximately half (42%) of the ETC abnormal fibers were positive for apoptotic and/or necrotic markers. 10% of the ETC abnormal fibers were positive for only apoptotic markers. A majority of these fibers immunostained for all three apoptotic markers (tBid, PUMA and cl-Cas3). 32% of the ETC abnormal fibers were positive for both apoptosis and necrosis with 37% staining positive for all five markers of apoptosis and necrosis **(Figure 2.3).**

ETC abnormality length is positively correlated with cell death pathway activation

Our histological approach, the sectioning of one hundred consecutive 10 micron sections, permitted measurement of ETC abnormal region length. We previously demonstrated that the length of ETC abnormal regions in an aged muscle fiber varies; fibers with longer ETC abnormalities being more prone to atrophy and fiber breakage (Bua, 2004). Fibers positive for cell death markers have significantly longer ETC abnormality lengths with a range of 200-1200 µm whereas fibers that did not immunostain with any cell death marker have shorter ETC abnormalities (range of 100-400 µm, **Figure 2.4A).** Myofibers positive for tBid exclusively and fibers positive for both tBid and PUMA had the shortest ETC abnormal regions. The range of ETC abnormality length for tBid positive fibers was 200-300 µm. tBid and PUMA positive fibers had an ETC abnormality length of 200-400 µm. Fibers positive for all 3 apoptotic markers, tBid, PUMA and cl-Cas3, had an ETC abnormality length of 200 -500 µm. Fibers staining for tBid, PUMA, cl-Cas3 and C5b-9 had an ETC abnormality length of 300-600 µm. ETC abnormal fibers positive for all apoptotic and necrotic markers (tBid, PUMA, cl-Cas3, C5b-9 and CD68) had the

longest ETC abnormal regions. All ETC abnormal fibers (n = 6 fibers) with an abnormality length of >600 μm were positive for all cell death markers **(Figure 2.4B)**.

ETC abnormality intra-fiber atrophy is positively correlated with cell death pathway activation

The cross-sectional area ratios (CSAR) of individual fibers were calculated and graphed to generate an intra-fiber atrophy profile. A CSAR value of 0 indicates fiber breakage and a value ≥1 indicates an absence of atrophy (Bua *et al.*, 2002). Significantly less atrophy was observed in ETC normal fibers of 12- and 36-month rats than in ETC abnormal fibers of 36-month rats **(Figure 2.5A)**. ETC abnormal fibers positive for cell death markers have a significant increase ($p=0.0016$) in intra-fiber atrophy with an average CSAR of 0.6 compared to ETC abnormal fibers that are negative for cell death, which have an average CSAR of 1 **(Figure 2.5B).** Atrophic and broken ETC abnormal fibers were consistently positive for apoptosis and necrosis**,** indicating that cell death pathway activation mediates fiber breakage and loss.

Fibers positive for cl-Cas3, C5b-9 and CD68 exhibited more intra-fiber atrophy. The average CSAR of fibers positive for tBid, PUMA and cl-Cas3 was 0.627±0.329. If C5b-9 is involved, the average CSAR was 0.457±0.169 and with CD68 the average CSAR was 0.544±0.234. Atrophy was not evident in fibers positive exclusively for tBid or tBid and PUMA. Furthermore, fiber breakage events within the ETC abnormal region were not detected when atrophy was not

present **(Figure 2.5C).** All broken fibers were positive for cl-Cas3, C5b9 and/or CD68 suggesting that these markers were involved in the terminal stage of ETC abnormal fibers.

Discussion

The decline in fiber number in the aged rat cohorts used in this study is consistent with previous observations (Wanagat *et al.*, 2001; Bua *et al.*, 2008). Numerous studies document increased cell death in aged skeletal muscle (Dirks & Leeuwenburgh, 2004; Marzetti *et al.*, 2009), reviewed by Alway (Alway *et al.*, 2011). Electron transport chain abnormalities also accumulate with age and are concomitant with fiber atrophy and fiber breakage (Lee *et al.*, 1998; Bua *et al.*, 2002; Bua *et al.*, 2006). The linkage between cell death processes and ETC abnormal fiber have not, however, previously been explored.

Apoptosis and necrosis in aged skeletal muscle fibers

Using a cell-by-cell scanning approach, we detected a significant increase in fibers positive for cleaved caspase 3 and necrosis markers within a subset of individual muscle fibers in aged rat quadriceps. Although previous studies have looked for activation of apoptosis in aged skeletal muscle, altered caspase activity has not been demonstrated with age (Dirks & Leeuwenburgh, 2004; Alway *et al.*, 2011). These studies were homogenate-based and, therefore, unable to discriminate between focal activation of apoptosis in a subset of muscle fibers versus a more generalized pro-apoptotic environment.

Necrotic fibers activate the complement system to assemble the C5b-9 membrane attack complex. This assembly of complement components occurs primarily in early stages of necrosis (Gaipl *et al.*, 2001) and allows for macrophage infiltration into the damaged fiber. We observed a significant increase in the number of fibers positive for necrosis markers (C5b-9 and CD68) in aged skeletal muscle. Fibers with ETC abnormalities were especially prone to necrosis. Our data suggest that cleaved caspase 3, C5b-9 and CD68 positive fibers are prevalent in the rectus femoris of aged rats and contribute to the age-dependent loss of myofibers. Furthermore, ETC abnormal fibers that are atrophic exhibit a significant increase for apoptotic and necrotic markers in the abnormal region.

Progression of Cell Death in Aged Muscle Fibers

Both apoptotic and necrotic cell death markers exhibited an age-dependent accumulation and segmental distribution in rat skeletal muscle. The majority of cell death marker positive regions were also concomitant with mitochondrial enzymatic abnormalities. This finding was unexpected because sarcopenia is generally considered to be multi-factorial. This observation led us to characterize cell death processes in ETC abnormal fibers and we determined that 42% of ETC abnormal fibers in aged quadriceps were positive for cell death markers. The length of ETC abnormalities varied from fiber to fiber. In general, fibers with small regions of ETC abnormalities were negative for markers of cell death. Longer ETC abnormal regions were more prone to fiber atrophy and exhibited high levels of staining for cell death markers. Furthermore, fibers positive for both apoptosis and necrosis markers are more likely to be ETC abnormal, providing strong evidence that majority of the cell death events are triggered by ETC

abnormalities. Fiber breakage was only observed in fibers undergoing both apoptosis and necrosis. Our data indicate that fiber loss observed in sarcopenia is due to the accumulation of ETC abnormalities and subsequent activation of apoptotic and necrotic pathways.

There is a correlation between the length of the ETC abnormality and cell death marker. For example, ETC abnormal fibers that did not stain positive for cell death markers tended to be of short length (100 - 400 μm), regions positive for tBid (while not staining for other cell death markers) were less than 300 μm, fibers positive for tBid and Puma were less than 400 μm. Fibers positive for tBid, PUMA and cl-Cas3 had a maximum length of 500 μm, with tBid, PUMA, cl-Cas3 and C5b-9 positive fibers at 600 μm while fibers positive for all five cell death markers were present in the longest ETC abnormal region, 1200 μm. These studies suggest a progression of cell death marker activation in ETC abnormal fibers with ETC abnormal regions initially not linked to cell death markers, as the ETC abnormality progressively expands, apoptosis markers (tBid, PUMA, cleaved caspase 3) are observed and finally, with the longer ETC abnormalities, necrosis markers (C5b-9 and CD68).

Proposed model of fiber loss

We have previously proposed a model of muscle fiber loss with age. The process begins with the generation and subsequent clonal accumulation of a mitochondrial DNA deletion mutation within an affected muscle fiber. The accumulation of deletion mutation-containing mtDNA genomes results in the loss of cytochrome c oxidase activity and the generation of numerous cellular responses. In this manuscript, we demonstrate that both apoptotic and necrotic responses occur with necrosis being tightly linked to fiber atrophy/fiber breakage. In the

regions of myofibers with mitochondrial dysfunction, activation of apoptosis is followed by necrosis. All breakage events are predominantly located within the ETC abnormal region, were positive for necrosis markers, suggesting that necrosis is responsible for fiber loss. We detected ~70-80% of the total apoptotic and necrotic fibers in aged rat quadriceps to be ETC abnormal further supporting the hypothesis that mtDNA deletions and the resultant mitochondrial enzymatic abnormalities play a causal role in the etiology of sarcopenia.

Methods

Tissue preparation

Adult 12-month (n=5) and aged 36-month (n=5) old male Fischer 344 x Brown Norway F1 hybrid rats were purchased from the National Institute on Aging colony maintained by Harlan Sprague Dawley (Indianapolis, IN). Animals were euthanized, the quadriceps muscles dissected from the animals, bisected at the midbelly, embedded in optimal cutting temperature compound (Sakura Finetek, Torrance, CA), flash frozen in liquid nitrogen and stored at -80°C. A minimum of one hundred 10µm thick consecutive transverse cross sections were cut with a cryostat at -20°C and placed on probe-on-plus slides. Slides were stored at -80°C until needed.

Immunohistochemistry and histochemistry

At 100µm intervals, the fifth, sixth, seventh, eighth and ninth tissue slides were fixed overnight in 10% buffered formalin. Antigens were retrieved by boiling in 10mM citrate buffer, pH 6.0. Slides were blocked in TBS-T containing 5% goat serum. Slides were incubated with primary

antibodies in blocking solution overnight, followed by TBS-T washes. Biotinylated goat anti-rabbit IgG (1:200) and avidin-peroxidase enzyme complex (1:50) from VECTASTAIN® ABC Kit were used according to the manufacturer's specification (Vector Laboratories). DAB was used for chromogenic detection. Primary antibodies used were rabbit anti-activated caspase 3 1:200 (Promega, Madison, WI), rabbit anti-PUMA 1:200 (Abcam, Cambridge, MA), rabbit anti-truncated Bid 1:200 (EMD Chemicals Inc., San Diego, CA), rabbit anti-C5b-9 1:500 (Abcam, Cambridge, MA), and rabbit anti-CD68 1:1000 (Abcam, Cambridge, MA). At 100 µm intervals, the first tissue slide was stained for COX, the second for SDH as previously described (Wanagat *et al.*, 2001). The third slide was dual stained, first for COX and secondly for SDH. Two slides within the series were used for haemotoxylin and eosin (H&E) staining. After histochemistry or immunohistochemistry, the slides were digitally scanned in the microscope (Nanozoomer, Hamamatsu). Individual muscle fibers were followed throughout the 1mm of tissue. Fibers positive for cell death markers and ETC abnormalities (COX^-/SDH^{+++}) were identified and annotated.

Measurements of cross-sectional area ratio, ETC abnormality and cell death region length

Cross-section area (CSA) of randomly selected individual ETC normal and ETC abnormal muscle fibers were measured throughout the 1,000µm using the Nanozoomer Digital Pathology imaging software. The minimum CSA value in the ETC abnormal region was divided by the average value of the fiber CSA in the ETC normal region within the same fiber. In ETC normal fibers, the ratio between minimum CSA and average CSA was determined. The CSA ratios of ETC abnormal and normal fibers were plotted on a histogram. The length of ETC abnormality was

determined by counting the number of slides the abnormality appeared in and multiplying by 10μm. Fibers that were ETC abnormal at the 100th slide were followed beyond 1,000μm until the fibers turned normal. Fibers that immunostained for each of the markers were annotated and followed throughout the 1,000μm. The length of cell death positive region was determined by counting the number of slides the staining was positive and multiplying by 10μm.

Statistical analysis

Data were presented as mean ± sem for 5 aged and adult rats. Three aged rats were used when analyzing length and atrophy of ETC abnormal fibers. All statistical analysis was performed using GraphPad Prism version 5.00 for Windows (GraphPad Software, San Diego California USA). Student's t-tests were performed for all analysis with a P-value < 0.05 being significant. A Welch's t-test was performed on analysis of length of ETC abnormality to correct for unequal variance between the two data sets (**Figure 2.4A**). To measure significant variance **(Figure 2.5A)**, F-tests were performed for fiber atrophy analysis. To calculate percent of incidences, 125 immunopositive fibers were analyzed in Figure 2B and 161 ETC abnormal fiber were analyzed in Figure 3.

Author Contributions

The experiments were designed by all authors. All experiments were performed by NC. Manuscript was prepared by NC and edited by AH, DM and JA.

Figure 2.1. Detection of myofiber cell death in the quadriceps of 12- and 36-month old rats. A) Representative micrographs containing a fiber positive for cell death. The tissue sections were stained with Haematoxylin and Eosin or immunostained using antibodies against truncated form of Bid, PUMA, cleaved caspase 3, C5b-9, CD68. The scale bar is 25 µm. B) Number of fibers per 1000 µm of tissue analyzed that stained positive for the cell death markers in 12- and 36-month rat quadriceps. Data presented in mean ± SEM.

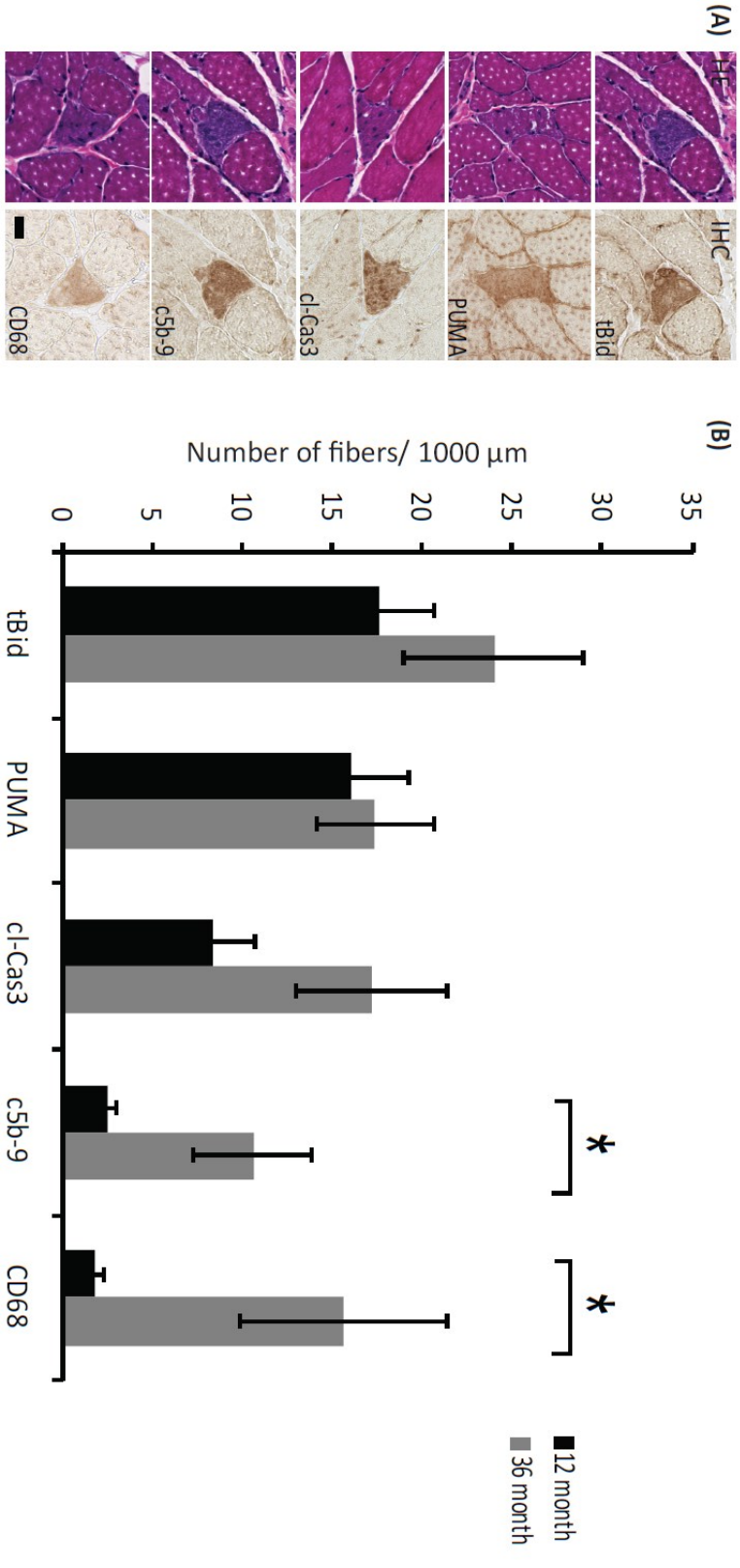
(A)
H&E
IHC
tBid
PUMA
cl-Cas3
c5b-9
CD68
(B)
Number of fibers/ 1000 µm
0
5
10
15
20
25
30
35
tBid
PUMA
cl-Cas3
c5b-9
CD68
*
*
12 month
36 month

Figure 2.2. Myofiber cell death in ETC abnormal fibers of 36-month old rats. A) Abundance of ETC abnormal fibers per 1,000 micron analyzed in the quadriceps of 12- and 36-month old rats. No ETC abnormal fibers were detected in 12-month old rats. Data presented in mean ± sem. B) The percent of ETC enzymatic phenotype of myofibers positive for apoptotic and necrotic markers in the rectus femoris of aged rats. C) Representative ETC abnormal fiber undergoing cell death. Micrographs of histochemical staining for COX and SDH activity and immunostaining with antibodies to cleaved caspase 3, C5b-9 and CD68 are presented. The scale bar is 25 μm. D) Digital reconstruction of the fiber in panel C). The red region indicates the ETC abnormal region and the yellow region depicts transition area within the fiber. Increased staining for cleaved caspase 3, C5b-9 and CD68 is depicted in blue, green and brown respectively.

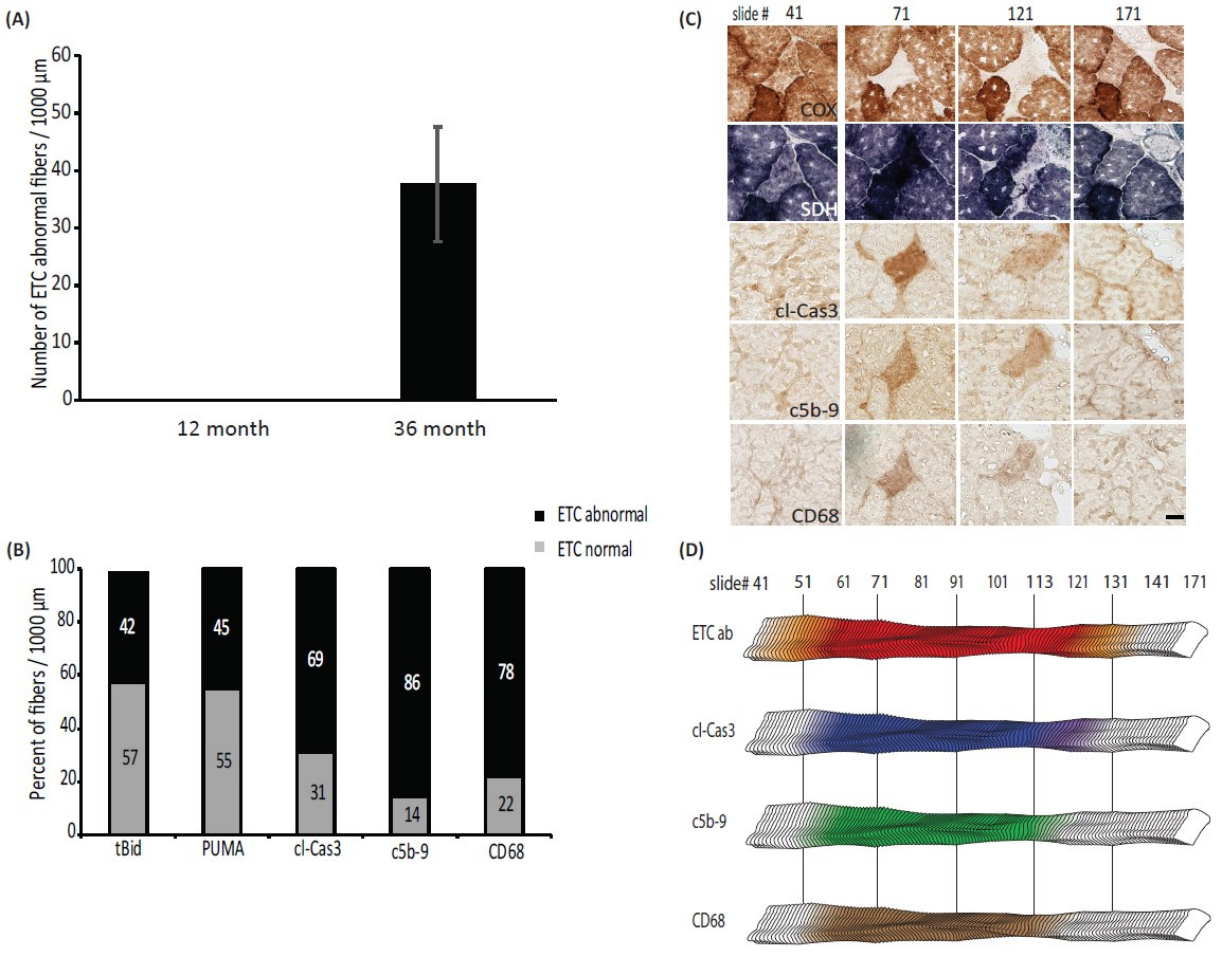
(A)
Number of ETC abnormal fibers / 1000 µm
60
50
40
30
20
10
0
12 month
36 month
(B)
ETC abnormal
ETC normal
Percent of fibers / 1000 µm
100
80
60
40
20
0
42
57
45
55
69
31
86
14
78
22
tBid
PUMA
cl-Cas3
c5b-9
CD68
(C)
slide # 41
71
121
171
COX
SDH
cl-Cas3
c5b-9
CD68
(D)
slide# 41
51
61
71
81
91
101
113
121
131
141
171
ETC ab
cl-Cas3
c5b-9
CD68

Figure 2.3. Prevalence of cell death in ETC abnormal fibers in 36-month old rat. The percent of ETC abnormal fibers from quadriceps of 36-month old rats that were positive for 1 or more cell death marker in the different combinations detected.

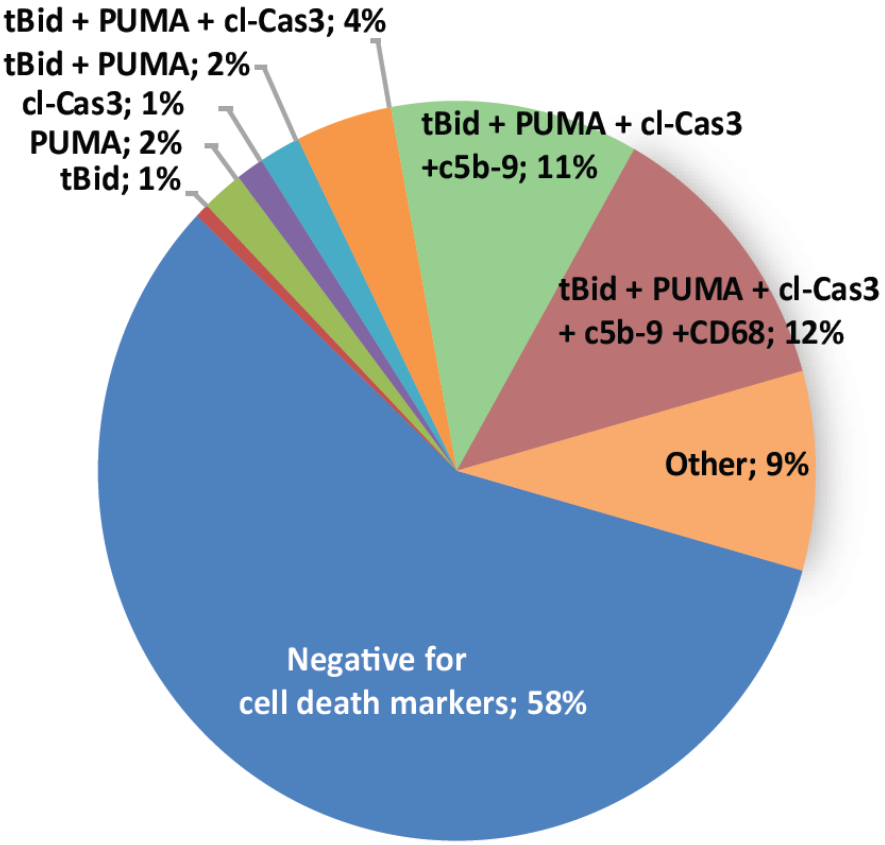
tBid + PUMA + cl-Cas3; 4%
tBid + PUMA; 2%
cl-Cas3; 1%
PUMA; 2%
tBid; 1%
tBid + PUMA + cl-Cas3 +c5b-9; 11%
tBid + PUMA + cl-Cas3 + c5b-9 +CD68; 12%
Other; 9%
Negative for cell death markers; 58%

Figure 2.4. Fibers with longer ETC abnormal regions are positive for cell death markers. A) A significant increase is observed in ETC abnormal length for fibers positive in cell death markers, p value < 0.0001 (n=68 fibers). B) The length of ETC abnormal region was measured for fibers positive for only tBid and subsequent addition of PUMA, cl-Cas3, C5b-9 and CD68. Fibers with the longest ETC abnormal region are positive for all five cell death markers. A total of 32 fibers were analyzed.

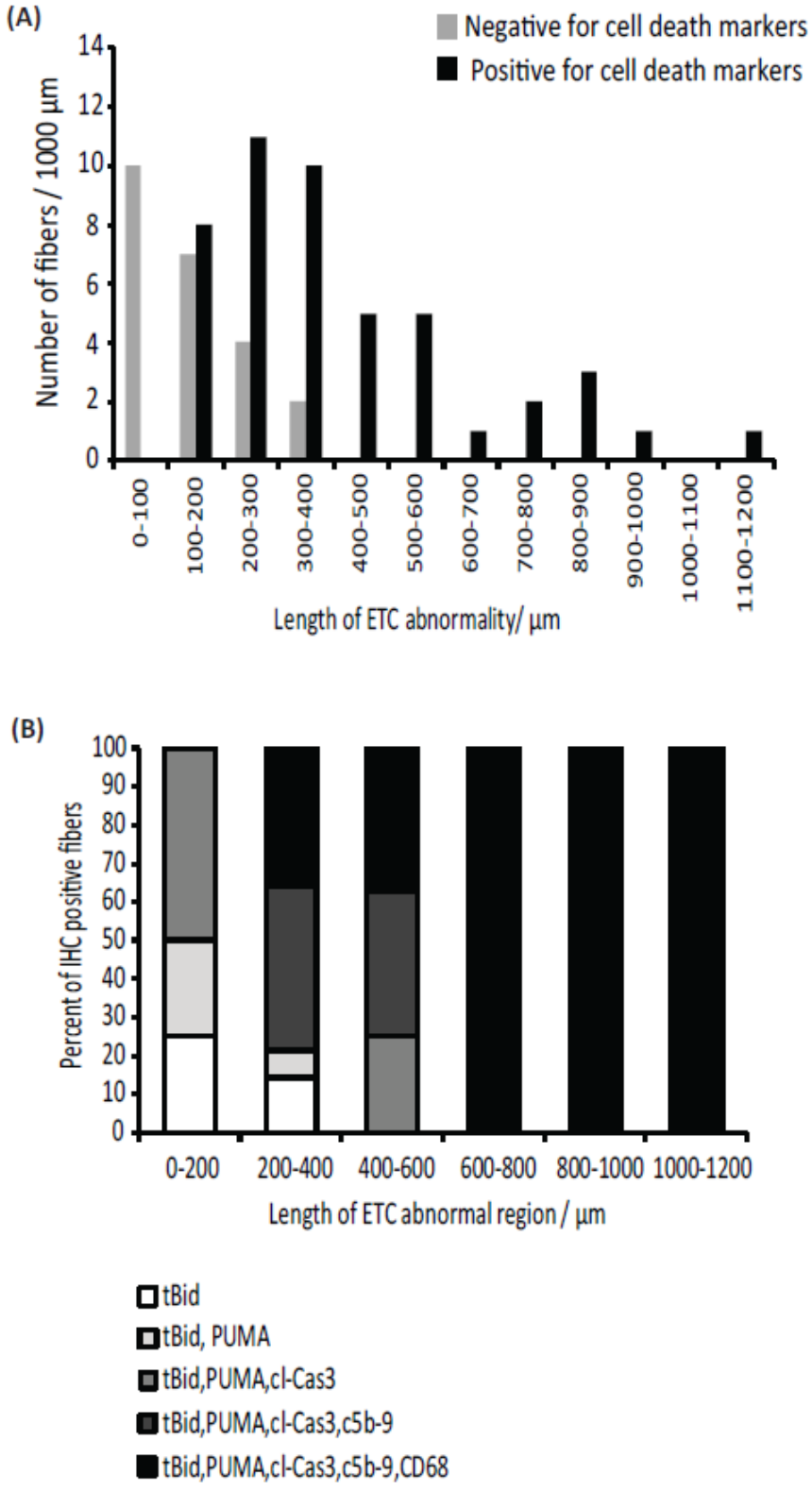
(A)
Negative for cell death markers
Positive for cell death markers
Number of fibers / 1000 µm
0
2
4
6
8
10
12
14
0-100
100-200
200-300
300-400
400-500
500-600
600-700
700-800
800-900
900-1000
1000-1100
1100-1200
Length of ETC abnormality/ µm
(B)
Percent of IHC positive fibers
0
10
20
30
40
50
60
70
80
90
100
0-200
200-400
400-600
600-800
800-1000
1000-1200
Length of ETC abnormal region / µm
tBid
tBid, PUMA
tBid,PUMA,cl-Cas3
tBid,PUMA,cl-Cas3,c5b-9
tBid,PUMA,cl-Cas3,c5b-9,CD68

Figure 2.5. Apoptosis and necrosis is prevalent in atrophic and broken ETC abnormal fibers. A) Intrafiber atrophy is more prevalent in ETC abnormal fibers (n=102 fibers) than in ETC normal fibers from either 36-month (n=99 fibers) or 12-month (n=30 fibers) rats. Significant variance (p value < 0.0001) in CSAR values between ETC abnormal and ETC normal. B) There is increased atrophy in ETC abnormal fibers positive for cell death. Cross-sectional area ratios of COX-/SDH++ fibers and COX normal/SDH normal fibers were determined. Significant atrophy in ETC abnormal fibers (p value = 0.0016). C) Atrophic and broken ETC abnormal fibers stain positive for cleaved caspase 3, c5b-9 and CD68. A total of 32 fibers were analyzed.

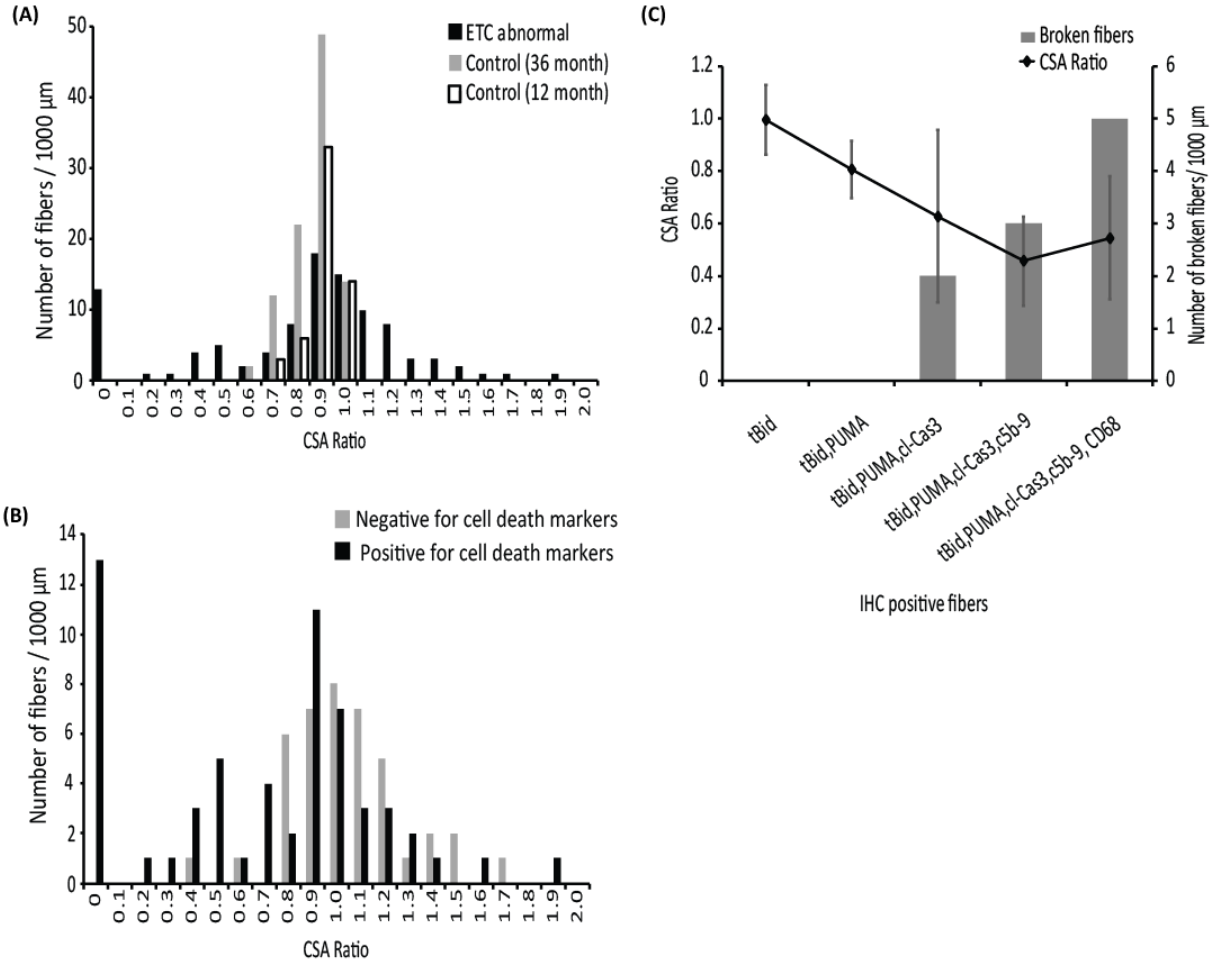
(A)
ETC abnormal
Control (36 month)
Control (12 month)
Number of fibers / 1000 µm
CSA Ratio
(B)
Negative for cell death markers
Positive for cell death markers
Number of fibers / 1000 µm
CSA Ratio
(C)
Broken fibers
CSA Ratio
CSA Ratio
Number of broken fibers/ 1000 µm
tBid
tBid,PUMA
tBid,PUMA,cl-Cas3
tBid,PUMA,cl-Cas3,c5b-9
tBid,PUMA,cl-Cas3,c5b-9, CD68
IHC positive fibers

Figure 2.6. Model of myofiber loss. A) Bundle of hypothetical fibers that contain wild type mtDNA with normal ETC function. B) A mtDNA deletion mutation, presumably resulting from an mtDNA replication error, is generated. The deletion-containing mtDNA genomes accumulates in a segment of fiber disrupting ETC enzymatic activity (grey) C) The deficiency results in activation of Bid and PUMA (black). D) As the ETC abnormal region expands, apoptosis is mediated by cl-Cas3 leading to intra-fiber atrophy. E) Upon the activation of apoptosis and necrosis, fiber breakage occurs within the ETC abnormal region. F) Apoptotic and necrotic region expands in the fiber. G) Fiber loss occurs. H) Another individual fiber, with accumulation of a deleted mtDNA genome, undergoes C-G again.

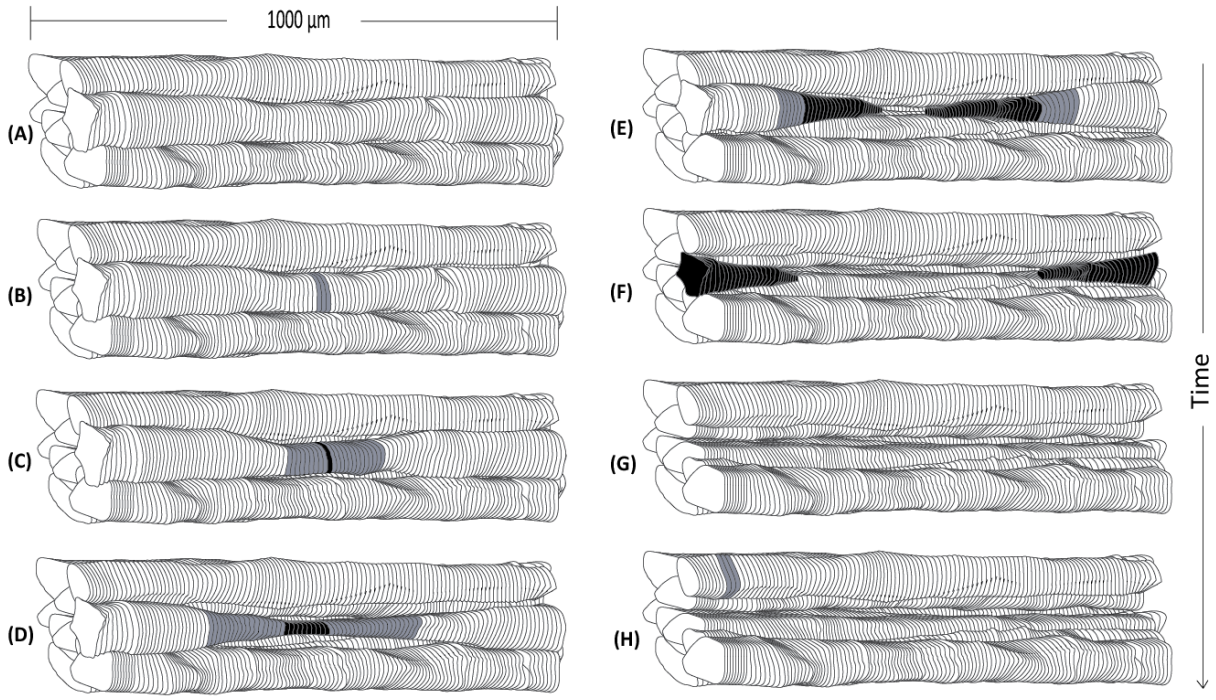
1000 µm
(A)
(B)
(C)
(D)
(E)
(F)
(G)
(H)
Time

Table 2.1. Abundance of fibers staining positive for cleaved caspase 3, C5b-9 and CD68 in 1,000 μm of rectus femoris from 12- and 36-month rats.

	Fibers staining positive		**Percentage of fibers**	
	Adult	**Aged**	**Adult**	**Aged**
cl-Cas3	1.2 ± 0.4	5.6 ± 2.0	0.012 ± 0.004	0.08 ± 0.02*
C5b-9	0.6 ± 0.2	2.4 ± 0.7*	0.006 ± 0.003	0.03 ± 0.02*
CD68	0.2 ± 0.2	2.0 ± 0.7*	0.002 ± 0.002	0.03 ± 0.01*
Fiber Number in RF muscle	9169 ± 447	6484 ± 477*		

*Significant, $p < 0.05$, myofibers positive for cell death markers in aged rats (n=5) and fiber loss (n=4) in rectus femoris. Data presented in mean ± sem.

Chapter 3

The chapter is published online:

Allen Herbst*†, Jonathan Wanagat*†, Nashwa Cheema*, Kevin Widjaja†, Debbie McKenzie, Judd M. Aiken (2016). Latent mitochondrial DNA deletion mutations drive muscle fiber loss at old age. *Aging Cell*, pp1-8.

*These authors contributed equally to this work.

†These authors generated Figure 3.4.

Abstract

With age, somatically-derived mitochondrial DNA (mtDNA) deletion mutations arise in many tissues and species. In skeletal muscle, deletion mutations clonally accumulate along the length of individual fibers. At high intra-fiber abundances, these mutations disrupt individual cell respiration and are linked to the activation of apoptosis, fiber atrophy, breakage, and necrosis, contributing to fiber loss. This sequence of molecular and cellular events suggests a putative mechanism for the 46% permanent loss of muscle fibers with age. To test whether mtDNA deletion mutation accumulation is a significant contributor to the fiber loss observed in aging muscle, we pharmacologically induced latent deletion mutation accumulation. We observed a 1,200% increase in mtDNA deletion mutation-containing electron transport chain abnormal muscle fibers, an 18% decrease in muscle fiber number and 22% loss of muscle mass. These data affirm the hypothesized role for mtDNA deletion mutation in the etiology of muscle fiber loss at old age.

Introduction

Sarcopenia is an increasingly prevalent and disabling consequence of aging, and the lack of a clear etiology is a critical barrier to developing treatments. This functional decline is a defining characteristic of the geriatric syndrome of frailty, which encompasses weight loss, muscle weakness, and slowed gait. A primary contributor to frailty is sarcopenia—the inevitable age-related process that results in the loss of skeletal muscle mass and function (Rosenberg, 1997). In humans, sarcopenia begins at ~25 years of age, approaches a 10% loss of muscle mass by age 50 and a 50% loss by the eighth decade (Lexell *et al.,* 1983; Goodpaster *et al.,* 2006). Muscle mass decline in humans has been attributed to both fiber loss and fiber atrophy (Lexell *et al.*, 1986; Klein *et al.*, 2003). The magnitude of this fiber loss in humans is estimated at ~25 muscle fibers per day at age 80 (Lexell *et al.*, 1986). In the F344xBN F1 hybrid rat, muscle mass and fiber loss begins at ~30 months of age and ~20 fibers are lost per day (Wanagat *et al.*, 2001; Lushaj *et al.*, 2008), paralleling the human data.The mechanisms that drive muscle fiber loss are mediated by apoptosis and necrosis in aged skeletal muscle (Dirks & Leeuwenburgh,2004; Marzetti *et al.*, 2010). Down-regulation of the apoptotic pathway reduces muscle mass loss and improves function in aged animals (Dupont-Versteegden, 2005). In aging human muscle, increased levels of apoptosis have been detected from biopsies (Malmgren *et al.*, 2001; Whitman *et al.*, 2005). Cellular necrosis is another mechanism of muscle fiber loss and is readily observed in aging rat muscle (Fujisawa, 1974). Electron transport chain (ETC) deficiencies trigger muscle fiber apoptosis and necrosis in aging skeletal muscle (Cheema *et al.*, 2015).

Electron transport chain (ETC) abnormal muscle fibers arise from a very specific molecular event, the intracellular, clonal accumulation of mitochondrial DNA deletion mutations. Mammalian mitochondria contain their own ~16-kb circular DNA genome that, together with nuclear components, encodes the proteins in the ETC. Muscle mitochondria exist as an extensive interconnected reticulum and cross sections of muscle contain thousands of mitochondrial genomes (Bakeeva *et al.*, 1978; Ogata & Yamasaki, 1997; Herbst *et al.*, 2007; Mishra *et al.*, 2015). When mtDNA deletion mutation-containing genomes accumulate to high levels, the defective genomes interfere with the normal transcription and translation of the mitochondrially encoded components of the ETC (NADH dehydrogenase, cytochrome b, cytochrome c oxidase-COX, ATP synthase). High levels of deletion-containing mtDNA genomes are localized to the ETC abnormal region of individual fibers (Müller-Höcker *et al.*, 1993; Cao *et al.*, 2001; Wanagat *et al.*, 2001). Although the specific deletion mutation differs from fiber to fiber, within a single fiber, ETC abnormal regions contain identical mtDNA deletion mutations suggesting that once a mitochondrial deletion mutation occurs, it expands clonally from its point of origin (Cao *et al.*, 2001). As multiple copies of the mtDNA exist in the mitochondrial reticulum, both wild-type and mutant mtDNA coexist in a state of heteroplasmy. The cellular impact of heteroplasmy is largely dependent on the mutant to wild-type mtDNA ratio. MtDNA deletion mutation abundance approaches 100% of the mitochondrial genomes within the ETC abnormal region of the fiber, and the threshold level for expression of the ETC abnormal phenotype is 90% (Herbst *et al.*, 2007). Low abundance mtDNA deletion mutations have been detected in ETC normal fibers and represent a pool of latent mutations that could give rise to

respiration deficiency and cell death given sufficient time or appropriate stimulation to accumulate(Pak & Aiken, 2004; Herbst *et al.*, 2007).

Gene expression measurements from diverse models of mitochondrial dysfunction and mitochondrial diseases (Alemi *et al.*, 2007; Subramaniam *et al.*, 2008) and studies from laser microdissected ETC abnormal regions of skeletal muscle fibers (Herbst *et al.*, 2013) identified the activation of mitochondrial biogenesis. Beta-guanidinopropionic acid (GPA), a creatine analogue, induces mitochondrial biogenesis primarily in skeletal muscle (Wiesner *et al.*, 1999; Reznick & Shulman, 2006). GPA, by inhibiting the creatine transporter, decreases intracellular creatine, high energy phosphocreatine, and ATP in skeletal muscle (Oudman *et al.*, 2013), increasing the AMP/ATP ratio (Bergeron *et al.*, 2001). The resulting energy deficit, likely through chronic AMPK activation, initiates mitochondrial biogenesis (Zong *et al.*, 2002; Chaturvedi *et al.*, 2009; Yang *et al.*, 2015). Similarly, creatine deficiency increased mitochondrial mass and respiratory enzyme activity in knockout mice (Schmidt *et al.*, 2004). In 28-month-old rats GPA treatment resulted in a twofold increase in skeletal muscle wild-type mtDNA, indicating mitochondrial biogenesis (Herbst *et al.*, 2013). These observations, taken together, suggest that somatically derived mtDNA deletion mutations clonally expand within individual fibers until a phenotypic threshold is surpassed resulting in the loss of cellular respiration, fiber atrophy, apoptosis, and necrosis with ensuing fiber breakage and loss. We hypothesized that, with advancing age, this process increasingly occurs in other muscle fibers—iteratively and cumulatively leading to the observed fiber loss that contributes to sarcopenia (Wanagat *et al.*, 2001; Herbst *et al.*, 2007; Cheema *et al.*, 2015). To test this hypothesis, we treated aged rats

with GPA, inducing latent deletion mutation accumulation and the formation of ETC abnormal fibers. We observe a significant increase in mtDNA deletion mutation frequency and ETC abnormality mediated fiber loss.

Results

To explore the role of ETC abnormal fibers in sarcopenia, we treated 30-month old hybrid rats with 1% beta-guanidinopropionic acid, compounded in chow, for four months. GPA treatment reduced quadriceps muscle mass 22% at 34-months of age **(Figure 3.1A, D)**. Muscle mass loss was accompanied by a 21% decline in rectus femoris cross-sectional area and an 18% loss of muscle fibers (1,589 fibers on average) in the GPA-treated rats **(Figure 3.1A,D)**. Concomitant with the loss of muscle mass and fibers was an increase in the abundance of excess fibrous connective tissue as detected by Masson's trichrome staining **(Figure 3.1B, C, D)**. In contrast to the typical interfascicular collagen deposition observed in normal muscle aging, we found fibrotic replacement of entire muscle fascicles **(Figure 3.1C)**. Muscle deterioration was most prominent in the muscle periphery with sparing in the vastus intermedius and central regions of the lateralis, medialis and femoris.

To estimate the difference in the tissue burden of ETC abnormal muscle fibers between GPA and control rats, we counted the number of enzymatically abnormal fibers in single muscle cross-sections that were histochemically stained for cytochrome c oxidase (COX) and succinate dehydrogenase (SDH) activities. Whereas COX is partially encoded by the mitochondrial

genome, SDH is encoded entirely in the nucleus. Individual (COX or SDH) and dual (COX and SDH) staining was used to reveal respiration deficient (COX^-, SDH^{++}) ETC abnormal skeletal muscle fiber segments **(Figure 3.2A)**. GPA-treatment resulted in a 1,200% increase in the number of ETC abnormal fibers as compared to normally-aged control rats within a single muscle section **(Figure 3.2B)**. By examining 119 randomly-selected fibers along their length, through one mm of quadriceps from GPA-treated rats, the abundance of ETC abnormal fibers was determined to be 15.1%. In contrast to normally aged rats, we observed clustering of ETC abnormal fibers, including the appearance of adjacent ETC abnormal fibers, which were not the result of fiber splitting. As observed in normally aged rats, ETC abnormal fibers tended to appear on the exterior surface of the fascicles and some ETC abnormal fibers split into multiple branches. As with collagen deposition, COX- fibers were most prominent in the muscle periphery. ETC abnormal fibers were not as frequent in the vastus intermedius and more central regions of the lateralis, medialis and femoris. In addition to increasing the abundance of ETC abnormal fibers, GPA treatment also affected the morphological characteristics of ETC abnormal fibers. The population of ETC abnormal fibers from GPA treated rats possessed, on average, shorter ETC abnormal segments. The mean ETC abnormality segment length in control rats was 442 ± 49.0 microns versus 345 ± 19.4 microns following GPA treatment **(Figure 3.2C)**.

In aging muscle, ETC abnormal fiber segments initiate apoptosis and necrosis (Cheema *et al.*, 2015). If ETC abnormal fibers are sufficient for fiber loss with age, then an increase in ETC abnormal fibers undergoing apoptosis and necrosis should be observed following GPA treatment. Immunohistochemical staining of GPA treated and control rat skeletal muscle

(Figure 3.3A) localized cleaved caspase-3 (cl-cas3) and complement-mediated membrane attack complex component c5b-9 to ETC abnormal segments. These markers indicate activation of apoptotic and necrotic cell death processes in ETC abnormal fibers. 80% of ETC abnormal fibers were positive for cell death markers in GPA treated rats as compared to 50% in control animals. Most of this difference was accounted for by an increase in the fraction of fibers undergoing necrosis in GPA treated rats **(Figure 3.3B)**. 20-25% of ETC abnormal fibers stained positive only for cl-Cas3, however, all c5b-9 positive fibers were cl-cas3 positive in GPA-treated and control rat quadriceps. In addition to an increased incidence of cell death positive ETC abnormal fibers from GPA treated rats, GPA treatment also resulted in necrotic ETC abnormal segments whose length was <200 microns **(Figure 3.3C)**. By contrast, in control rats, ETC abnormal fibers underwent necrosis only when greater than 200 microns in length. A final indicator of cell death in ETC abnormal fiber segments is the presence of broken fibers. In GPA treated rats, 23% of ETC abnormal fibers were broken, compared to 15% of the ETC abnormal fibers broken in control rats.

The mtDNA deletion mutations that accumulate with age are large, with 4-10kb lost, occur in the major arc and remove up to 11 protein encoding genes and 13 transfer RNAs. The gene encoding ND4 is routinely deleted (Kowald and Kirkwood, 2014), while minor arc genes such as ND1 are preserved. To quantitate mtDNA deletion burden in muscle homogenates, we exploited differences in copy number between ND4 and ND1 as an estimate of mtDNA deletion mutation frequency (Grady *et al.*, 2014) using a digital PCR approach (Taylor *et al.*, 2014). In a hypothetical sample comprised of only full length, intact mtDNA molecules, the expected ratio

would be 1 and this is what we observed in tissue homogenate DNA samples from control rats. In GPA-treated rats however, the ratio was depressed with an average ratio of 0.8 **(Figure 3.4A)** indicating a 20% mtDNA deletion mutation frequency in rat muscle following four months of GPA treatment.

While the abundance of deletion mutations in tissue homogenates gives an overall estimation of the mutation frequency, it is the focal distribution of deletion mutations that leads to their cellular impact. Therefore, we coupled laser microdissection and long extension PCR to define the mtDNA genotype within individual COX- fibers from GPA-treated rats. Each ETC abnormal fiber contained a unique mtDNA deletion mutation with a loss of 6-10kb **(Figure 3.4B)**. To interrogate heteroplasmy in single COX- fibers, we quantitated the ND4 and ND1 copy numbers by digital PCR. In COX^{+} control fibers, we found the expected 1:1 ratio between ND4 and ND1 genes. COX- fibers, however, possessed large increases in total mtDNA copy number (ND1) but a depression of the ND4 target site encompassed by the deletion event **(Figure 3.4C)**. These copy numbers demonstrate greater than 90% heteroplasmy for mtDNA deletion mutations within single ETC abnormal muscle fibers. DNA sequencing of the LX-PCR products from one of the COX- fibers identified a breakpoint between nucleotides 6,344 and 15,002 of the F344x BN F1 mtDNA genome (AY769440.1) which included a four base-pair repeat. This deletion mutation disrupted 11 protein coding and nine tRNA genes in the major arc while maintaining the minor arc genes including ND1 **(Figure 3.4D)**.

GPA treatment induces a metabolic shift from glycolytic to oxidative metabolism (reviewed in Oudman *et al.*, 2013). It is possible that in GPA treated rats we might observe a similar effect. Therefore, we determined the percent of oxidative slow twitch fibers (type I) in the rectus femoris muscle of control and treated rats. We observed no significant difference. In control and GPA treated rats, the muscle was composed of 2 ± 0.4% and 2.7 ± 1.2 % type I fibers respectively **(Figure 3.5A)**. Controls had a smaller range of 1 - 3% whereas in GPA 0.2 - 6% of the RF was type I. Type I fibers tended to cluster in GPA treated rats which was not as frequently observed in controls **(Figure 3.5B)**. In addition to the difference detected in fiber type clustering, type I fibers were identified in the periphery of the rectus femoris rather than in the central regions of the muscle in GPA-treated rats **(Figure 3.5C)**. These data suggest that GPA has an effect on the periphery of the muscle as it was also prone to increased collagen deposition and higher number of COX- fibers.

The two main fiber types, type I and type II, are morphologically and biochemically distinct. Oxidative fibers have a smaller cross sectional area and are enriched in more mitochondria whereas glycolytic fibers have a larger CSA and have a lower mitochondrial content. Even though, there was no significant difference in fiber type distribution, mitochondrial activity and fiber CSA differed in GPA rats suggesting a possible shift to oxidative metabolism. Higher mitochondrial content may be visualised by enzymatic activity staining of mitochondrial enzymes. In COX and SDH staining, fibers tended to stain darker in the GPA-treated muscles than the controls indicating an increase in enzymatic activity. Furthermore, we observed smaller fiber CSA in GPA rats. We measured the fiber CSA of GPA-treated rats and controls in

1mm^2 area in the rectus femoris. A significant decline of 47% in fiber CSA was observed in GPA-treated muscle **(Figure 3.6A)**. Fibers from GPA muscle had an average CSA of 1517 ± 34.30 μm^2 with a range from 25 – 5,583 μm^2 whereas in the age-matched controls, fibers had a larger average CSA of 2853 ± 110.7 μm^2 with a range from 137 – 13,170 μm^2 **(Figure 3.6B)**.

There was no significant difference in mortality between GPA-treated and control rats. At the end of the experiment, control rats and GPA treated rats had a survival percent of 86% and 74% respectively **(Figure 3.7)**. The daily consumption of food was monitored with control rats consuming 37g and GPA-treated rats consuming 25g. A significant decline of 12 grams was observed in the daily food intake of GPA-treated rats (p value < 0.0001) **(Figure 3.8A)**. A gradual decline in the body weight of rats was observed in GPA treatment, whereas, control rats remained at a constant body weight of 569 grams **(Figure 3.8B)**. Although, there was a 28% decrease in body mass in GPA-treated rats, no differences were observed in cardiac and brain tissue between GPA-treated and control rats **(Table 3.1).**

Discussion

The physiological impact of mitochondrial mutations is demonstrated by the effect of AZT treatment (Rayapureddi *et al.*, 2010), accelerated aging of mitochondrial DNA polymerase gamma mutator mice (Trifunovic *et al.*, 2004), and cardiac arrhythmias in Twinkle mitochondrial helicase mutant mice (Baris *et al.*, 2015). Previous experiments demonstrated that a 7 weeks GPA treatment of 27-month-old rats resulted in an increased incidence (3.7-fold) of ETC

abnormal fibers, but did not result in measureable fiber loss (Herbst *et al.*, 2013). Clonally expanded mtDNA deletion mutations first appear as ETC abnormal fibers at approximately 28 months of age in the hybrid rat (Herbst *et al.*, 2013). We hypothesized that inducing mitochondrial biogenesis at older ages, when deletion mutation frequency is higher, would explicitly test the role of these mutations in muscle fiber loss. Four months of GPA treatment in 30-month-old rats resulted in a 12-fold increase in ETC abnormal fibers, accelerating cell death, fiber loss and fibrosis, leading to a 22% loss of muscle mass. This loss encompasses individual fiber loss and atrophy (e.g. due to reduced protein synthesis or increased protein degradation), but is offset by positive contributions to muscle mass from fibrotic replacement. Loss of muscle mass and rectus femoris fiber number in control rats was consistent with previous data (Lushaj *et al.*, 2008). The sparing of muscle deterioration in the central areas of the quadriceps follows from the muscle fiber type distribution (predominantly type I) in these regions. Type II fibers, which predominate in the muscle periphery, have been shown to be more susceptible to deletion mutation accumulation and are preferentially lost with age (Wanagat *et al.*, 2001; Bua *et al.*, 2002). GPA treatment, however, could also be acting in these areas independent of mitochondrial genotype as GPA is known to cause a type I to type II fiber shift (Oudman *et al.*, 2013). Increased deposition of fibrotic tissue in GPA-treated rat quadriceps muscle is consistent with the inflammatory loss of necrotic ETC-deficient muscle fibers.

In muscle aging, activation of apoptosis and necrosis predominantly occurs in ETC abnormal muscle fibers (Cheema *et al.*, 2015). The ETC abnormality results from the focal accumulation of mtDNA deletion mutations (Wanagat *et al.*, 2001; Herbst *et al.*, 2007). As GPA treatment

promotes sarcopenic changes through an increase in ETC abnormal fiber abundance, treatment should also accelerate the mitochondrial genotypic changes observed with muscle aging. To test this relationship, we quantitated mtDNA deletion mutation abundances in both muscle tissue homogenates and single muscle fibers. The mtDNA deletion frequency (20%) in tissue homogenates mirrored the increased abundance of ETC abnormal fibers. Similarly, in single fibers, GPA treatment resulted in deletion mutation abundances that exceed the90%phenotypic threshold for presentation of a respiration deficiency. The mtDNA deletions are clonal, involve only the major arc, and ranged in size from 4 to 10 kb. The deletion mutations induced by GPA treatment appear similar to those observed previously (Cao *et al.*, 2001; Wanagat *et al.*, 2001). Previously, in rats, we observed that the abundance of wild-type genomes was maintained in ETC abnormal regions (Herbst *et al.*, 2007). Subsequent data in humans showed a diminished abundance of wild-type genomes (Herbst *et al.*, 2007). The data presented here are more similar to the latter, a slight reduction in wild-type mtDNA abundance.

The approach to quantitation of ETC abnormal fibers and mitochondrial deletion mutations depends upon the underlying abundance (Greaves *et al.*, 2014). The abundance of mtDNA deletion mutations in normally aged muscle contrasts dramatically with abundances following GPA treatment illustrating the need for different approaches to quantitation. Determining ETC abnormal fiber number in normally aged muscle requires counting all lesions within a given tissue volume to account for the three-dimensional structure, distribution, and abundances of these lesions (Wanagat *et al.*, 2001). In contrast, the elevated abundance of ETC abnormal fibers following GPA treatment required a sampling approach; volume density techniques were

no longer practical due to the massive increase in ETC abnormal fiber number. Detection of deletion mutation events from tissue homogenates during normal aging is exceedingly difficult due to the large range between deletion mutation-containing and wild-type mtDNA genome abundances. Deletion mutation-containing mitochondrial genomes have been quantitated at between 20 parts per million in human brain homogenates (Taylor *et al.*, 2014) and one part per million in aged mouse muscle (Guo *et al.*, 2010) vs. 20 parts per hundred in homogenates from GPA-treated rats and > 90 parts per hundred in single ETC abnormal fibers. The absolute mutation frequency in aged control rats is below the detection range using the loss of the major arc primer/probe site quantitation method, which results in a ND4:ND1 ratio approximating one. The higher deletion mutation abundance in homogenates from GPA-treated rat muscles or single muscle fibers allowed detection of deletion mutation frequencies ranging from 20% in homogenates to 98% in single fibers.

The induction of ETC abnormal fibers by GPA treatment suggested two possibilities: (i) GPA treatment generated mtDNA deletion mutations de novo or (ii) GPA enhanced the accumulation of latent pre-existing, age-induced deletion mutations. GPA is not known to be mutagenic despite numerous studies of its activity in mammals (reviewed by Oudman) (Oudman *et al.*, 2013; Karamat *et al.*, 2015), and we did not observe any ETC abnormalities in young rats treated with GPA (Herbst *et al.*, 2013). GPA inhibits creatine-dependent energy metabolism leading to fiber atrophy in young and old rodents and induces mitochondrial biogenesis in skeletal muscle (Mahanna *et al.*, 1980; Wiesner *et al.*, 1999; Zong *et al.*, 2002; Herbst *et al.*, 2013). Sampling individual respiration competent fibers determined that 10–25%

of these ETC normal fibers from 36-month-old rat skeletal muscles harbored mtDNA deletion mutations at intrafiber abundances of 0.01–2.17% (Pak & Aiken, 2004).

The increased incidence of respiratory-deficient muscle fibers by expansion of latent mtDNA deletion mutations demonstrates the existence of specific pathways that control mitochondrial DNA mutation accumulation and, more importantly, that these pathways can be modulated in vivo. While the activation of mitochondrial biogenesis is suspected to have beneficial effects on aging (Martin-Montalvo *et al.*, 2013; Yang *et al.*, 2015), if that process lacks selectivity for competent mitochondrial genomes, adverse effects may accrue due to the expansion of mtDNA deletion mutations in mammals (Lin *et al.*, 2016). Similarly, treatments designed to affect aging phenotypes by manipulating mitochondrial quality control require examination of those interventions on both normal and mutant mtDNA populations.

GPA treatment in aged rats increased the accumulation of mtDNA deletion mutations, which manifests as an increased abundance of ETC abnormal muscle fibers. In addition to increasing the abundance of ETC abnormal segments, GPA accelerated the progression of ETC abnormal

fiber segments as evidenced by shorter abnormalities, increased cell death activation and cell death activation in shorter segments, and increased incidence of broken fibers. Finally, GPA treatment accelerated the loss of muscle mass and fiber number that defines sarcopenia. The experimental manipulation of mtDNA deletion mutation abundance by a pharmacological intervention in old animals accelerated phenotypes of muscle aging. These data strengthen the causal link between mtDNA deletion mutation and fiber loss and underscore the significance of latent mtDNA deletion mutations. The exogenous pharmacological induction of ETC

abnormalities implicates specific pathways that regulate mtDNA deletion mutation accumulation in vivo. Modulation of these pathways is likely to be pleiotropic with beneficial effects on bioenergetics confounded by the antagonistic induction of mutant mtDNA accumulation.

Material and Methods

Ethics Statement

This study was carried out in accordance with the recommendations in the NIH Guide for Care and Use of Laboratory Animals and the guidelines of the Canadian Council on Animal Care. The protocols used were approved by the Institutional Animal Care and Use Committees at the University of Alberta.

Animals, GPA treatments & tissue preparation

Thirty-month old male Fischer 344 x Brown Norway F1 hybrid rats (*Rattus norvegicus*) were purchased from the National Institute on Aging colony maintained by Harlan Sprague Dawley (Indianapolis, IN). β-guanidinopropionic acid was synthesized as described (Rowley *et al.*, 1971; Herbst *et al.*, 2013) from cyanamide and β-alanine. GPA was purified by recrystallization and the synthesis confirmed by mass-spectrometry and IR spectroscopy. β-GPA was formulated to 1% by weight in 6% fat rodent chow (Harlan-Teklad, Madison, WI) and fed for 4-months *ad libitum*. Rats were housed on a 12 hour light/dark cycle. No significant difference was observed in the survival of rats treated with β-GPA vs controls. Animals were euthanized, the quadriceps

muscles dissected from the animals, weighed, bisected at the mid belly, embedded in optimal cutting temperature compound (Sakura Finetek, Torrance, CA), flash frozen in liquid nitrogen and stored at -80°C. A minimum of one hundred 10µm thick consecutive transverse cross-sections were cut with a cryostat at -20°C and placed on Probe-On-Plus slides or PEN membrane glass slides (Life Technologies) for laser microdissection. Slides were stored at -80°C until needed.

Histochemical and immunohistochemical staining

At 100um intervals, sections were stained for COX (brown) or SDH (blue) as previously described (Wanagat *et al.*, 2001). A third slide was dual stained, first for COX and secondly for SDH. ETC abnormal fibers appear blue on a brown background following dual staining. Two slides within the series were used for hematoxylin and eosin (H&E) staining. Fibrotic tissue was stained using Masson's trichrome, as described [Lushaj, 2008]. Immunohistochemical staining using anti-activated caspase 3 (Promega, Madison, WI;1:200) and anti-C5b-9 (Abcam, Cambridge, MA;1:500) was performed as described[Cheema, 2015]. Fiber typing was performed using anti-My32 (Abcam, Cambridge, MA; 1:500). After histochemistry or immunohistochemistry, slides were digitized by a scanning microscope (Nanozoomer, Hamamatsu).

Image analysis, counts and quantitation

Cross-sectional area measurements and fiber counts of the rectus femoris were obtained from digital images. Rectus femoris muscle is used for CSA measurements and fiber counts because it

is entirely encapsulated by the quadriceps and has low pennation angle to the muscle fibers, facilitating accurate and precise quantification. The absolute number of ETC abnormal fibers (COX-/SDH++) were identified and annotated throughout 10 µm of tissue in both GPA treated and control rats. 119 individual randomly selected fibers from GPA treated rats were followed throughout one millimeter of tissue to measure the abundance of ETC abnormal regions. Fibers that stained positive for cleaved caspase 3 at a 100-µm interval were counted, annotated, and followed throughout the 1 mm of rectus femoris tissue. The length of ETC abnormality segments was determined by counting the number of slides the abnormality appeared in and multiplying by 10 µm. Fiber cross sectional area (CSA) was measured by annotating fibers in $1mm^2$ area using the NDP.view software (Nanozoomer, Hamamatsu).

DNA isolation

This was performed by Dr. Allen Herbst. Rat quadriceps muscle was ground to a powder using a mortar, pestle, and liquid nitrogen. Total DNA was extracted using the Maxwell 16 tissue preparation kit (Promega, Madison, WI). Total DNA quantity and quality was measured using spectrophotometry at A230, A260, and A280 (Thermo Scientific Nanodrop 2000 Spectrophotometer) and integrity examined by gel electrophoresis. DNA isolation from individual muscle fiber cross-sections was performed subsequent to laser microdissection. Muscle sections on membrane slides were dehydrated in absolute ethanol and air dried. ETC abnormal fibers were identified on adjacent serial sections by staining for COX and SDH as described above. Single muscle fiber sections were captured using a Leica LMD 7000, digested in one microliter of proteinase K digestion solution as described (Wanagat *et al.*, 2001; Herbst

et al., 2007), and re-suspended to a total volume of ten microliters with nuclease- free water. Initial estimation of mtDNA copy number from all DNA samples was obtained by quantitative PCR (qPCR) using primers and probes to the rat mitochondrial genome (ND4, ND1) purchased from Integrated DNA Technologies (IDT; Coralville, Iowa). qPCR reactions for both ND4 and ND1 were 1ul of target DNA, 1.25ul of 20X ND4/ND1 primer probe mix, 12.5ul of 2X AmpliTaq Master Mix (ThermoFisher; Waltham, MA), and 10.25ul of H_2O for each 25ul reaction. qPCR cycling conditions for ND4 were Taq-Polymerase activation at 95°C for ten minutes, denaturation at 95°C for ten seconds, annealing at 58°C for ten seconds, extension at 72°C for 30 seconds, plate read, and repeat steps 2-5, for a total of 40 cycles. ND1 was cycled similarly, except the annealing temperature was decreased to 54°C.

Digital PCR quantitation of mtDNA deletion mutation abundance

This was performed by Dr. Jonathan Wanagat and Kevin Widjaja. Samples were diluted to the target range of the Quantstudio 3D digital PCR (dPCR) 20K Chip (Version 2, ThermoFisher; Waltham, MA) and the mtDNA copy number determined in each sample. ND4 and ND1 reactions were performed on separate, individual digital PCR chips according to the manufacturer's instructions. DPCR cycling conditions for ND4 and ND1 were the same as for qPCR described above. MtDNA copy numbers per microliter were calculated using QuantStudio 3D Analysis Suite Cloud Software (Version 3, ThermoFisher; Waltham, MA). In the case of tissue homogenates, mtDNA copy numbers were normalized to the control samples.

Long Extension PCR amplification of mtDNA deletions from single muscle fibers

This was performed by Dr. Allen Herbst. Deletion-containing mtDNAs were amplified using the 16S-F and 12S-R primer set purchased from IDT. Long extension PCR reactions were assembled according to the manufacturer's instructions, Go-Taq Long PCR master mix (Promega, Madison, WI). PCR cycling conditions were polymerase activation at 95°C for two minutes, denaturation at 94°C for twenty seconds, and annealing at 68°C for ten minutes, then repeated for 40 cycles. PCR products were fractionated on 1% agarose gels, stained with ethidium bromide, and visualized under UV light.

Statistical analysis

Data are presented as mean ± SEM. Reported p-values were obtained using Student's t-tests with a p-value < 0.05 being significant. All statistical analysis was performed using GraphPad Prism version 5.00 for Windows (GraphPad Software, San Diego, California USA).

Figure 3.1. Morphometric data collected from aged control and GPA-treated rats. (A) Representative muscle cross-sectional images stained with hematoxylin and eosin. The bar denotes 5mm. The encircled area delineates the rectus femoris muscle with cross-sectional areas of 39.5 and 33.2 mm^2 for control and GPA-treated, respectively. (B) Quadriceps muscle sections stained with Masson's trichrome to identify collagen (blue) deposition. The bar denotes 5mm. (C) Higher magnification imaging of fibrotic tissue deposited in aged rats. The bar denotes 100 microns. (D) Quadriceps muscle mass, rectus femoris fiber number and cross-sectional area and quadriceps fibrotic tissue abundance in control and GPA treated aged rats.

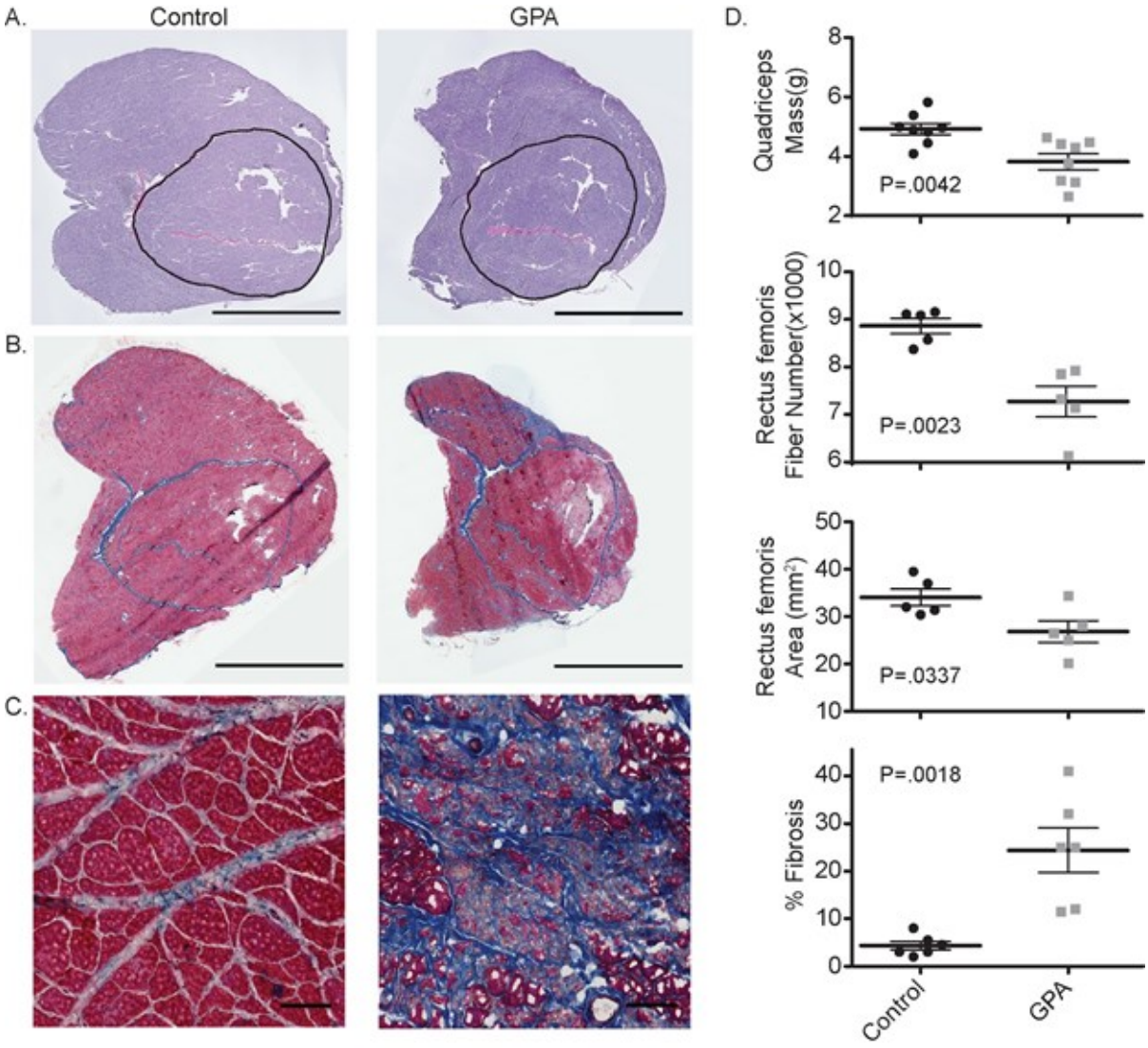
A.
Control
GPA
B.
C.
D.
Quadriceps Mass(g)
P=.0042
Rectus femoris Fiber Number(x1000)
P=.0023
Rectus femoris Area (mm²)
P=.0337
% Fibrosis
P=.0018
Control
GPA

Figure 3.2. GPA treatment of aged rats results in a 1200% increase in the abundance of segmental ETC abnormal fibers. (A) COX negative SDH hyper ETC abnormal muscle fibers are prevalent in GPA treated rat muscle. The scale bar in each image is 0.25mm. (B) Quantification of ETC abnormality abundances in rectus femoris and whole quadriceps muscles. (C) GPA treatment decreases ETC abnormal segment length. Frequency distributions are fitted with Gaussian curves using a least squares approach.

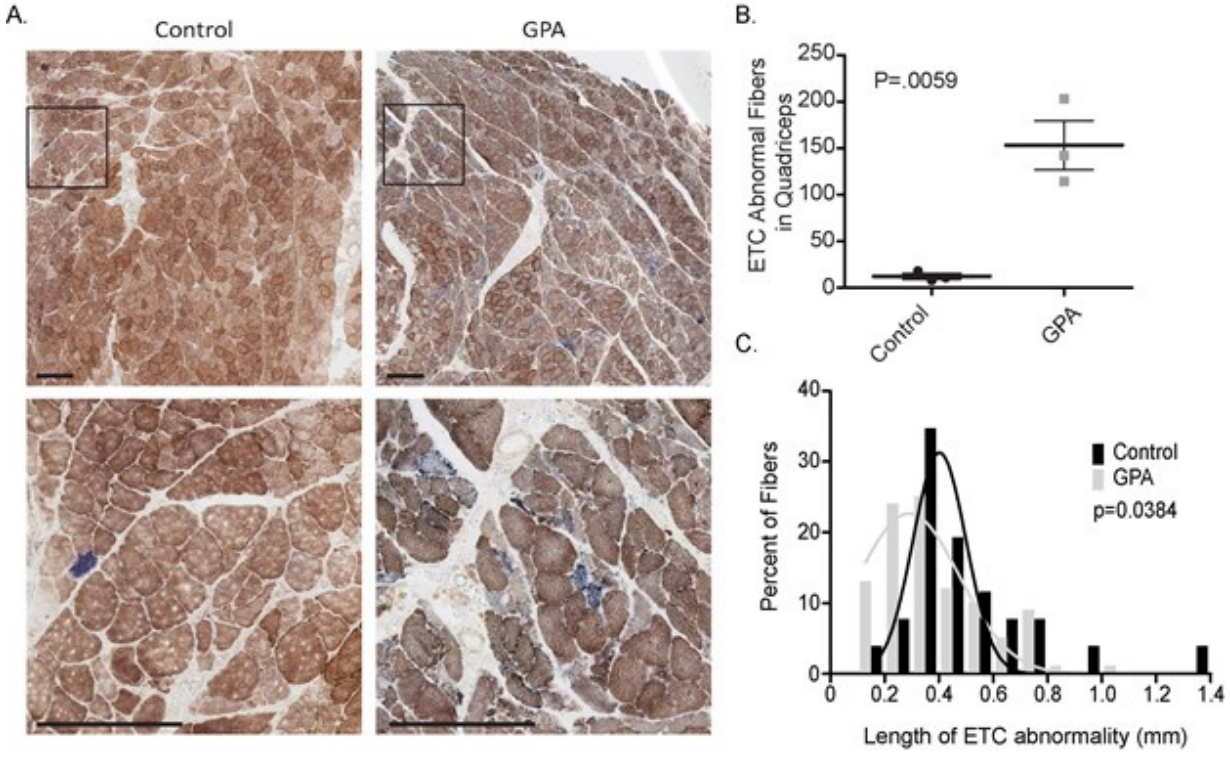
A.
Control
GPA
B.
P=.0059
ETC Abnormal Fibers in Quadriceps
250
200
150
100
50
0
Control
GPA
C.
Percent of Fibers
40
30
20
10
0
Control
GPA
p=0.0384
0
0.2
0.4
0.6
0.8
1.0
1.2
1.4
Length of ETC abnormality (mm)

Figure 3.3. Fiber death in GPA-induced ETC abnormal fibers. ETC abnormal fibers, induced by GPA treatment activate apoptosis and undergo necrosis. A. ETC abnormal fiber undergoing apoptosis and necrosis. Dual and single Histochemical staining for COX and SDH. Immunohistochemical staining for cl-Cas3 and c5b-9. The scale bar denotes 50 microns. B. 80% of ETC abnormal fibers are positive for apoptotic (cl-Cas3) and necrotic (c5b-9) cell death. C. Cell death processes are activated in shorter ETC abnormal fiber segments of GPA treated rats than in controls.

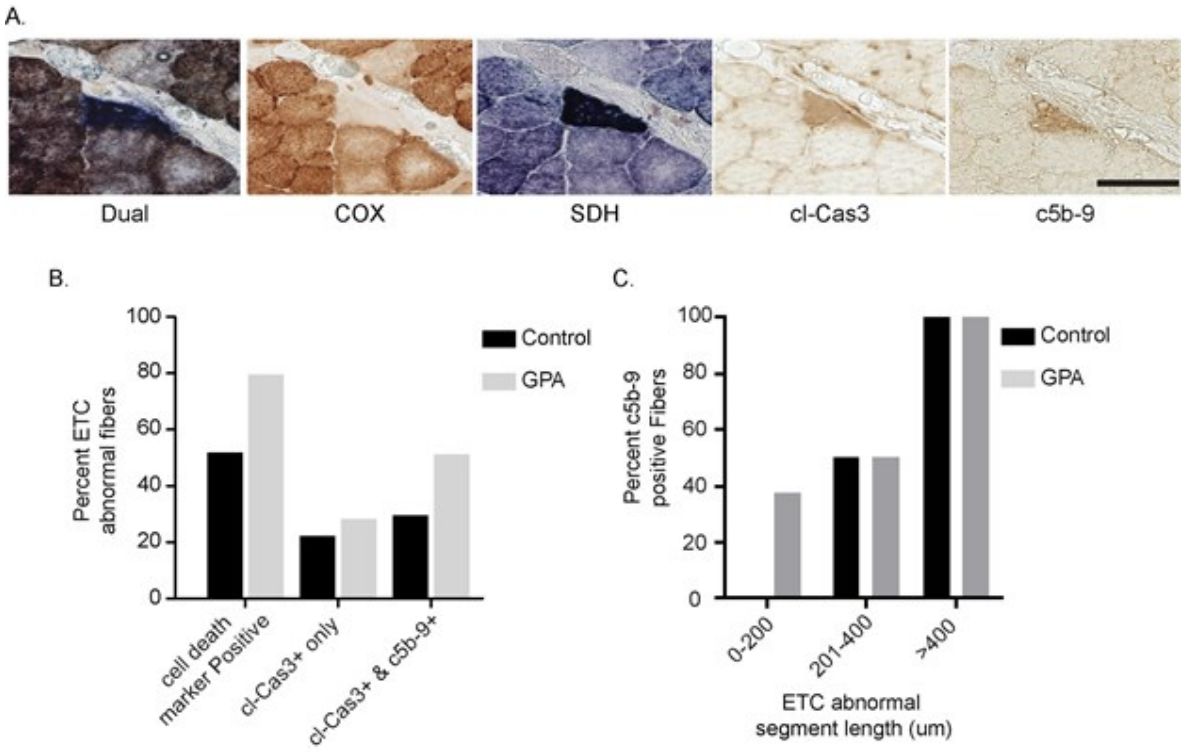
A.
Dual
COX
SDH
cl-Cas3
c5b-9
B.
Percent ETC abnormal fibers
100
80
60
40
20
0
Control
GPA
cell death marker Positive
cl-Cas3+ only
cl-Cas3+ & c5b-9+
C.
Percent c5b-9 positive Fibers
100
80
60
40
20
0
Control
GPA
0-200
201-400
>400
ETC abnormal segment length (um)

Figure 3.4. Induction of mtDNA deletion mutation accumulation by GPA treatment in aged rats. A. Elevated mtDNA deletion mutation frequency in GPA-treated rat quadriceps muscles. B. Mitochondrial DNA deletion mutations from GPA-treated rats amplified by long extension PCR from laser capture microdissected COX- fibers C. Copy numbers of total mtDNA as compared to WT mtDNA in single, microdissected control or COX- fibers showing degrees of heteroplasmy. D. Sequencing of mtDNA deletion mutation breakpoint from a single microdissected COX- fiber shown in panels B and C - Lane 1 and fiber 1, respectively. This figure is a courtesy of Dr. Allen Herbst, Dr. Jonathan Wanagat and Kevin Widjaja.

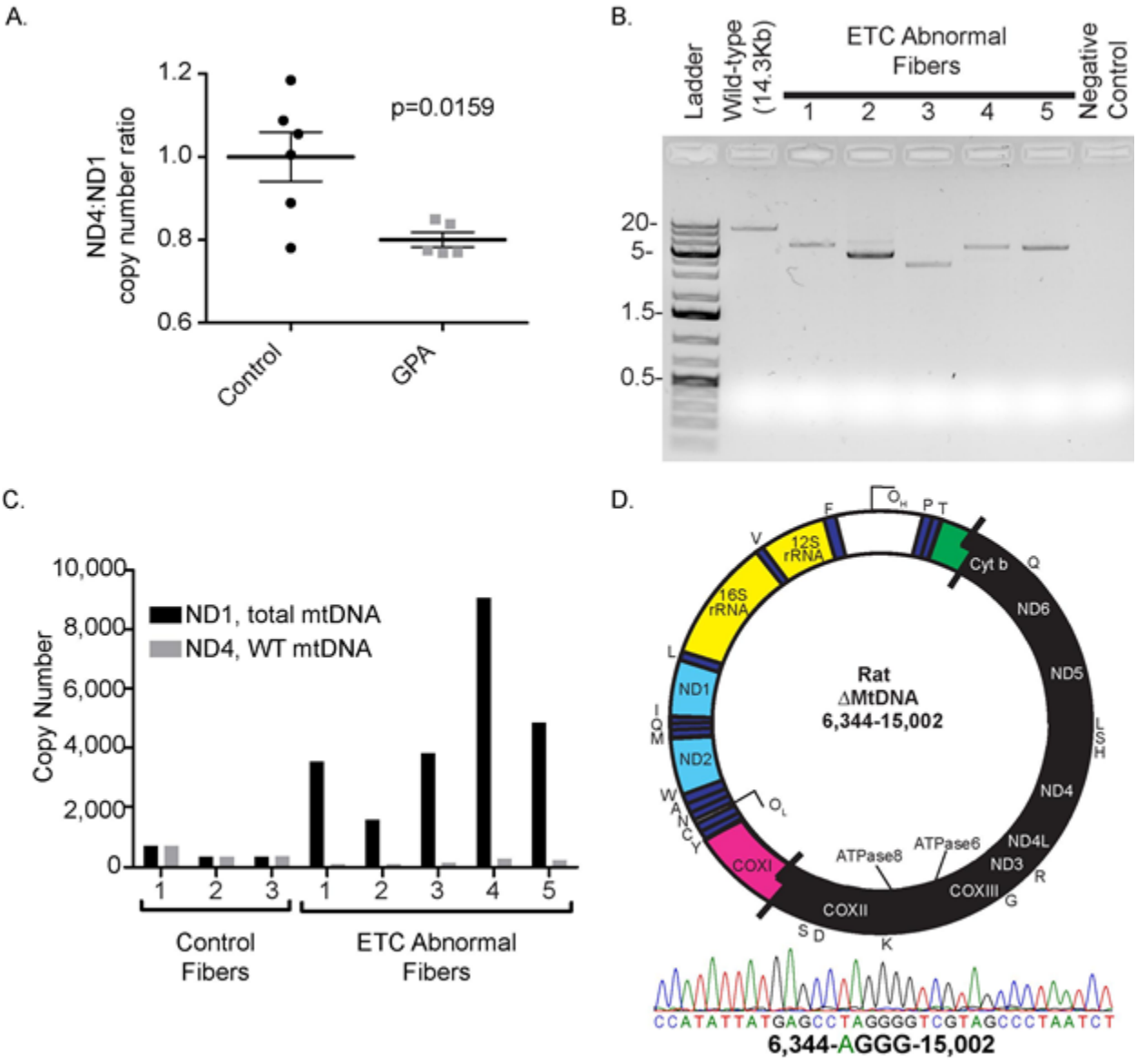
A.
ND4:ND1
copy number ratio
1.2
1.0
0.8
0.6
p=0.0159
Control
GPA
B.
Ladder
Wild-type
(14.3Kb)
ETC Abnormal
Fibers
1
2
3
4
5
Negative
Control
20-
5-
1.5-
0.5-
C.
Copy Number
10,000
8,000
6,000
4,000
2,000
0
ND1, total mtDNA
ND4, WT mtDNA
1
2
3
1
2
3
4
5
Control
Fibers
ETC Abnormal
Fibers
D.
Rat
ΔMtDNA
6,344-15,002
12S
rRNA
16S
rRNA
Cyt b
ND6
ND5
ND4
ND4L
ND3
COXIII
COXII
ATPase6
ATPase8
COXI
ND2
ND1
CCATATTATGAGCCTAGGGGTCGTAGCCCTAATCT
6,344-AGGG-15,002

Figure 3.5. Fiber typing in control and GPA treated rats. (A) Percent of type 1 fibers in the rectus femoris muscle in control and GPA rats. (B) Representative micrographs of My32 immunostained vastus lateralis muscle. My32 recognizes type II fibers. Fiber type I clustering observed in GPA treated muscle. (C) Fiber type distribution in rectus femoris (RF) muscle. Type 1 fibers observed in the RF periphery facing the vastus medialis (VM) muscle. Scale bar is 100 μm.

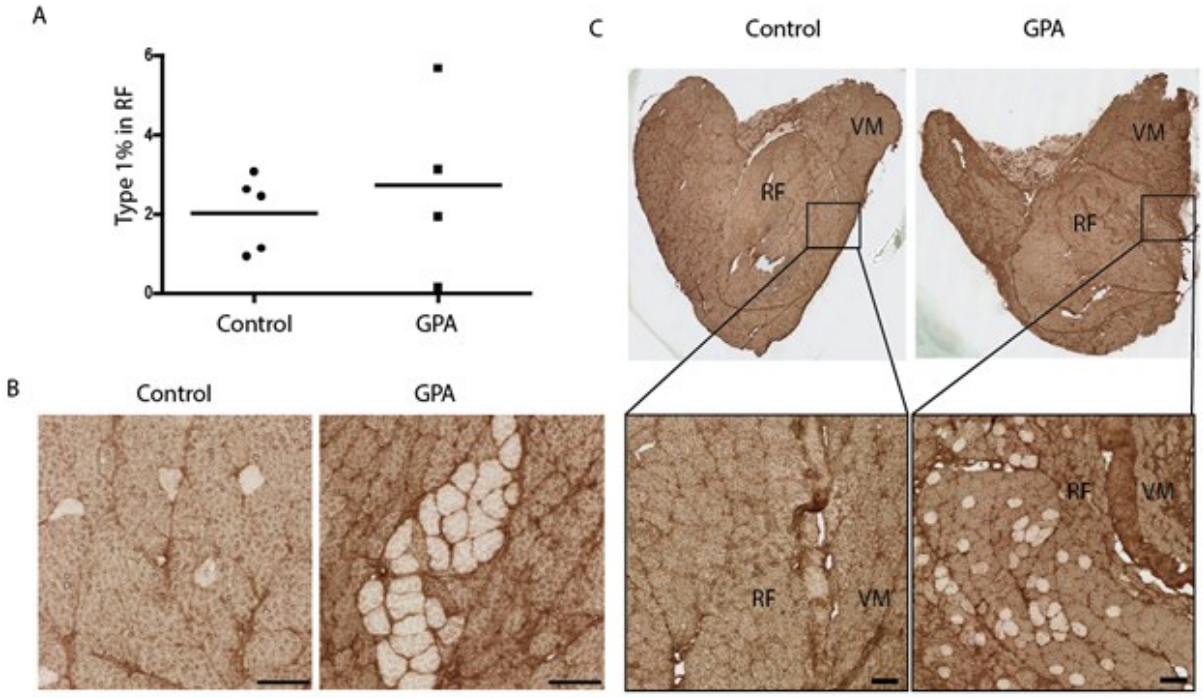
A
Type 1% in RF
6
4
2
0
Control
GPA
B
Control
GPA
C
Control
GPA
VM
RF
VM
RF
RF
VM
RF
VM

Figure 3.6. Myofiber CSA in control and GPA rectus femoris muscle. (A) Average fiber CSA measurement in control and GPA rats. (B) Percent of fibers in control and GPA rats with fiber CSA. Maximum fiber CSA in control was 13,170 μm^2.

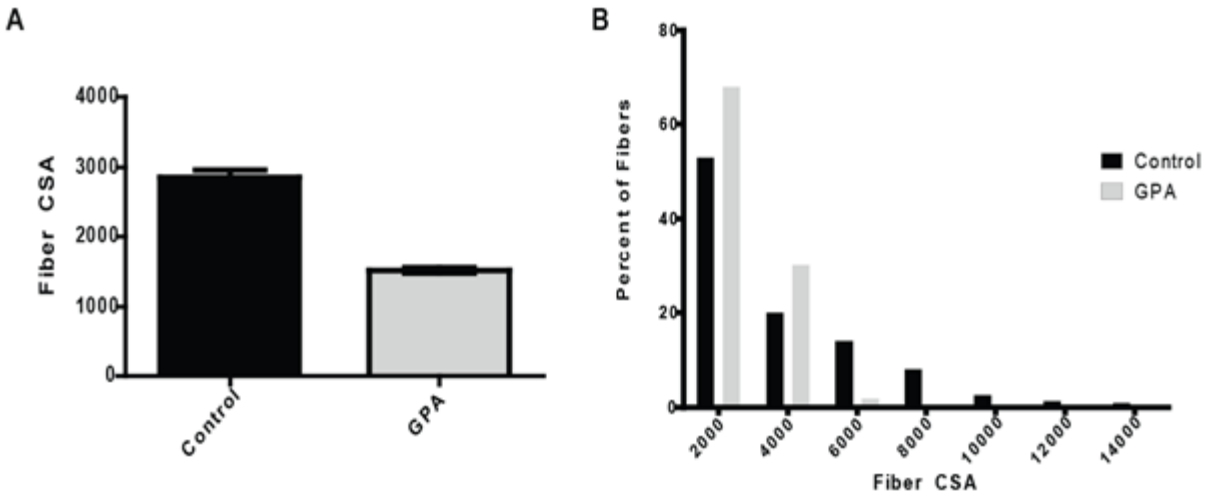
A
Fiber CSA
4000
3000
2000
1000
0
Control
GPA
B
Percent of Fibers
80
60
40
20
0
Control
GPA
2000
4000
6000
8000
10000
12000
14000
Fiber CSA

Figure 3.7. Survival curve for 30 month FBN rats on normal rodent chow (solid line) and 1% β-GPA chow (dashed line) for 4 month *ad libitum.*

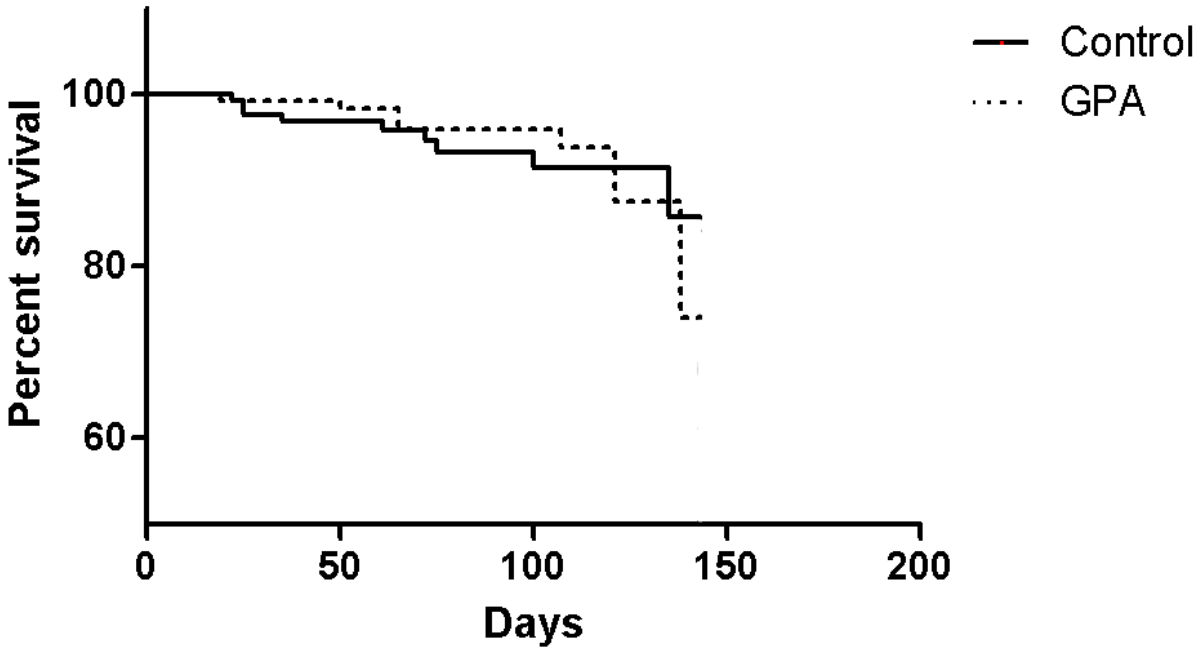
Control
GPA
Percent survival
100
80
60
0
50
100
150
200
Days

Figure 3.8 Food consumption and body weight of rats on normal and GPA feed. (A) Food consumption of controls and GPA fed rats during 4 month period (g/day). (B) Body weight of controls (open circle) and GPA fed rats (filled square) over the course of the experiment. Surviving rats were sacrificed at 143 days.

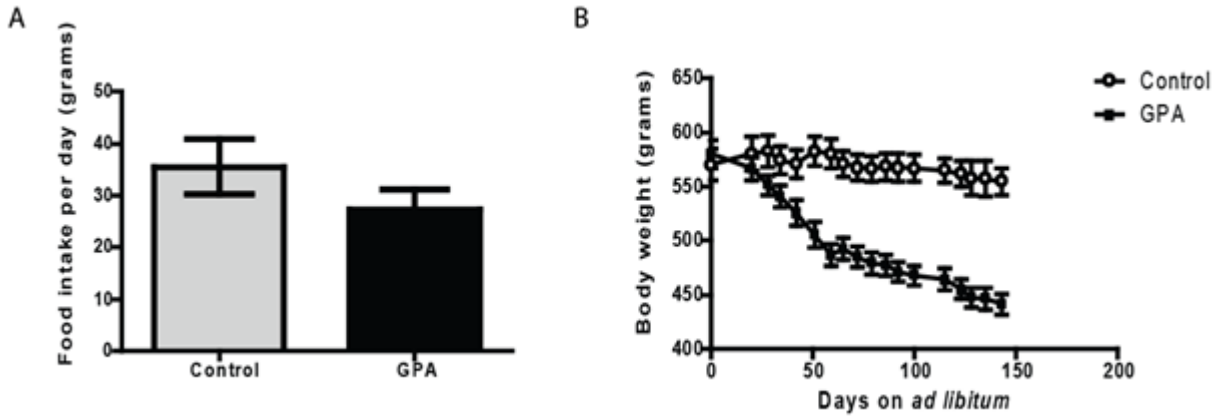
A
Food intake per day (grams)
50
40
30
20
10
0
Control
GPA
B
Body weight (grams)
650
600
550
500
450
400
0
50
100
150
200
Days on ad libitum
Control
GPA

Table 3.1. Wet weights of body, brain and heart of control and GPA rats at end of study (n=7-8).

	Weight (grams)		
	Body	**Brain**	**Heart**
Control	515±68	2.3±0.1	1.4±0.2
GPA	402±52	2.3±0.1	1.4±0.1

Chapter 4: Future Directions and Conclusions

Mitochondrial dysfunction plays a strong role in sarcopenia. The role of ETC abnormalities and cell death in aged heart, brain and kidney is, however, unknown. Studies in multiple tissues would support a universal biological mechanisms of ETC abnormalities in the aging process. In chapter 2, I identify the role of the two cell death pathways, apoptosis and necrosis, in aged tissue. In ETC abnormal fibers, apoptosis was triggered in shorter abnormalities and necrosis was involved with longer abnormalities. Currently, caloric restriction is the only intervention that has delayed ETC abnormality accumulation and attenuated apoptotic signalling in aged skeletal muscle. In this chapter, I outline some future studies on caloric restriction. Based on our findings in chapter 3, GPA can be utilised to address questions regarding different mechanisms in muscle aging. An additional experiment on GPA-treated rats, performed in our laboratory, provided surprising results on regenerative capacity in aged rat muscles and raised many intriguing questions. The experiment, along with future studies regarding GPA, ETC abnormalities in post mitotic tissues and interventions of sarcopenia are listed below.

Future Directions

1. Fiber number restoration in aged rat muscle

Multiple mechanisms contribute to age-related decline in muscle mass and strength. There is a decline in nutrient uptake, anabolic capacity, physical activity, innervation and regenerative capacity in aged tissue. Satellite cells, the progenitor cells of muscle involved in repair, have

reduced regenerative and functional capability in aged tissue (reviewed in Demontis *et al.,* 2013). Parabiotic experiments, where a young and old rat are surgically joined to share a circulatory system, suggest that changes in extrinsic factors such as circulating hormones and cytokines contribute to age-related decline in regeneration (reviewed in Jones and Rando, 2011). There is, however, data suggesting that, at very old age, rats can recover muscle mass. In 34 month FBN rats, antioxidant treatment following muscle disuse reversed muscle atrophy in plantaris muscle. Treated rats had hypertrophic fibers, activation of satellite cells and reduced apoptosis (Alway *et al.,* 2014).

To observe the effect of GPA removal on aged tissue, 30 month old FBN rats were fed 1% GPA or normal food chow for 4 months (n=12 per group). At 34 months, FBN rats were given normal food chow for 2 months and were euthanized at 36 months of age. At the end of the experiment, 10 controls rats and 9 GPA-treated rats were euthanized and quadriceps were extracted to determine muscle mass and embedded in optimal cutting media for histochemistry and immunohistochemical analysis.

In chapter 3, I observed that GPA treatment of 4 months induced significant decline in body weight, muscle mass and fiber number. RF muscle in 34 month controls had 8859 ± 162 and GPA treated had 7270 ± 324 fibers, a loss of 1589 fibers. After 2 months of recovery, however, there was no detectable difference in body weight, muscle mass and fiber number between 36 month control and GPA-treated rats. Fiber count in rectus femoris in controls was 8269 ± 271 and in GPA rats, 8619 ± 224. Interestingly, a significant increase (p value = 0.006) in RF fiber number was detected between 4 month GPA treatment and 2 month GPA recovered rats

(Figure 4.1A). This finding suggests that, in a span of 2 months, biological processes were activated reversing the decline in muscle mass and fiber number. Similar to our observations, DeTata *et al.*(1993) reported a complete restoration of muscle mass of young GPA treated rats following 1 month of removal.

As described in chapter 3, 119 fibers were randomly selected and followed through 1000 µm. In GPA treated rats, 15.1% of the fibers were ETC abnormal, in the control rats, all randomly selected fibers were ETC normal. This suggests that GPA treatment of 4 months induced the accumulation of latent mtDNA deletions which was phenotypically observed by the increased incidence of respiratory-deficient muscle fibers. After 2 months on normal food chow, 36 month GPA-treated rats had muscle mass and fiber number similar to controls, however, the ETC abnormalities were significantly increased. In a single 10µm section, 36 month aged rats had 17 ± 4 (Cheema *et al.,* 2015) ETC abnormal fibers while in 36 month GPA rats there were 101 ± 33 abnormal fibers **(Figure 4.1B)**. Prior to the 2 month recovery, 34 month GPA-treated rats had an ETC abnormality abundance of 159 ± 23. When comparing ETC abnormality abundance in 36 month GPA-treated versus 34 month GPA-treated, there is a decline of 58 ETC abnormal fibers. The decline in the abundance of ETC abnormal fibers and not in ETC normal fibers in RF suggests, that in the 36 month recovered rats, ETC abnormal fibers are being preferentially lost (~1 ETC abnormal fiber is lost per day). This leads to an intriguing question that once all ETC abnormalities are generated, how long does it take for the muscle to completely abolish them? If some recovered rats were allowed to live a month longer, this hypothesis could have been tested by detecting a lower abundance of ETC abnormal fibers.

Additionally, 36 month FBN rats are very old rats, therefore, for the recovery process to be most fruitful, either i) GPA treatment should be shorter than 4 months to allow for a longer recovery period and ii) the onset of 4 month treatment should be earlier than 30 months.

36 month GPA recovered rats also had a significant increase in fiber number compared to 34 month GPA-treated rats. This might be due to hypertrophic fibers splitting into several fibers. Interestingly, 36 month GPA-treated rats had hypertrophic fibers compared to controls **(Figure 4.1C)**. This phenomenon of fiber splitting has been observed in birds (Alway *et al.,* 1989), cats (Mikesky *et al.,* 1989) and rats in resistance exercise studies (Tamaki *et al.,* 1992). This increase in fiber number was associated with increase in muscle function. However, it is unknown if muscle function improved in 36 month GPA recovered rats. It would be interesting to perform muscle functional studies such as treadmill and swimming experiments on the 36 month recovered rat to determine that the restoration of muscle mass and fiber number also restores muscle function in aged rats.

The 36 month rat samples can be used to address the question whether 4 month of GPA treatment induced the accumulation of all mtDNA deletions. In aged rats, 10-25% of ETC normal fibers had low abundance of mtDNA deletions (Pak *et al.,* 2004). GPA-treatment would induce mitochondrial biogenesis accelerating the accumulation of mtDNA deletions. These mtDNA deletions would disrupt ETC function and induce cell death. Hence, it can be hypothesized that, after GPA treatment, 36 month recovered rats would have a lower frequency of mtDNA deletions in ETC normal fibers as 10-25% are probably lost or are now ETC abnormal.

As shown in chapter 3, GPA treatment resulted in a significant increase in fibrotic tissue in treated rats accompanied with muscle atrophy. Our preliminary data indicates that muscle mass was regained in the 36 month old rats that were withdrawn from GPA. The effect of GPA removal on fibrotic tissue has not been experimentally analyzed. Histological analysis indicated that 36 month GPA rats have similar muscle morphology as to 36 month old control rats. This suggests that GPA removal did reduce fibrotic tissue. A study in aged hearts in mice has shown that fibrosis can be reversed by caloric restriction (Yan *et al.,* 2013). Old mice on normal food had significant fibrosis in heart tissue. Caloric restriction was initiated after cardiomyopathy had developed in aged mice. After 2 months on CR diet, fibrosis was significantly reduced in the old mice to similar levels observed in young mice on normal food suggesting that fibrosis can be repaired. As there is evidence of repairing fibrotic tissue, it would be intriguing to determine if the 2 months on normal chow affected fibrotic tissue by removing the collagen deposition induced by the 4 month GPA treatment.

Our data suggest that, upon GPA removal, there was complete restoration of muscle mass and fiber number. Additionally, we observed that the fibers had become hypertrophied. These findings indicate that, within 2 months of GPA removal, most processes have been activated and we are observing the end stage of muscle adaptations. Once rodents are removed from GPA, the drug is cleared from tissue relatively quickly and creatine levels return to normal within 1 month with complete recovery of mitochondrial perturbations by 4 months (DeTata *et al.,* 1993). All previous studies using GPA have, however, been reported in young animals and GPA withdrawal has not been studied in old rats. Therefore, the specific effects of GPA removal

on rats should be studied at early, middle and late time periods of the treatment duration to fully understand when the changes are activated in old muscles.

2. Future studies with GPA

GPA has a similar effect in muscle as exercise. Exercise induces mitochondrial biogenesis via AMPK activation. This results in increases in number of mitochondria and mtDNA, muscle mass increase and fiber hypertrophy. Increase in fiber CSA is contributed to the activation of satellite cells by physical stimuli. Similar to exercise, satellite cells have been shown to become activated by GPA treatment *ex vivo*. GPA supplementation in C2C12, a mouse muscle cell line, induced myoblasts to differentiate into myotubes. Myotubes had larger nuclear domains and diameters in GPA supplementation (Ohira *et al.,* 2011). Following 4 month GPA treatment, interstitial nuclei adjacent to myofibers (these could be myoblasts) are positive for activated caspase 3. This suggests either that i) satellite cells were undergoing apoptosis or ii) satellite cells were undergoing differentiation. Activated caspase 3 plays a significant role in initiation of myogenic differentiation by inhibiting satellite cell self-renewal via the cleavage of Pax 7 (Dick *et al.,* 2015). After 2 months on normal chow, 36 month GPA treated rats had an increase in fiber CSA. This increase may be due to satellite cell activation and increase in nuclear domain size. There was a trend of increase in cl-Cas3 in interstitial nuclei at 4 months of treatment, however, this trend was not observed 2 months post-GPA treatment. It is possible that, during GPA treatment, satellite cells were activated and fused with existing myofibers, leading to fiber hypertrophy observed upon GPA removal. To experimentally confirm this effect, satellite cells

in their activated or quiescent state can be immunostained in GPA-treated muscle sections. To observe hypertrophy induced by GPA removal, rats can be treated with BrdU. Satellite cells, once activated, will incorporate BrdU in proliferating cells and will fuse with the existing myofibers. Hypertrophic fibers will have internal myonuclei that are BrdU positive.

Mitochondrial biogenesis has many advantageous effects and has been implicated in healthy aging (Martin-Montalvo *et al.,* 2013), caloric restriction (Lopez-Lluch *et al.,* 2006) and exercise (Hood *et al.,* 2009). Furthermore, GPA administration of 8 weeks induced mitochondrial biogenesis in young rats as increased levels of mitochondrial density, PGC 1-alpha mRNA and cytochrome c levels were detected in skeletal muscle (Reznick *et al.,* 2007). As most studies have largely focused on younger ages, age-dependent effects with GPA treatment are unknown. Recent studies have suggested that GPA may have beneficial effects on aging as GPA administration increased lifespan in Drosophila (Yang *et al.,* 2015) and delayed neurodegeneration in mice (Horvath *et al.,* 2011). Therefore, it is possible that GPA may have beneficial effects on 75-90% healthy muscle fibers that contain only wild-type mtDNA copies (Pak *et al.,* 2004). To determine the positive effects of GPA, a future study should compare the transcriptional profile of GPA-treated ETC normal fibers with aged ETC normal fibers. ETC normal fibers in GPA treatment may have upregulation of anabolic pathways compared to natural aged fibers.

In the initial GPA experiment (Herbst *et al.,* 2013), 7 weeks of treatment resulted in a 2 fold increase in mtDNA copy number and 3 fold increase in ETC abnormalities without loss in muscle mass. Other researchers found that short GPA treatment of 2 months induces mitochondrial

biogenesis in rodents (Reznick *et al,* 2007; reviewed in Oudman *et al.,* 2013). In this current study, fiber loss in muscle was induced by a longer treatment and administered to older rats that have a greater burden of mtDNA deletions. We detected an increase in ETC abnormalities and accumulation of mtDNA deletions in rats treated with GPA for 4 months. Interestingly, wild-type mtDNA copy numbers in GPA-treated muscle were similar to controls and preliminary analysis detected no change in PGC-1 alpha, PPAR or cleaved caspase 3. It is possible, however, that GPA induced mitochondrial biogenesis within the first 7 weeks of the 4 month treatment. This suggests that GPA might be acting differently in short versus long exposures. In longer exposures, the muscle initially responds to the GPA treatment, however, after a certain period, the biological processes return to homeostasis. To test this hypothesis, aged rats should be treated with GPA for 0-6 months with cohorts sacrificed every month. This would allow us to determine the chronological order of induction of mitochondrial biogenesis, ETC abnormality appearance and fiber loss.

There is strong literature supporting a glycolytic to oxidative metabolic switch induced by GPA administration. Affected muscles have a higher percent of the oxidative fiber type which results in treated rats exhibiting a higher endurance capacity in swimming and treadmill exercises. Rodents have an increase in mitochondrial oxidative proteins in their skeletal muscle, increase in type I fibers and decline in type II fiber CSA (Oudman *et al.,* 2013; van Deursen *et al.,* 1994; Mahanna *et al.,* 1980). These findings suggest that GPA has a preferential effect on different fiber types and muscles. It has been previously reported that in young rats, 2 months of GPA treatment induced type II fiber atrophy (glycolytic fibers) whereas oxidative fibers were

unaffected (van Deursen *et al.,* 1994). Oxidative fibers have a smaller cross sectional area and are enriched in mitochondria whereas glycolytic fibers have a larger CSA and a lower mitochondrial content. In chapter 3, increase in mitochondrial activity and decline in fiber CSA in 34 month GPA-treated rats suggested a possible shift to oxidative metabolism. A significant decline of 47% in fiber CSA was observed in GPA-treated muscle. However, fiber type specific effect was not determined. It is possible that GPA induced type II fiber atrophy in our experiments as we have focused on quadricep tissue, a glycolytic muscle susceptible to sarcopenia. However, the effect of chronic GPA treatment on oxidative fibers in old rats is unknown. In longer periods, GPA may affect oxidative fibers to a lesser degree than glycolytic fibers. As GPA has a fiber type effect, it would be interesting to delineate the molecular mechanisms involved in fiber atrophy in GPA-treated muscles and identify pathways present in sarcopenia-resistant muscles.

3. Mitochondrial DNA deletions as general cause of aging in post-mitotic tissues.

Post-mitotic tissues such as skeletal muscle, heart and brain are composed of terminally differentiated cells. As these cells do not proliferate, they accumulate damaging signals over time which contribute to the aging phenotype. As stated in the mitochondrial theory of aging, one of the damaging signals is the accumulation of mtDNA mutations. The role of mitochondrial DNA deletions has been well described in aging of skeletal muscle. Mutant mitochondrial genomes have been detected in other post-mitotic tissues such as aged heart (Mohamed *et al.,* 2006) and brain (Kraytsberg *et al.,* 2006). The molecular mechanism of age-dependent cell loss

due to mtDNA deletions as observed in aged skeletal muscle fibers has not been delineated in other post-mitotic tissues. The identification of similar molecular pathways will provide a ubiquitous role of mtDNA deletions, providing a strong support of mitochondrial damage in the aging process. The following section will outline evidence in aged heart and brain suggesting that the role of mtDNA deletions may be a universal phenomenon.

Myocardial efficiency declines with progressing age (Yaniv *et al.,* 2013). In the aging heart, the left ventricle is enlarged, fibrotic tissue is increased and systolic/diastolic function is impaired (Sheydina *et al.,* 2011). At the cellular and molecular level, aged cardiac myocytes have defects in ATP dysregulation, mitochondrial calcium homeostasis, altered mitochondrial protein expression and function (Yaniv *et al.,* 2013). In humans, past the age of 50, all aged hearts had increased abundance of COX- cells (Müller-Höcker, 1989). The levels of ETC complex subunits, such as complexes 1, 2 and 3, decrease with age (Gomez *et al.,* 2009), the number of ETC abnormal myocytes increase (Wanagat *et al.*, 2002) and enzymatic activities decline (Suh *et al.,* 2003). mtDNA deletions have been identified in aged cardiomyocytes from humans (Arai *et al.,* 2003) (Mohamed *et al.,* 2006) and rats (Wanagat *et al.,* 2002) as well as in adult cardiac stem cells from mice (Lushaj *et al.,* 2012). In a transgenic mouse model expressing mutant mitochondrial helicase, accumulation of mtDNA deletions in cardiomyocytes is accelerated, and is phenotypically observed by cardiac dysfunction (Baris *et al.,* 2015). Similar to skeletal muscle, mtDNA deletions colocalize with COX- cardiomyocytes suggesting the clonal expansion of mtDNA deletions disrupts ETC function in cardiomyocytes (Müller-Höcker, 1989; Wanagat *et al.,* 2002) and there is age-dependent susceptibility to apoptosis (reviewed in Sheydina *et al.,*

2011). In skeletal muscle, ETC abnormal fibers predominantly undergo apoptosis and necrosis and are the contributing factor of age-dependent fiber loss (Cheema *et al.,* 2015) with many studies reporting increased apoptosis in aged skeletal muscle tissue (Alway *et al.,* 2011). A causative association of ETC dysfunction and cell death was reported in a Drosophila transgenic model of cardiomyopathy. Cardiac dysfunction was induced by knocking down COX assembly factors which induced mitochondrial dysfunction, increase in ETC abnormal cardiac cells and apoptotic cells (Martinez-Morentin *et al.,* 2015). This suggests a similar role of ETC abnormalities inducing cell death in heart cells as seen in skeletal muscle. However, in aged heart tissue it is still unknown whether COX- cardiac cells are the leading cause of apoptotic cells.

Age-dependent declines in neuronal number has been debated for several years. Unlike skeletal muscle and heart, the decline in neuronal number with age is not clear. In aged rats there is no reported difference in the neuronal numbers when comparing old rats of 12 month and 22 months age (Mortera and Herculano-Houzel, 2012). As technology progresses, more sensitive and accurate techniques are being developed, therefore, studies should confirm the age-dependent change of neuronal numbers. There is, however, a consensus, that with increasing age, there is a functional decline in cognition. There is an age-dependent increase in brain atrophy and decline in cognitive function. Gene expression studies from aged brain tissue of C.elegans, rats, rhesus monkeys and humans have indicated a strong role for mitochondrial dysfunction in the ageing brain (Bishop *et al.,* 2010). In aged prefrontal cortex from humans, genes involved in mitochondrial function and oxidative stress response were detected (Lu *et al.,*

2004). Impairment of mitochondrial function in aged human neurons is due to the abundance of mtDNA deletions (Kraytsberg *et al.,* 2006). Similar to skeletal muscle and heart, there is an age-dependent increase in COX- neurons in hippocampal regions from individuals (Cottrell *et al.,* 2001) and the COX deficient phenotype is associated with high thresholds of unique mtDNA deletions (Kraytsberg *et al.,* 2006). As described in Chapter 2, COX- cells are more prone to apoptosis. In brain, apoptosis has been extensively studied in neurodegenerative diseases. Stimuli such as calcium dysregulation, increased excitotoxicity, decline in neurotrophic factors and mitochondria perturbations induce apoptosis (reviewed in Mattson and Magnus, 2006). In aging, these stimuli exist, albeit to a lesser degree. A recent study in aged rat brain determined a pro-apoptotic protein, AIF, translocated to the nucleus only in aged rat brain indicating an increased apoptotic potential (Yu *et al.,* 2011). Therefore, cell death may be implicated in the age-dependent decline in neuronal function. Cognitive dysfunction in aged brain is primarily thought to be due to alterations in neuronal morphology. Gene expression analysis identified significant changes with ageing in the expression of synaptic genes (reviewed in Bishop *et al.,* 2010). Aged neurons have fewer synapses, declines in dendrite number and cellular function. Even though there is no detectable difference in neuronal number, COX- aged neurons may have a significant role in changes in neuronal morphology.

4. Interventions for sarcopenia that delay ETC abnormalities

In skeletal muscle, accumulation of ETC abnormalities with increasing age has been observed in a number of species from rats, rhesus monkeys and humans. Muscles that exhibit the most

atrophy are more susceptible to ETC abnormalities. These studies suggest a strong biological role of ETC abnormalities in the ageing process and interventions that delay or reduce the ETC abnormalities in aged individuals would be of great interest. Currently, caloric restriction is the only intervention that reduces the ETC abnormality load in aged rats (Bua *et al.,* 2004) and rhesus monkeys (McKiernan *et al.,* 2011).

Caloric restriction extends longevity and healthspan from yeast to mammals and its effects have been documented in a number of biological systems, e.g., ameliorating sarcopenia (McKiernan *et al.,* 2011) and age-associated cardiomyopathy (Yan *et al.,* 2013). Rats on a 40% calorie restricted diet maintained their muscle mass and had lower ETC abnormalities compared to *ad libitum* fed rats. Interestingly, the length of the focal defects did not differ between the *ad libitum* and CR rats suggesting that the molecular mechanisms activated by CR affected the formation of ETC abnormalities and not their progression (Bua *et al.,* 2004). Similar findings were also observed in rhesus monkeys (McKiernan *et al.,* 2011). Although, the effect of CR on humans is relatively unknown due to their longer lifespan and a limited sample number, caloric restriction does improve healthspan (Anderson and Weindruch, 2012), reduces cardiomyopathy and increases cardiovascular function (Bales and Kraus, 2013) similar to observations in rodent studies. Caloric restriction is not a feasible intervention for humans as it requires strong motivation. Therefore, identifying CR mimetics has been of great interest.

The mechanism by which CR delays aging is unknown. Many studies have implicated a strong role of mitochondria in CR. With caloric restriction, mitochondria produce less ROS, there is a decline in oxidative damage and the induction of mitophagy increases the turnover rate of

damaged mitochondria. The mitochondrial biogenesis pathway involving AMPK/Sirtuin/ PGC1alpha is upregulated in CR rodents with the metabolic sensors, AMPK and Sirtuins, activating PGC1-alpha. Sirtuins also play a significant role in autophagy which is also elevated in CR animals (Sharples *et al.,* 2015). Hence, CR mimetic compounds that activate mitochondrial biogenesis, induce autophagy and antioxidants seem to be the most promising (Lopez-Lluch and Navas, 2016).

The majority of the CR studies have focused on onset at young age as animals with old age onset do not respond so robustly (Lopez-Lluch and Navas, 2016). The benefits of caloric restriction are still observed when CR is initiated at middle age. In old rats, fiber number of the vastus lateralis muscles was preserved and ETC abnormality abundances were reduced in CR onset at middle age (Aspnes *et al.,* 1997). A recent study, however, suggests that CR onset in old animals can reverse age-associated cardiomyopathy (Yan *et al.,* 2013). Additionally, the combination of CR and exercise can be synergistic. In mice, intermittent fasting and exercise was shown to elevate antioxidant response only in old animals suggesting an age-dependent effect (Rodriguez-Bies *et al.,* 2015). Our studies with GPA, an AMPK activator, indicates that mitochondrial biogenesis, when activated in aged animals, is deleterious to fibers with mitochondrial dysfunction. There is, however, a decline in mitochondrial quality control with age. It would be interesting to study the additive effect of induction of autophagy and mitochondrial biogenesis in aged rats. ETC abnormalities might accumulate as there is an age-dependent lag in mitochondrial quality control. Thus, upon induction of mitophagy, dysfunctional mitochondria might be degraded preferentially. Rapamycin is a pharmacological

drug that induces autophagy and can extend lifespan in mice (Ehninger *et al.,* 2014). This extension is, however, due to prevention of cancer rather than delay of the aging process (Neff *et al.,* 2013). Another CR mimetic, resveratrol, activates AMPK, sirtuins and mitophagy (Testa *et al.,* 2014) and might be an ideal candidate to study the additive effect of autophagy upon mitochondrial biogenesis induction in muscle ageing.

Conclusion

Sarcopenia is the age-dependent loss of muscle mass and function and has been observed in a variety of species from yeast, flies, rats, monkeys and humans. The muscle wasting phenomena is prevalent in elderly posing a huge risk to health and mortality. Muscles can be susceptible or resistant to age-dependent fiber loss as not all muscles undergo sarcopenia due to differences in muscle fiber type composition. Only muscles that are susceptible to sarcopenia exhibit age-dependent accumulation of fibers with mitochondrial abnormalities and accumulation of mtDNA deletion e.g. rectus femoris and vastus lateralis. Muscles that do not exhibit age-dependent muscle atrophy do not have any mitochondrial abnormalities and mtDNA deletions e.g. adductor longus muscle. ETC abnormal fibers have been demonstrated to contain unique mtDNA deletions in focal regions of the affected fiber in rats (Cao *et al.,* 2001; Wanagat *et al.,* 2001), monkeys (Gokey *et al.,* 2004) and humans (Bua *et al.,* 2006). Research in our laboratory has demonstrated a strong link between ETC abnormalities and mtDNA deletions, revealing that, unique mtDNA deletions accumulate via mitochondrial biogenesis (Herbst *et al.,* 2013) to a threshold of 95-98% which than disrupts the electron transport chain (Herbst *et al.,* 2007).

My contribution to understanding sarcopenia was to determine the role of ETC abnormal fibers in fiber loss. Our lab has previously identified that ETC abnormal fibers are more prone to intrafiber atrophy which also, in some severe cases, results in the fiber breaking within the abnormal segment. It was also identified that there is an inverse relationship between ETC abnormalities length and intra-fiber atrophy (Bua *et al.,* 2004). The longer the length of the abnormal segment, the more atrophic the fiber is in that regions. It was also observed that ETC abnormal segments had oxidative damage (Wanagat *et al.,* 2001) and expression of cell death markers (Herbst *et al.,* 2013). As ETC abnormal fibers are atrophic and appear in muscles prone to fiber loss, we hypothesized that ETC abnormal fibers are undergoing apoptosis and necrosis. In Chapter 2, I observed that ~80% of the necrotic fibers detected in aged rat tissue were ETC abnormal. Similarly ~70% of cleaved caspase 3 fibers detected in aged rat tissue were ETC abnormal. These data suggest that the major sources of necrotic and apoptotic fibers in aged muscle tissue are ETC abnormal fibers. I also identified that apoptosis and necrosis occur simultaneously in longer abnormal segments and were always detected in the case of broken fibers. Furthermore, in rats, the number of fibers lost per day correlated with the number of fibers that were cleaved caspase 3 positive. In Chapter 2, at 36 months of age, the rectus femoris muscle had ~6 fibers that were immunopositive for cleaved caspase 3 within the tissue sample. In line with this finding, between 33-36 months a rat loses ~11 fibers per day in the rectus femoris muscle (Bua *et al.,* 2008). These data suggest that ETC abnormal fibers are a significant source of fiber loss in sarcopenia.

My findings in Chapter 2 suggest a strong role of mitochondria in fiber loss. In Chapter 3, I establish a causative role of mitochondrial dysfunction in sarcopenia by inducing ETC abnormalities via a pharmacological compound. Our lab has previously found that ETC abnormal fibers activate mitochondrial biogenesis, possibly to correct for the energy deficiency in the cell. Microarray analysis revealed that genes involved in mitochondrial biogenesis, lipid oxidation and cellular metabolism were upregulated in ETC abnormal segments. The results were immunohistochemically validated and transcription factor for mitochondrial genes (PGC 1 alpha), mitochondrial DNA polymerase (Polg) and energy sensing molecule (AMPK) have been detected in ETC abnormal segments. Induction of mitochondrial biogenesis in 28 month old rats by guanidinopropionic acid resulted in 3 fold increase in ETC abnormalities and mtDNA genome copy number (Herbst *et al.,* 2013). We used this pharmacological compound to test the causal role of ETC abnormalities in sarcopenia. We hypothesized that GPA onset administration at an older age would result in fiber loss. In Chapter 3, I observed a significant decline in the fiber number of 34 month GPA-treated rats. This was accompanied by an increase in ETC abnormal fibers, apoptotic myofibers, intra-fiber atrophy, broken fibers and fibrosis. Interestingly, abnormalities that were short in length were necrotic in GPA-treated rats. This was not observed in natural aging, as seen in Chapter 2, suggesting that GPA-treated rats accelerated the molecular events triggered by ETC abnormal fibers. These data suggest that ETC abnormal fibers contribute to fiber loss seen in aged muscle tissue. In conclusion, our studies have delineated a molecular pathway of fiber loss in sarcopenia where mitochondrial dysfunction is the primary cause of cell death. Studying mechanisms induced in ETC dysfunctional cells may allow us to identify certain pathways to delay the occurrence of cell death. Based on our

findings and the fact that there is a decline in mitochondrial function with increasing age detected in various tissues, COX- cells may play an integral role in the aging process.

Figure 4.1. GPA withdrawal induces increase in fiber number and fiber CSA. (A) Increase in fiber number after GPA withdrawal in rectus femoris muscle of 34 month GPA-treated, 36 month GPA-treated and 36 month control rats. Rats were fed GPA for four months prior to 2 month withdrawal. Controls received *ad libitum* food for 6 months. (B) ETC abnormal fiber counts from one 10μm section in rectus femoris muscle of 34 month GPA-treated, 36 month GPA-treated and 36 month control rats. (C) Fiber cross-sectional area measurements in 36-month controls and GPA-treated rats. Significant p-value < 0.001.

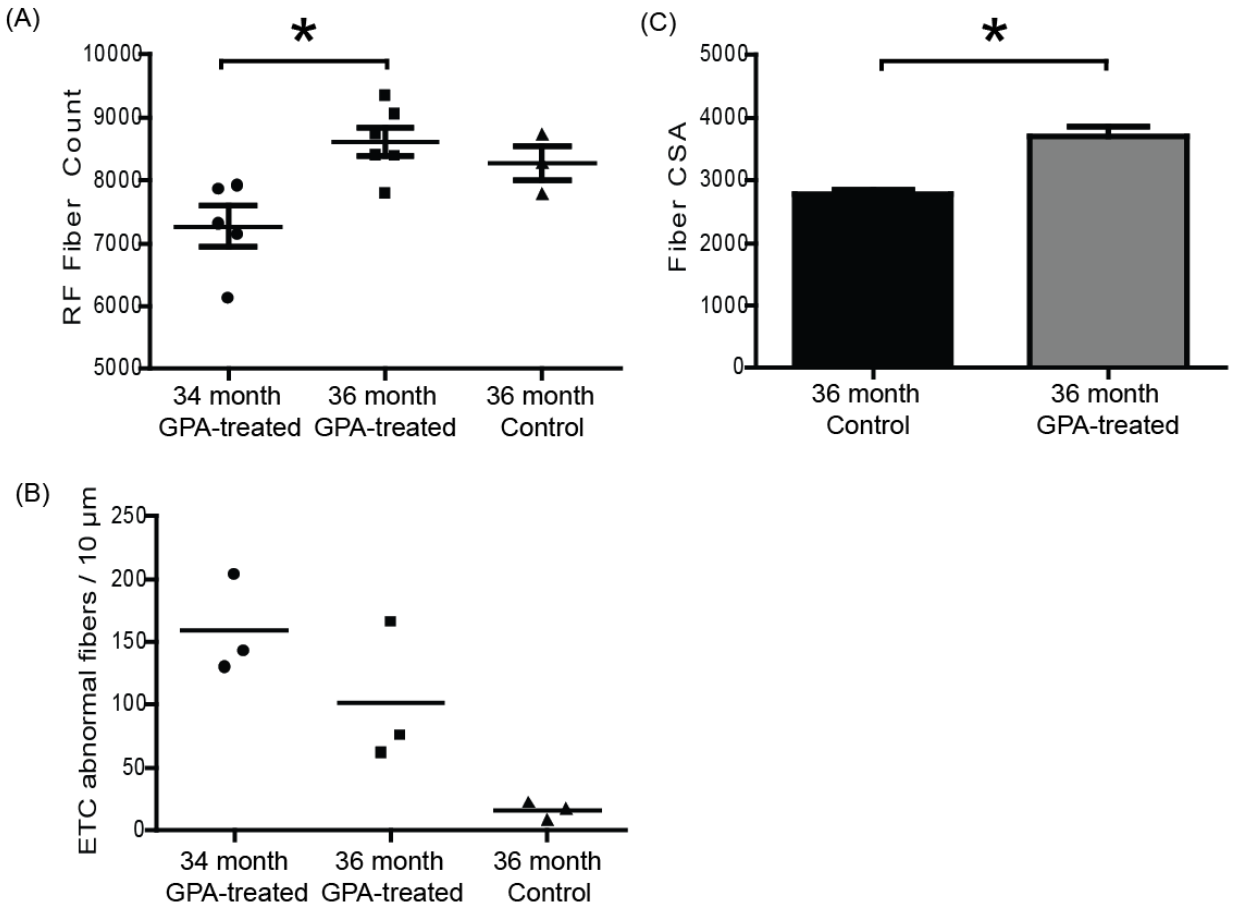
(A)
*
10000
9000
8000
7000
6000
5000
RF Fiber Count
34 month GPA-treated
36 month GPA-treated
36 month Control
(C)
*
5000
4000
3000
2000
1000
0
Fiber CSA
36 month Control
36 month GPA-treated
(B)
250
200
150
100
50
0
ETC abnormal fibers / 10 µm
34 month GPA-treated
36 month GPA-treated
36 month Control

REFERENCES

Abmayr, S., R.W. Crawford, and J.S. Chamberlain. 2004. Characterization of ARC, apoptosis repressor interacting with CARD, in normal and dystrophin-deficient skeletal muscle. *Hum Mol Genet*. 13:213-221.

Akpek, E.K., and R.A. Smith. 2013. Overview of Age-Related Ocular Conditions. *Am J Manag Care*. 19:S67-S75.

Alemi, M., A. Prigione, A. Wong, R. Schoenfeld, S. DiMauro, M. Hirano, F. Taroni, and G. Cortopassi. 2007. Mitochondrial DNA deletions inhibit proteasomal activity and stimulate an autophagic transcript. *Free Radical Biology and Medicine*. 42:32-43.

Alnaqeeb, M.A., and G. Goldspink. 1987. Changes in Fiber Type, Number and Diameter in Developing and Aging Skeletal-Muscle. *J Anat*. 153:31-45.

Alway, S.E., B.T. Bennett, J.C. Wilson, N.K. Edens, and S.L. Pereira. 2014. Epigallocatechin-3-gallate improves plantaris muscle recovery after disuse in aged rats. *Experimental Gerontology*. 50:82-94.

Alway, S.E., M.R. Morissette, and P.M. Siu. 2011. Chapter 4 - Aging and Apoptosis in Muscle. *In* Handbook of the Biology of Aging (Seventh Edition). E.J. Masoro and S.N. Austad, editors. Academic Press, San Diego. 63-118.

Alway, S.E., P.K. Winchester, M.E. Davis, and W.J. Gonyea. 1989. Regionalized Adaptations and Muscle-Fiber Proliferation in Stretch-Induced Enlargement. *Journal of Applied Physiology*. 66:771-781.

Anderson, R.M., and R. Weindruch. 2012. The caloric restriction paradigm: Implications for healthy human aging. *Am J Hum Biol*. 24:101-106.

Anderson, S., A.T. Bankier, B.G. Barrell, M.H.L. de Bruijn, A.R. Coulson, J. Drouin, I.C. Eperon, D.P. Nierlich, B.A. Roe, F. Sanger, P.H. Schreier, A.J.H. Smith, R. Staden, and I.G. Young. 1981. Sequence and organization of the human mitochondrial genome. *Nature*. 290:457-465.

Arai, T., K. Nakahara, H. Matsuoka, M. Sawabe, K. Chida, S. Matsushita, K. Takubo, N. Honma, K. Nakamura, N. Izumiyama, and Y. Esaki. 2003. Age-related mitochondrial DNA deletion in human heart: Its relationship with cardiovascular diseases. *Aging Clin Exp Res*. 15:1-5.

Artal-Sanz, M., and N. Tavernarakis. 2005. Proteolytic mechanisms in necrotic cell death and neurodegeneration. *Febs Lett*. 579:3287-3296.

Aspnes, L.E., C.M. Lee, R. Weindruch, S.S. Chung, E.B. Roecker, and J.M. Aiken. 1997. Caloric restriction reduces fiber loss and mitochondrial abnormalities in aged rat muscle. *The FASEB Journal*. 11:573-581.

Austad, S.N. 1993. Retarded Senescence in an Insular Population of Virginia Opossums (Didelphis-Virginiana). *J Zool*. 229:695-708.

Bakeeva, L.E., Y.S. Chentsov, and V.P. Skulachev. 1978. Mitochondrial framework (reticulum mitochondriale) in rat diaphragm muscle. *Biochimica et Biophysica Acta (BBA) - Bioenergetics*. 501:349-369.

Baker, D.J., and R.T. Hepple. 2006. Elevated caspase and AIF gene expression correlate with progression of sarcopenia during aging in male F344BN rats. *Experimental Gerontology*. 41:1149-1156.

Bales, C.W., and W.E. Kraus. 2013. Caloric Restriction IMPLICATIONS FOR HUMAN CARDIOMETABOLIC HEALTH. *J Cardiopulm Rehabil*. 33:201-208.

Baris, O.R., S. Ederer, J.F.G. Neuhaus, J.C. von Kleist-Retzow, C.M. Wunderlich, M. Pal, F.T. Wunderlich, V. Peeva, G. Zsurka, W.S. Kunz, T. Hickethier, A.C. Bunck, F. Stockigt, J.W. Schrickel, and R.J. Wiesner. 2015. Mosaic Deficiency in Mitochondrial Oxidative Metabolism Promotes Cardiac Arrhythmia during Aging. *Cell Metab*. 21:667-677.

Barja, G. 2004. Aging in vertebrates, and the effect of caloric restriction: a mitochondrial free radical production-DNA damage mechanism? *Biological reviews of the Cambridge Philosophical Society*. 79:235-251.

Barja, G., and A. Herrero. 2000. Oxidative damage to mitochondrial DNA is inversely related to maximum life span in the heart and brain of mammals. *Faseb J*. 14:312-318.

Baumgartner, R.N., K.M. Koehler, D. Gallagher, L. Romero, S.B. Heymsfield, R.R. Ross, P.J. Garry, and R.D. Lindeman. 1998. Epidemiology of sarcopenia among the elderly in New Mexico. *Am J Epidemiol*. 147:755-763.

Behrens, M.I., M. Silva, A. Schmied, F. Salech, H. Manzur, R. Rebolledo, R. Bull, V. Torres, M. Henriquez, and A.F.G. Quest. 2011. Age-Dependent Increases in Apoptosis/Necrosis Ratios in Human Lymphocytes Exposed to Oxidative Stress. *The Journals of Gerontology Series A: Biological Sciences and Medical Sciences*. 66A:732-740.

Beregi, E., and O. Regius. 1987. Comparative Morphological-Study of Age-Related Mitochondrial Changes of the Lymphocytes and Skeletal-Muscle Cells. *Acta Morphol Hung*. 35:219-224.

Bergeron, R., J.M. Ren, K.S. Cadman, I.K. Moore, P. Perret, M. Pypaert, L.H. Young, C.F. Semenkovich, and G.I. Shulman. 2001. Chronic activation of AMP kinase results in NRF-1 activation and mitochondrial biogenesis. *Am J Physiol-Endoc M*. 281:E1340-E1346.

Bhakdi, S., and J. Tranum-Jensen. 1978. Molecular nature of the complement lesion. *Proceedings of the National Academy of Sciences of the United States of America*. 75:5655-5659.

Bishop, N.A., T. Lu, and B.A. Yankner. 2010. Neural mechanisms of ageing and cognitive decline. *Nature*. 464:529-535.

Blackwood, J.K., S.C. Williamson, L.C. Greaves, L. Wilson, A.C. Rigas, R. Sandher, R.S. Pickard, C.N. Robson, D.M. Tumbull, R.W. Taylor, and R. Heer. 2011. In situ lineage tracking of human prostatic epithelial stem cell fate reveals a common clonal origin for basal and luminal cells. *J Pathol*. 225:181-188.

Blagosklonny, M.V. 2010. Revisiting the antagonistic pleiotropy theory of aging TOR-driven program and quasi-program. *Cell Cycle*. 9:3151-3156.

Boore, J.L. 1999. Animal mitochondrial genomes. *Nucleic Acids Research*. 27:1767-1780.

Bota, D.A., H. Van Remmen, and K.J.A. Davies. 2002. Modulation of Lon protease activity and aconitase turnover during aging and oxidative stress. *Febs Lett*. 532:103-106.

Boveris, A., N. Oshino, and B. Chance. 1972. The cellular production of hydrogen peroxide. *The Biochemical journal*. 128:617-630.

Braga, M., A.P.S. Hikim, S. Datta, M.G. Ferrini, D. Brown, E.L. Kovacheva, N.F. Gonzalez-Cadavid, and I. Sinha-Hikim. 2008. Involvement of oxidative stress and caspase 2-mediated intrinsic pathway signaling in age-related increase in muscle cell apoptosis in mice. *Apoptosis*. 13:822-832.

Brandes, N., S. Schmitt, and U. Jakob. 2009. Thiol-Based Redox Switches in Eukaryotic Proteins. *Antioxidants & redox signaling*. 11:997-1014.

Bratic, A., and N.-G. Larsson. 2013. The role of mitochondria in aging. *The Journal of Clinical Investigation*. 123:951-957.

Bua, E., J. Johnson, A. Herbst, B. Delong, D. McKenzie, S. Salamat, and J.M. Aiken. 2006. Mitochondrial DNA–Deletion Mutations Accumulate Intracellularly to Detrimental Levels in Aged Human Skeletal Muscle Fibers. *American Journal of Human Genetics*. 79:469-480.

Bua, E., J.K. Johnson, D. McKenzie, and J.M. Aiken. 2008. Sarcopenia Accelerates at Advanced Ages in Fisher 344×Brown Norway Rats. *The journals of gerontology. Series A, Biological sciences and medical sciences*. 63:921-927.

Bua, E., S.H. McKiernan, and J.M. Aiken. 2004. Calorie restriction limits the generation but not the progression of mitochondrial abnormalities in aging skeletal muscle. *The FASEB Journal*.

Bua, E., S.H. McKiernan, J. Wanagat, D. McKenzie, and J.M. Aiken. 2002. Mitochondrial abnormalities are more frequent in muscles undergoing sarcopenia. 2617-2624 pp.

Burke, S.N., and C.A. Barnes. 2006. Neural plasticity in the ageing brain. *Nat Rev Neurosci*. 7:30-40.

Campisi, J. 2013. Aging, Cellular Senescence, and Cancer. *Annual review of physiology*. 75:685-705.

Canada, S. 2012. Life Tables, Canada, Provinces and Territories

2010 to 2012. StatCan, Ottawa, ON.

Canada, S. 2015. Canada's population estimates: Age and sex, July 1, 2015 Ottawa.

Cao, Z., J. Wanagat, S.H. McKiernan, and J.M. Aiken. 2001. Mitochondrial DNA deletion mutations are concomitant with ragged red regions of individual, aged muscle fibers: analysis by laser-capture microdissection. *Nucleic Acids Research*. 29:4502-4508.

Capel, F., V. Rimbert, D. Lioger, A. Diot, P. Rousset, P.P. Mirand, Y. Boirie, B. Morio, and L. Mosoni. 2005. Due to reverse electron transfer, mitochondrial H2O2 release increases with age in human vastus lateralis muscle although oxidative capacity is preserved. *Mechanisms of ageing and development*. 126:505-511.

Cappola, A.R., K. Bandeen-Roche, G.S. Wand, S. Volpato, and L.P. Fried. 2001. Association of IGF-I levels with muscle strength and mobility in older women. *J Clin Endocr Metab*. 86:4139-4146.

Carroll, M.C. 2004. The complement system in regulation of adaptive immunity. *Nat Immunol*. 5:981-986.

Carter, A.J., and A.Q. Nguyen. 2011. Antagonistic pleiotropy as a widespread mechanism for the maintenance of polymorphic disease alleles. *BMC Medical Genetics*. 12:1-13.

Chabi, B., V. Ljubicic, K.J. Menzies, J.H. Huang, A. Saleem, and D.A. Hood. 2008. Mitochondrial function and apoptotic susceptibility in aging skeletal muscle. *Aging Cell*. 7:2-12.

Chan, D.C. 2006. Mitochondria: Dynamic organelles in disease, aging, and development. *Cell*. 125:1241-1252.

Chaturvedi, R.K., P. Adhihetty, S. Shukla, T. Hennessy, N. Calingasan, L. Yang, A. Starkov, M. Kiaei, M. Cannella, J. Sassone, A. Ciammola, F. Squitieri, and M.F. Beal. 2009. Impaired PGC-1α function in muscle in Huntington's disease. *Hum Mol Genet*. 18:3048-3065.

Cheema, N., A. Herbst, D. McKenzie, and J.M. Aiken. 2015. Apoptosis and necrosis mediate skeletal muscle fiber loss in age-induced mitochondrial enzymatic abnormalities. *Aging Cell*. 14:1085-1093.

Chen, H.L., D. Cangello, S. Benson, J. Folmer, H. Zhu, M.A. Trush, and B.R. Zirkin. 2001. Age-related increase in mitochondrial superoxide generation in the testosterone-producing cells of Brown Norway rat testes: relationship to reduced steroidogenic function? *Experimental Gerontology*. 36:1361-1373.

Christensen, K., G. Doblhammer, R. Rau, and J.W. Vaupel. 2009. Ageing populations: the challenges ahead. *Lancet*. 374:1196-1208.

Coggan, A.R., A.M. Abduljalil, S.C. Swanson, M.S. Earle, J.W. Farris, L.A. Mendenhall, and P.M. Robitaille. 1993. Muscle Metabolism during Exercise in Young and Older Untrained and Endurance-Trained Men. *Journal of Applied Physiology*. 75:2125-2133.

Cohen, B.J., M.R. Anver, D.H. Ringler, and R.C. Adelman. 1978. Age-Associated Pathological-Changes in Male Rats. *Fed Proc*. 37:2848-2850.

COLE, D.S., and B.P. MORGAN. 2003. Beyond lysis: how complement influences cell fate. *Clin Sci*. 104:455-466.

Conley, K.E., S.A. Jubrias, and P.C. Esselman. 2001. Oxidative capacity and ageing in human muscle (vol 526, pg 203, 2000). *J Physiol-London*. 533:921-921.

Cooney, C.A. 1993. Are somatic cells inherently deficient in methylation metabolism? A proposed mechanism for DNA methylation loss, senescence and aging. *Growth Dev Aging.* . 57:261-273.

Cortopassi, G.A., and N. Arnheim. 1990. Detection of a specific mitochondrial DNA deletion in tissues of older humans. *Nucleic Acids Research*. 18:6927-6933.

Cortopassi, G.A., D. Shibata, N.W. Soong, and N. Arnheim. 1992. A Pattern of Accumulation of a Somatic Deletion of Mitochondrial-DNA in Aging Human Tissues. *Proceedings of the National Academy of Sciences of the United States of America*. 89:7370-7374.

Cottrell, D.A., E.L. Blakely, M.A. Johnson, P.G. Ince, G.M. Borthwick, and D.M. Turnbull. 2001. Cytochrome c oxidase deficient cells accumulate in the hippocampus and choroid plexus with age. *Neurobiology of Aging*. 22:265-272.

Creagh, E.M. 2014. Caspase crosstalk: integration of apoptotic and innate immune signalling pathways. *Trends in Immunology*. 35:631-640.

Cree, L.M., S.K. Patel, A. Pyle, S. Lynn, D.M. Turnbull, P.F. Chinnery, and M. Walker. 2008. Age-related decline in mitochondrial DNA copy number in isolated human pancreatic islets. *Diabetologia*. 51:1440-1443.

Demontis, F., R. Piccirillo, A.L. Goldberg, and N. Perrimon. 2013. Mechanisms of skeletal muscle aging: insights from Drosophila and mammalian models. *Dis Model Mech*. 6:1339-1352.

D'Erchia, A.M., A. Atlante, G. Gadaleta, G. Pavesi, M. Chiara, C. De Virgilio, C. Manzari, F. Mastropasqua, G.M. Prazzoli, E. Picardi, C. Gissi, D. Horner, A. Reyes, E. Sbisa, A. Tullo, and G. Pesole. 2015. Tissue-specific mtDNA abundance from exome data and its correlation with mitochondrial transcription, mass and respiratory activity. *Mitochondrion*. 20:13-21.

Detata, V., G. Cavallini, M. Pollera, Z. Gori, and E. Bergamini. 1993. The Induction of Mitochondrial Myopathy in the Rat by Feeding Beta-Guanidinopropionic Acid and the Reversibility of the Induced Mitochondrial Lesions - a Biochemical and Ultrastructural Investigation. *International Journal of Experimental Pathology*. 74:501-509.

Dick, S.A., N.C. Chang, N.A. Dumont, R.A.V. Bell, C. Putinski, Y. Kawabe, D.W. Litchfield, M.A. Rudnicki, and L.A. Megeney. 2015. Caspase 3 cleavage of Pax7 inhibits self-renewal of satellite cells. *Proceedings of the National Academy of Sciences of the United States of America*. 112:E5246-E5252.

Dirks, A., and C. Leeuwenburgh. 2004. Aging and lifelong calorie restriction result in adaptations of skeletal muscle apoptosis repressor, apoptosis-inducing factor, X-linked inhibitor of apoptosis, caspase-3, and caspase-12. *Free Radical Biology and Medicine*. 36:27-39.

Dirks, A., and C. Leeuwenburgh. 2005. The Role of Apoptosis in Age-Related Skeletal Muscle Atrophy. *Sports Med*. 35:473-483.

Donato, A.J., I. Eskurza, A.E. Silver, A.S. Levy, G.L. Pierce, P.E. Gates, and D.R. Seals. 2007. Direct evidence of endothelial oxidative stress with aging in humans - Relation to impaired endothelium-dependent dilation and upregulation of nuclear factor-kappa B. *Circ Res*. 100:1659-1666.

Drew, B., S. Phaneuf, A. Dirks, C. Selman, R. Gredilla, A. Lezza, G. Barja, and C. Leeuwenburgh. 2003. Effects of aging and caloric restriction on mitochondrial energy production in gastrocnemius muscle and heart. *Am J Physiol-Reg I*. 284:R474-R480.

Driver, J.A., L. Djousse, G. Logroscino, J.M. Gaziano, and T. Kurth. 2008. Incidence of cardiovascular disease and cancer in advanced age: prospective cohort study. *Brit Med J*. 337.

Dupont-Versteegden, E.E. 2005. Apoptosis in muscle atrophy: Relevance to sarcopenia. *Experimental Gerontology*. 40:473-481.

Edris, W., B. Burgett, O.C. Stine, and C.R. Filburn. 1994. Detection and Quantitation by Competitive Pcr of an Age-Associated Increase in a 4.8-Kb Deletion in Rat Mitochondrial-DNA. *Mutat Res-Dnaging G*. 316:69-78.

Ehninger, D., F. Neff, and K. Xie. 2014. Longevity, aging and rapamycin. *Cell Mol Life Sci*. 71:4325-4346.

Everitt, A.V. 1980. The neuroendocrine system and aging. *Gerontology. 1980;26(2):108-19.*

Failla, G. 1958. The Aging Process and Cancerogenesis. *Ann Ny Acad Sci*. 71:1124-1140.

Fano, G., P. Mecocci, J. Vecchiet, S. Belia, S. Fulle, M.C. Polidori, G. Felzani, U. Senin, L. Vecchiet, and M.F. Beal. 2001. Age and sex influence on oxidative damage and functional status in human skeletal muscle. *J Muscle Res Cell M*. 22:345-351.

Fantin, F., V. Di Francesco, G. Fontana, A. Zivelonghi, L. Bissoli, E. Zoico, A. Rossi, R. Micciolo, O. Bosello, and M. Zamboni. 2007. Longitudinal body composition changes in old men and women: Interrelationships with worsening disability. *J Gerontol a-Biol*. 62:1375-1381.

Figueiredo, P.A., S.K. Powers, R.M. Ferreira, H.J. Appell, and J.A. Duarte. 2009. Aging Impairs Skeletal Muscle Mitochondrial Bioenergetic Function. *J Gerontol a-Biol*. 64:21-33.

Forner, F., L.J. Foster, S. Campanaro, G. Valle, and M. Mann. 2006. Quantitative proteomic comparison of rat mitochondria from muscle, heart, and liver. *Mol Cell Proteomics*. 5:608-619.

Franceschi, C. 1989. Cell proliferation, cell death and aging. *Aging (Milano)*. 1:3-15.

Frontera, W.R., V.A. Hughes, R.A. Fielding, M.A. Fiatarone, W.J. Evans, and R. Roubenoff. 2000. Aging of skeletal muscle: a 12-yr longitudinal study. *Journal of Applied Physiology*. 88:1321-1326.

Fujisawa, K. 1974. Some observations on the skeletal musculature of aged rats: Part 1. Histological aspects. *J Neurol Sci*. 22:353-366.

Gabaldon, T., and M.A. Huynen. 2004. Shaping the mitochondrial proteome. *Bba-Bioenergetics*. 1659:212-220.

Gaipl, U.S., S. Kuenkele, R.E. Voll, T.D. Beyer, W. Kolowos, P. Heyder, J.R. Kalden, and M. Herrmann. 2001. Complement binding is an early feature of necrotic and a rather late event during apoptotic cell death. *Cell Death Differ*. 8:327-334.

Gallegly, J.C., N.A. Turesky, B.A. Strotman, C.M. Gurley, C.A. Peterson, and E.E. Dupont-Versteegden. 2004. Satellite cell regulation of muscle mass is altered at old age. *Journal of Applied Physiology*. 97:1082-1090.

Gianni, P., J.J. Kaczor, M.J. Douglas, P.M. Stuart, and M.A. Tarnopolsky. 2004. Oxidative stress and the mitochondrial theory of aging in human skeletal muscle. *Experimental Gerontology*. 39:1391-1400.

Gokey, N.G., Z. Cao, J.W. Pak, D. Lee, S.H. McKiernan, D. McKenzie, R. Weindruch, and J.M. Aiken. 2004. Molecular analyses of mtDNA deletion mutations in microdissected skeletal muscle fibers from aged rhesus monkeys. *Aging Cell*. 3:319-326.

Gomez, L.A., J.S. Monette, J.D. Chavez, C.S. Maier, and T.M. Hagen. 2009. Supercomplexes of the mitochondrial electron transport chain decline in the aging rat heart. *Arch Biochem Biophys*. 490:30-35.

Goodpaster, B.H., S.W. Park, T.B. Harris, S.B. Kritchevsky, M. Nevitt, A.V. Schwartz, E.M. Simonsick, F.A. Tylavsky, M. Visser, and A.B. Newman. 2006. The loss of skeletal muscle strength, mass, and quality in older adults: The health, aging and body composition study. *J Gerontol a-Biol*. 61:1059-1064.

Grady, J.P., G. Campbell, T. Ratnaike, E.L. Blakely, G. Falkous, V. Nesbitt, A.M. Schaefer, R.J. McNally, G.S. Gorman, R.W. Taylor, D.M. Turnbull, and R. McFarland. 2014. Disease progression in patients with single, large-scale mitochondrial DNA deletions. *Brain*. 137:323-334.

Greaves, L.C., M. Nooteboom, J.L. Elson, H.A.L. Tuppen, G.A. Taylor, D.M. Commane, R.P. Arasaradnam, K. Khrapko, R.W. Taylor, T.B.L. Kirkwood, J.C. Mathers, and D.M. Turnbull. 2014. Clonal Expansion of Early to Mid-Life Mitochondrial DNA Point Mutations Drives Mitochondrial Dysfunction during Human Ageing. *Plos Genet*. 10.

Grinberg, M., M. Schwarz, Y. Zaltsman, T. Eini, H. Niv, S. Pietrokovski, and A. Gross. 2005. Mitochondrial carrier homolog 2 is a target of tBID in cells signaled to die by tumor necrosis factor alpha. *Mol Cell Biol*. 25:4579-4590.

Grist, S.A., M. McCarron, A. Kutlaca, D.R. Turner, and A.A. Morley. 1992. In vivo human somatic mutation: frequency and spectrum with age. *Mutation research*. 266:189-196.

Guo, X.H., E. Kudryavtseva, N. Bodyak, A. Nicholas, I. Dombrovsky, D.Y. Yang, Y. Kraytsberg, D.K. Simon, and K. Khrapko. 2010. Mitochondrial DNA deletions in mice in men: Substantia nigra is much less affected in the mouse. *Bba-Bioenergetics*. 1797:1159-1162.

Hamrick, M.W., M.E. McGee-Lawrence, and D.M. Frechette. 2016. Fatty Infiltration of Skeletal Muscle: Mechanisms and Comparisons with Bone Marrow Adiposity. *Front Endocrinol*. 7.

Harman, D. 1972. The Biologic Clock: The Mitochondria? *J Am Geriatr Soc*. 20:145-147.

Hasty, P., and B.A. Christy. 2013. p53 as an intervention target for cancer and aging. *Pathobiol Aging Age Relat Dis*. 3.

Hayashi, J., S. Ohta, A. Kikuchi, M. Takemitsu, Y. Goto, and I. Nonaka. 1991. Introduction of disease-related mitochondrial DNA deletions into HeLa cells lacking mitochondrial DNA results in mitochondrial dysfunction. *Proceedings of the National Academy of Sciences of the United States of America*. 88:10614-10618.

Hayflick, L., and P.S. Moorhead. 1961. The serial cultivation of human diploid cell strains. *Experimental Cell Research*. 25:585-621.

He, L., P.F. Chinnery, S.E. Durham, E.L. Blakely, T.M. Wardell, G.M. Borthwick, R.W. Taylor, and D.M. Turnbull. 2002. Detection and quantification of mitochondrial DNA deletions in individual cells by real-time PCR. *Nucleic Acids Research*. 30:e68-e68.

Hebert, S.L., P. Marquet-de Rougé, I.R. Lanza, S.K. McCrady-Spitzer, J.A. Levine, S. Middha, R.E. Carter, K.A. Klaus, T.M. Therneau, E.W. Highsmith, and K.S. Nair. 2015. Mitochondrial Aging and Physical Decline: Insights From Three Generations of Women. *The Journals of Gerontology Series A: Biological Sciences and Medical Sciences*. 70:1409-1417.

Heinrich, A., F. Balszuweit, H. Thiermann, and K. Kehe. 2009. Rapid simultaneous determination of apoptosis, necrosis, and viability in sulfur mustard exposed HaCaT cell cultures. *Toxicol Lett*. 191:260-267.

Henriquez, M., R. Armisen, A. Stutzin, and A.F. Quest. 2008. Cell death by necrosis, a regulated way to go. *Current molecular medicine*. 8:187-206.

Herbst, A., C.J. Johnson, K. Hynes, D. McKenzie, and J.M. Aiken. 2013. Mitochondrial Biogenesis Drives a Vicious Cycle of Metabolic Insufficiency and Mitochondrial DNA Deletion Mutation Accumulation in Aged Rat Skeletal Muscle Fibers. *PLoS ONE*. 8:e59006.

Herbst, A., J.W. Pak, D. McKenzie, E. Bua, M. Bassiouni, and J.M. Aiken. 2007. Accumulation of Mitochondrial DNA Deletion Mutations in Aged Muscle Fibers: Evidence for a Causal Role in Muscle Fiber Loss. *The journals of gerontology. Series A, Biological sciences and medical sciences*. 62:235-245.

Herbst, A., J. Wanagat, N. Cheema, K. Widjaja, D. McKenzie, and J.M. Aiken. 2016. Latent mitochondrial DNA deletion mutations drive muscle fiber loss at old age. *Aging Cell*. 15:1132-1139.

Herndon, L.A., P.J. Schmeissner, J.M. Dudaronek, P.A. Brown, K.M. Listner, Y. Sakano, M.C. Paupard, D.H. Hall, and M. Driscoll. 2002. Stochastic and genetic factors influence tissue-specific decline in ageing C-elegans. *Nature*. 419:808-814.

Herrero, A., and G. Barja. 1998. H2O2 production of heart mitochondria and aging rate are slower in canaries and parakeets than in mice: sites of free radical generation and mechanisms involved. *Mechanisms of ageing and development*. 103:133-146.

Hiona, A., A. Sanz, G.C. Kujoth, R. Pamplona, A.Y. Seo, T. Hofer, S. Someya, T. Miyakawa, C. Nakayama, A.K. Samhan-Arias, S. Servais, J.L. Barger, M. Portero-Otín, M. Tanokura, T.A. Prolla, and C. Leeuwenburgh. 2010. Mitochondrial DNA Mutations Induce Mitochondrial Dysfunction, Apoptosis and Sarcopenia in Skeletal Muscle of Mitochondrial DNA Mutator Mice. *PLoS ONE*. 5:e11468.

Holloszy, J.O., M. Chen, G.D. Cartee, and J.C. Young. 1991. Skeletal muscle atrophy in old rats: Differential changes in the three fiber types. *Mechanisms of ageing and development*. 60:199-213.

Holmes, D.J. 2003. F344 Rat. *Sci. Aging Knowl. Environ.* 2003:as2-.

Holmes, D.J. 2004. Brown Norway Rat. *Sci. Aging Knowl. Environ.* 2004:as3-.

Holmes, D.J. 2004. F344BNF1 and BNF344F1 Hybrid Rats. *Sci. Aging Knowl. Environ.* 2004:as4-.

Honda, K., K. Kato, N. Dairaku, K. Iijima, T. Koike, A. Imatani, H. Sekine, S. Ohara, H. Matsui, and T. Shimosegawa. 2003. High levels of intracellular ATP prevent nitric oxide-induced apoptosis in rat gastric mucosal cells. *International Journal of Experimental Pathology*. 84:281-288.

Hood, D.A. 2009. Mechanisms of exercise-induced mitochondrial biogenesis in skeletal muscle. *Appl Physiol Nutr Me*. 34:465-472.

Horvath, T.L., D.M. Erion, J.D. Elsworth, R.H. Roth, G.I. Shulman, and Z.B. Andrews. 2011. GPA protects the nigrostriatal dopamine system by enhancing mitochondrial function. *Neurobiol Dis*. 43:152-162.

Information, C.I.f.H. 2014. National Health Expenditure Trends, 1975
to 2014. CIHI, Ottawa, ON.

Iqbal, S., O. Ostojic, K. Singh, A.M. Joseph, and D.A. Hood. 2013. Expression of Mitochondrial Fission and Fusion Regulatory Proteins in Skeletal Muscle during Chronic Use and Disuse. *Muscle & Nerve*. 48:963-970.

Izyumov, D.S., A.V. Avetisyan, O.Y. Pletjushkina, D.V. Sakharov, K.W. Wirtz, B.V. Chernyak, and V.P. Skulachev. 2004. "Wages of fear": Transient threefold decrease in intracellular ATP level imposes apoptosis. *Biochimica et Biophysica Acta - Bioenergetics*. 1658:141-147.

Jang, Y.C., M.S. Lustgarten, Y. Liu, F.L. Muller, A. Bhattacharya, H. Liang, A.B. Salmon, S.V. Brooks, L. Larkin, C.R. Hayworth, A. Richardson, and H. Van Remmen. 2010. Increased superoxide in vivo accelerates age-associated muscle atrophy through mitochondrial dysfunction and neuromuscular junction degeneration. *The FASEB Journal*. 24:1376-1390.

Janssen, I., S.B. Heymsfield, and R. Ross. 2002. Low relative skeletal muscle mass (sarcopenia) in older persons is associated with functional impairment and physical disability. *J Am Geriatr Soc*. 50:889-896.

Jemt, E., G. Farge, S. Backstrom, T. Holmlund, C.M. Gustafsson, and M. Falkenberg. 2011. The mitochondrial DNA helicase TWINKLE can assemble on a closed circular template and support initiation of DNA synthesis. *Nucleic Acids Research*. 39:9238-9249.

Johnson, C.R., and W.D. Jarvis. 2004. Caspase-9 regulation: An update. *Apoptosis*. 9:423-427.

Johnston, A.P.W., M. De Lisio, and G. Parise. 2008. Resistance training, sarcopenia, and the mitochondrial theory of aging. *Appl Physiol Nutr Me*. 33:191-199.

Johnston, W., G. Karpati, S. Carpenter, D. Arnold, and E.A. Shoubridge. 1995. Late-Onset Mitochondrial Myopathy. *Ann Neurol*. 37:16-23.

Jones, D.L., and T.A. Rando. 2011. Emerging models and paradigms for stem cell ageing. *Nat Cell Biol*. 13:506-512.

Kajstura, J., W. Cheng, R. Sarangarajan, P. Li, B.S. Li, J.A. Nitahara, S. Chapnick, K. Reiss, G. Olivetti, and P. Anversa. 1996. Necrotic and apoptotic myocyte cell death in the aging heart of Fischer 344 rats. *Am J Physiol-Heart C*. 271:H1215-H1228.

Karamat, F.A., D.L. Horjus, Y.C. Haan, L. van der Woude, I. Oudman, G.A. van Montfrans, J.F. Clark, and L.M. Brewster. 2015. The acute effect of beta-guanidinopropionic acid versus creatine or placebo in healthy men (ABC Trial): study protocol for a randomized controlled trial. *Trials*. 16.

Kennedy, S.R., L.A. Loeb, and A.J. Herr. 2012. Somatic mutations in aging, cancer and neurodegeneration. *Mechanisms of ageing and development*. 133:118-126.

Kharraz, Y., J. Guerra, C.J. Mann, A.L. Serrano, Mu, #xf1, oz-C, #xe1, and P. noves. 2013. Macrophage Plasticity and the Role of Inflammation in Skeletal Muscle Repair. *Mediators of Inflammation*. 2013:9.

Khodorov, B., V. Pinelis, O. Vergun, T. Storozhevykh, and N. Vinskaya. 1996. Mitochondrial deenergization underlies neuronal calcium overload following a prolonged glutamate challenge. *Febs Lett*. 397:230-234.

Kirkwood, T.B.L. 1993. The Disposable Soma Theory - Evidence and Implications. *Neth J Zool*. 43:359-363.

Klein, C.S., G.D. Marsh, R.J. Petrella, and C.L. Rice. 2003. Muscle fiber number in the biceps brachii muscle of young and old men. *Muscle & Nerve*. 28:62-68.

Koch, C.M., C.V. Suschek, Q.O. Lin, S. Bork, M. Goergens, S. Joussen, N. Pallua, A.D. Ho, M. Zenke, and W. Wagner. 2011. Specific Age-Associated DNA Methylation Changes in Human Dermal Fibroblasts. *PLoS ONE*. 6.

Kovacheva, E.L., A.P. Sinha Hikim, R. Shen, I. Sinha, and I. Sinha-Hikim. 2010. Testosterone Supplementation Reverses Sarcopenia in Aging through Regulation of Myostatin, c-Jun NH(2)-Terminal Kinase, Notch, and Akt Signaling Pathways. *Endocrinology*. 151:628-638.

Kowald, A., and T.B.L. Kirkwood. 2014. Transcription could be the key to the selection advantage of mitochondrial deletion mutants in aging. *Proceedings of the National Academy of Sciences of the United States of America*. 111:2972-2977.

Kraytsberg, Y., E. Kudryavtseva, A.C. Mckee, C. Geula, N.W. Kowall, and K. Khrapko. 2006. Mitochondrial DNA deletions are abundant and cause functional impairment in aged human substantia nigra neurons. *Nat Genet*. 38:518-520.

Kudin, A.P., N.Y.B. Bimpong-Buta, S. Vielhaber, C.E. Elger, and W.S. Kunz. 2004. Characterization of superoxide-producing sites in isolated brain mitochondria. *Journal of Biological Chemistry*. 279:4127-4135.

Kujoth, G.C., A. Hiona, T.D. Pugh, S. Someya, K. Panzer, S.E. Wohlgemuth, T. Hofer, A.Y. Seo, R. Sullivan, W.A. Jobling, J.D. Morrow, H. Van Remmen, J.M. Sedivy, T. Yamasoba, M. Tanokura, R. Weindruch, C. Leeuwenburgh, and T.A. Prolla. 2005. Mitochondrial DNA mutations, oxidative stress, and apoptosis in mammalian aging. *Science*. 309:481-484.

Lane, N., and W. Martin. 2010. The energetics of genome complexity. *Nature*. 467:929-934.

Leduc-Gaudet, J.-P., M. Picard, F.S.-J. Pelletier, N. Sgarioto, M.-J. Auger, J. Vallée, R. Robitaille, D.H. St-Pierre, and G. Gouspillou. 2015. Mitochondrial morphology is altered in atrophied skeletal muscle of aged mice. *Oncotarget*. 6:17923-17937.

Ledvina, M., and M. Hodanova. 1980. The effect of simultaneous administration of tocopherol and sunflower oil on the life-span of female mice. *Experimental Gerontology*. 15:67-71.

Lee, C.M., S.S. Chung, J.M. Kaczkowski, R. Weindruch, and J.M. Aiken. 1993. Multiple Mitochondrial-DNA Deletions Associated with Age in Skeletal-Muscle of Rhesus-Monkeys. *J Gerontol*. 48:B201-B205.

Lee, C.M., P. Eimon, R. Weindruch, and J.M. Aiken. 1994. Direct repeat sequences are not required at the breakpoints of age-associated mitochondrial DNA deletions in rhesus monkeys. *Mechanisms of ageing and development*. 75:69-79.

Lee, C.M., M.E. Lopez, R. Weindruch, and J.M. Aiken. 1998. Association of age-related mitochondrial abnormalities with skeletal muscle fiber atrophy. *Free Radical Biology and Medicine*. 25:964-972.

Lee, J.H., K.J. Jung, J.W. Kim, H.J. Kim, B.P. Yu, and H.Y. Chung. 2004. Suppression of apoptosis by calorie restriction in aged kidney. *Experimental Gerontology*. 39:1361-1368.

Lee, W.S., W.H. Cheung, L. Qin, N. Tang, and K.S. Leung. 2006. Age-associated decrease of type IIA/B human skeletal muscle fibers. *Clin Orthop Relat R*:231-237.

Lexell, J., D. Downham, and M. Sjostrom. 1986. Distribution of different fibre types in human skeletal muscles. Fibre type arrangement in m. vastus lateralis from three groups of healthy men between 15 and 83 years. *J Neurol Sci*. 72:211-222.

Lexell, J., K. Henrikssonlarsen, B. Winblad, and M. Sjostrom. 1983. Distribution of Different Fiber Types in Human Skeletal-Muscles - Effects of Aging Studied in Whole Muscle Cross-Sections. *Muscle & Nerve*. 6:588-595.

Lexell, J., C.C. Taylor, and M. Sjöström. 1988. What is the cause of the ageing atrophy?: Total number, size and proportion of different fiber types studied in whole vastus lateralis muscle from 15- to 83-year-old men. *J Neurol Sci*. 84:275-294.

Lin, Y.F., A.M. Schulz, M.W. Pellegrino, Y. Lu, S. Shaham, and C.M. Haynes. 2016. Maintenance and propagation of a deleterious mitochondrial genome by the mitochondrial unfolded protein response. *Nature*. 533:416-+.

Linnane, A.W., A. Baumer, R.J. Maxwell, H. Preston, C.F. Zhang, and S. Marzuki. 1990. Mitochondrial Gene Mutation - the Aging Process and Degenerative Diseases. *Biochem Int*. 22:1067-1076.

Linnane, A.W., S. Kovalenko, and E.B. Gingold. 1998. The Universality of Bioenergetic Disease: Age-associated Cellular Bioenergetic Degradation and Amelioration Therapy. *Ann Ny Acad Sci*. 854:202-213.

Lopez, M.E., N.L. Van Zeeland, D.B. Dahl, R. Weindruch, and J.M. Aiken. 2000. Cellular phenotypes of age-associated skeletal muscle mitochondrial abnormalities in rhesus monkeys. *Mutat Res-Fund Mol M*. 452:123-138.

Lopez-Lluch, G., N. Hunt, B. Jones, M. Zhu, H. Jamieson, S. Hilmer, M.V. Cascajo, J. Allard, D.K. Ingram, P. Navas, and R. de Cabo. 2006. Calorie restriction induces mitochondrial biogenesis and bioenergetic efficiency. *Proceedings of the National Academy of Sciences of the United States of America*. 103:1768-1773.

Lopez-Lluch, G., and P. Navas. 2016. Calorie restriction as an intervention in ageing. *J Physiol-London*. 594:2043-2060.

Lu, T., Y. Pan, S.-Y. Kao, C. Li, I. Kohane, J. Chan, and B.A. Yankner. 2004. Gene regulation and DNA damage in the ageing human brain. *Nature*. 429:883-891.

Lushaj, E.B., L. Lozonschi, M. Barnes, E. Anstadt, and T. Kohmoto. 2012. Mitochondrial DNA deletion mutations in adult mouse cardiac side population cells. *Mutat Res-Fund Mol M*. 734:62-68.

Mahanna, D.A., C.D. Fitch, and V.W. Fischer. 1980. Effects of β-guanidinopropionic acid on murine skeletal muscle. *Experimental Neurology*. 68:114-121.

Malagelada, C., X. Xifró, A. Miñano, J. Sabriá, and J. Rodríguez-Alvarez. 2005. Contribution of caspase-mediated apoptosis to the cell death caused by oxygen–glucose deprivation in cortical cell cultures. *Neurobiol Dis*. 20:27-37.

Malhi, H., G.J. Gores, and J.J. Lemasters. 2006. Apoptosis and necrosis in the liver: A tale of two deaths? *Hepatology*. 43:S31-S44.

Malmgren, L.T., C.E. Jones, and L.M. Bookman. 2001. Muscle Fiber and Satellite Cell Apoptosis in the Aging Human Thyroarytenoid Muscle: A Stereological Study with Confocal Laser Scanning Microscopy. *Otolaryngology -- Head and Neck Surgery*. 125:34-39.

Mansouri, A., F.L. Muller, Y.H. Liu, R. Ng, J. Faulkner, M. Hamilton, A. Richardson, T.T. Huang, C.J. Epstein, and H. Van Remmen. 2006. Alterations in mitochondrial function, hydrogen peroxide release and oxidative damage in mouse hind-limb skeletal muscle during aging. *Mechanisms of ageing and development*. 127:298-306.

Marschallinger, J., I. Schaffner, B. Klein, R. Gelfert, F.J. Rivera, S. Illes, L. Grassner, M. Janssen, P. Rotheneichner, C. Schmuckermair, R. Coras, M. Boccazzi, M. Chishty, F.B. Lagler, M. Renic, H.C. Bauer, N. Singewald, I. Blumcke, U. Bogdahn, S. Couillard-Despres, D.C. Lie, M.P. Abbracchio, and L. Aigner. 2015. Structural and functional rejuvenation of the aged brain by an approved anti-asthmatic drug. *Nat Commun*. 6.

Martin, G.M., C.E. Ogburn, L.M. Colgin, A.M. Gown, S.D. Edland, and R.J. Monnat. 1996. Somatic mutations are frequent and increase with age in human kidney epithelial cells. *Hum Mol Genet*. 5:215-221.

Martinez-Morentin, L., L. Martinez, S. Piloto, H. Yang, E.A. Schon, R. Garesse, R. Bodmer, K. Ocorr, M. Cervera, and J.J. Arredondo. 2015. Cardiac deficiency of single cytochrome oxidase assembly factor scox induces p53-dependent apoptosis in a Drosophila cardiomyopathy model. *Hum Mol Genet*. 24:3608-3622.

Martin-Montalvo, A., and R. de Cabo. 2013. Mitochondrial Metabolic Reprogramming Induced by Calorie Restriction. *Antioxidants & redox signaling*. 19:310-319.

Martin-Montalvo, A., E.M. Mercken, S.J. Mitchell, H.H. Palacios, P.L. Mote, M. Scheibye-Knudsen, A.P. Gomes, T.M. Ward, R.K. Minor, M.J. Blouin, M. Schwab, M. Pollak, Y.Q. Zhang, Y.B. Yu, K.G. Becker, V.A. Bohr, D.K. Ingram, D.A. Sinclair, N.S. Wolf, S.R. Spindler, M. Bernier, and R. de Cabo. 2013. Metformin improves healthspan and lifespan in mice. *Nat Commun*. 4.

Marzetti, E., C.S. Carter, S.E. Wohlgemuth, H.A. Lees, S. Giovannini, B. Anderson, L.S. Quinn, and C. Leeuwenburgh. 2009. Changes in IL-15 expression and death-receptor apoptotic signaling in rat gastrocnemius muscle with aging and life-long calorie restriction. *Mechanisms of ageing and development*. 130:272-280.

Marzetti, E., J.C.Y. Hwang, H.A. Lees, S.E. Wohlgemuth, E.E. Dupont-Versteegden, C.S. Carter, R. Bernabei, and C. Leeuwenburgh. 2010. Mitochondrial death effectors: Relevance to sarcopenia and disuse muscle atrophy. *Bba-Gen Subjects*. 1800:235-244.

Marzetti, E., S.E. Wohlgemuth, H.A. Lees, H.Y. Chung, S. Giovannini, and C. Leeuwenburgh. 2008. Age-related activation of mitochondrial caspase-independent apoptotic signaling in rat gastrocnemius muscle. *Mechanisms of ageing and development*. 129:542-549.

Masoro, E.J. 1990. Animal models in aging research. Academic Press, San Diego,CA. 72-94 pp.

Mattson, M.P., and T. Magnus. 2006. Ageing and neuronal vulnerability. *Nat Rev Neurosci*. 7:278-294.

McArdle, A., A. Maglara, P. Appleton, A.J. Watson, I. Grierson, and M.J. Jackson. 1999. Apoptosis in multinucleated skeletal muscle myotubes. *Lab Invest*. 79:1069-1076.

McBride, H.M., M. Neuspiel, and S. Wasiak. 2006. Mitochondria: More than just a powerhouse. *Curr Biol*. 16:R551-R560.

McConkey, D.J. 1998. Biochemical determinants of apoptosis and necrosis. *Toxicol Lett*. 99:157-168.

Mcdonald, S.A.C., L.C. Greaves, L. Gutierrez-Gonzalez, M. Rodriguez-Justo, M. Deheragoda, S.J. Leedham, R.W. Taylor, C.Y. Lee, S.L. Preston, M. Lovell, T. Hunt, G. Elia, D. Oukrif, R. Harrison, M.R. Novelli, I. Mitchell, D.L. Stoker, D.M. Turnbull, J.A.Z. Jankowski, and N.A. Wright. 2008. Mechanisms of field cancerization in the human stomach: The expansion and spread of mutated gastric stem cells. *Gastroenterology*. 134:500-510.

McKiernan, S.H., R. Colman, M. Lopez, T.M. Beasley, R. Weindruch, and J.M. Aiken. 2009. Longitudinal analysis of early stage sarcopenia in aging rhesus monkeys. *Experimental Gerontology*. 44:170-176.

McKiernan, S.H., R.J. Colman, M. Lopez, T.M. Beasley, J.M. Aiken, R.M. Anderson, and R. Weindruch. 2011. Caloric restriction delays aging-induced cellular phenotypes in rhesus monkey skeletal muscle. *Experimental Gerontology*. 46:23-29.

Melov, S., P.E. Coskun, and D.C. Wallace. 1999. Mouse models of mitochondrial disease, oxidative stress, and senescence. *Mutat Res-DNA Repair*. 434:233-242.

Metter, E.J., L.A. Talbot, M. Schrager, and R. Conwit. 2002. Skeletal muscle strength as a predictor of all-cause mortality in healthy men. *J Gerontol a-Biol*. 57:B359-B365.

Michikawa, Y., F. Mazzucchelli, N. Bresolin, G. Scarlato, and G. Attardi. 1999. Aging-Dependent Large Accumulation of Point Mutations in the Human mtDNA Control Region for Replication. *Science*. 286:774-779.

Mikesky, A.E., W. Matthews, C.J. Giddings, and W.J. Gonyea. 1989. Muscle Enlargement and Exercise Performance in the Cat. *The Journal of Strength & Conditioning Research*. 3:85-92.

Mishra, P., G. Varuzhanyan, A.H. Pham, and D.C. Chan. 2015. Mitochondrial Dynamics Is a Distinguishing Feature of Skeletal Muscle Fiber Types and Regulates Organellar Compartmentalization. *Cell Metab*. 22:1033-1044.

Mohamed, S.A., T. Hanke, A.W. Erasmi, M.J.F. Bechtel, M. Scharfschwerdt, C. Meissner, H.H. Sievers, and A. Gosslau. 2006. Mitochondrial DNA deletions and the aging heart. *Experimental Gerontology*. 41:508-517.

Moon, S.K., L.J. Thompson, N. Madamanchi, S. Ballinger, J. Papaconstantinou, C. Horaist, M.S. Runge, and C. Patterson. 2001. Aging, oxidative responses, and proliferative capacity in cultured mouse aortic smooth muscle cells. *Am J Physiol-Heart C*. 280:H2779-H2788.

Morterá, P., and S. Herculano-Houzel. 2012. Age-related neuronal loss in the rat brain starts at the end of adolescence. *Frontiers in Neuroanatomy*. 6:45.

Mugatroyd, C., Y. Wu, Y. Bockmühl, and D. Spengler. 2010. The Janus face of DNA methylation in aging. *Aging (Albany NY)*. 2:107-110.

Muller, F.L., Y. Liu, and H. Van Remmen. 2004. Complex III Releases Superoxide to Both Sides of the Inner Mitochondrial Membrane. *Journal of Biological Chemistry*. 279:49064-49073.

Mullerhocker, J. 1989. Cytochrome-C-Oxidase Deficient Cardiomyocytes in the Human-Heart - an Age-Related Phenomenon - a Histochemical Ultracytochemical Study. *Am J Pathol*. 134:1167-1173.

Mullerhocker, J. 1990. Cytochrome-C-Oxidase Deficient Fibers in the Limb Muscle and Diaphragm of Man without Muscular Disease - an Age-Related Alteration. *J Neurol Sci*. 100:14-21.

Müller-Höcker, J., K. Schneiderbanger, F.H. Stefani, and B. Kadenbach. 1992. Progressive loss of cytochrome c oxidase in the human extraocular muscles in ageing — a cytochemical-immunohistochemical study. *Mutation Research/DNAging*. 275:115-124.

Müller-Höcker, J., P. Seibel, K. Schneiderbanger, and B. Kadenbach. 1993. Different in situ hybridization patterns of mitochondrial DNA in cytochrome c oxidase-deficient extraocular muscle fibres in the elderly. *Vichows Archiv A Pathol Anat*. 422:7-15.

Neff, F., D. Flores-Dominguez, D.R. Ryan, M. Horsch, S. Schroder, T. Adler, L.C. Afonso, J.A. Aguilar-Pimentel, L. Becker, L. Garrett, W. Hans, M.M. Hettich, R. Holtmeier, S.M. Holter, K. Moreth, C. Prehn, O. Puk, I. Racz, B. Rathkolb, J. Rozman, B. Naton, R. Ordemann, J. Adamski, J. Beckers, R. Bekeredjian, D.H. Busch, G. Ehninger, J. Graw, H. Hofler, M. Klingenspor, T. Klopstock, M. Ollert, J. Stypmann, E. Wolf, W. Wurst, A. Zimmer, H. Fuchs, V. Gailus-Durner, M.H. de Angelis, and D. Ehninger. 2013. Rapamycin extends murine lifespan but has limited effects on aging. *J Clin Invest*. 123:3272-3291.

Neupert, W., and J.M. Herrmann. 2007. Translocation of proteins into mitochondria. *Annual Review of Biochemistry*. 76:723-749.

Newman, A.B., V. Kupelian, M. Visser, E. Simonsick, B. Goodpaster, M. Nevitt, S.B. Kritchevsky, F.A. Tylavsky, S.M. Rubin, T.B. Harris, and H.A.S. Investigators. 2003. Sarcopenia: Alternative definitions and associations with lower extremity function. *J Am Geriatr Soc*. 51:1602-1609.

Nicotera, P., M. Leist, and E. Ferrando-May. 1998. Intracellular ATP, a switch in the decision between apoptosis and necrosis. *Toxicol Lett*. 103:139-142.

Nooteboom, M., R. Johnson, R.W. Taylor, N.A. Wright, R.N. Lightowlers, T.B.L. Kirkwood, J.C. Mathers, D.M. Turnbull, and L.C. Greaves. 2010. Age-associated mitochondrial DNA mutations lead to small but significant changes in cell proliferation and apoptosis in human colonic crypts. *Aging Cell*. 9:96-99.

Ogata, T., and Y. Yamasaki. 1997. Ultra-high-resolution scanning electron microscopy of mitochondria and sarcoplasmic reticulum arrangement in human red, white, and intermediate muscle fibers. *Anat Rec*. 248:214-223.

Ohira, Y., Y. Matsuoka, F. Kawano, A. Ogura, Y. Higo, T. Ohira, M. Terada, Y. Oke, and N. Nakai. 2011. Effects of Creatine and Its Analog, beta-Guanidinopropionic Acid, on the Differentiation of and Nucleoli in Myoblasts. *Biosci Biotech Bioch*. 75:1085-1089.

Olfert, I.M., J. Balouch, and O. Mathieu-Costello. 2004. Oxygen consumption during maximal exercise in Fischer 344 x Brown Norway F1 hybrid rats. *J Gerontol a-Biol*. 59:801-808.

Olivetti, G., M. Melissari, J.M. Capasso, and P. Anversa. 1991. Cardiomyopathy of the aging human heart. Myocyte loss and reactive cellular hypertrophy. *Circ Res*. 68:1560-1568.

Olson, W., G.O. Walsh, R. Einaugler, and W.K. Engel. 1972. Oculocraniosomatic Neuromuscular Disease with Ragged-Red Fibers. *Arch Neurol-Chicago*. 26:193-+.

Oudman, I., J.F. Clark, and L.M. Brewster. 2013. The Effect of the Creatine Analogue Beta-guanidinopropionic Acid on Energy Metabolism: A Systematic Review. *PLoS ONE*. 8:e52879.

Overend, T.J., D.A. Cunningham, D.H. Paterson, and M.S. Lefcoe. 1992. Thigh Composition in Young and Elderly Men Determined by Computed-Tomography. *Clin Physiol*. 12:629-640.

Pak, J.W., and J.M. Aiken. 2004. Low levels of mtDNA deletion mutations in ETS normal fibers from aged rats. *Strategies for Engineered Negligible Senescence: Why Genuine Control of Aging May Be Foreseeable*. 1019:289-293.

Panieri, E., V. Gogvadze, E. Norberg, R. Venkatesh, S. Orrenius, and B. Zhivotovsky. 2013. Reactive oxygen species generated in different compartments induce cell death, survival, or senescence. *Free Radical Biology and Medicine*. 57:176-187.

Pansarasa, O., L. Castagna, B. Colombi, J. Vecchiet, G. Felzani, and F. Marzatico. 2000. Age and sex differences in human skeletal muscle: Role of reactive oxygen species. *Free Radical Res*. 33:287-293.

Passarino, G., A. Montesanto, F. De Rango, S. Garasto, M. Berardelli, F. Domma, V. Mari, E. Feraco, C. Franceschi, and G. De Benedictis. 2007. A cluster analysis to define human aging phenotypes. *Biogerontology*. 8:283-290.

Pérez, V.I., A. Bokov, H.V. Remmen, J. Mele, Q. Ran, Y. Ikeno, and A. Richardson. 2009. Is the oxidative stress theory of aging dead? *Biochimica et Biophysica Acta (BBA) - General Subjects*. 1790:1005-1014.

Pistilli, E.E., J.R. Jackson, and S.E. Alway. 2006. Death receptor-associated pro-apoptotic signaling in aged skeletal muscle. *Apoptosis*. 11:2115-2126.

Pistilli, E.E., P.M. Siu, and S.E. Alway. 2006. Molecular Regulation of Apoptosis in Fast Plantaris Muscles of Aged Rats. *The journals of gerontology. Series A, Biological sciences and medical sciences*. 61:245-255.

Porta, E.A., N.S. Joun, and R.T. Nitta. 1980. Effects of the type of dietary fat at two levels of vitamin E in wistar male rats during development and aging: I. Life span, serum biochemical parameters and pathological changes. *Mechanisms of ageing and development*. 13:1-39.

Porter, A.G.a.J., R.U. 1999. Emerging roles of caspase-3 in apoptosis. *Cell Death Differ*. 6:99-104.

PorteraCailliau, C., D.L. Price, and L.J. Martin. 1997. Non-NMDA and NMDA receptor-mediated excitotoxic neuronal deaths in adult brain are morphologically distinct: Further evidence for an apoptosis-necrosis continuum. *J Comp Neurol*. 378:88-104.

Primeau, A.J., P.J. Adhihetty, and D.A. Hood. 2002. Apoptosis in heart and skeletal muscle. *Can J Appl Physiol*. 27:349-395.

RAY, P.S., J.L. MARTIN, E.A. SWANSON, H. OTANI, W.H. DILLMANN, and D.K. DAS. 2001. Transgene overexpression of αB crystallin confers simultaneous protection against cardiomyocyte apoptosis and necrosis during myocardial ischemia and reperfusion. *The FASEB Journal*. 15:393-402.

Rayapureddi, J.P., W.J. Tomamichel, S.T. Walton, and R.M. Payne. 2010. TAT Fusion Protein Transduction into Isolated Mitochondria Is Accelerated by Sodium Channel Inhibitors. *Biochemistry-Us*. 49:9470-9479.

Regmi, S.G., Rolland, S.G. and Conradt, B. 2014. Age dependent changes in mitochondrial morphology and volume are not predictors of lifespan. *Aging*. 6:118 -130.

Reznick, R.M., H.H. Zong, J. Li, K. Morino, I.K. Moore, H.J. Yu, Z.X. Liu, J.Y. Dong, K.J. Mustard, S.A. Hawley, D. Befroy, M. Pypaert, D.G. Hardie, L.H. Young, and G.I. Shulman. 2007. Aging-associated reductions in AMP-activated protein kinase activity and mitochondrial biogenesis. *Cell Metab*. 5:151-156.

Rice, C.L., D.A. Cunningham, D.H. Paterson, and M.S. Lefcoe. 1989. Arm and leg composition determined by computed tomography in young and elderly men. *Clin Physiol*. 9:207-220.

Rice, K.M., J.K. Linderman, R.S. Kinnard, and E.R. Blough. 2005. The Fischer 344/NNiaHSd X Brown Norway/BiNia is a better model of sareopenia than the Fischer 344/NNiaHSd: a comparative analysis of muscle mass and contractile properties in aging male rat models. *Biogerontology*. 6:335-343.

Rich, P.R. 2003. The molecular machinery of Keilin's respiratory chain. *Biochem Soc T*. 31:1095-1105.

Rocca, W.A., C.M. Boyd, B.R. Grossardt, W.V. Bobo, L.J. Finney Rutten, V.L. Roger, J.O. Ebbert, T.M. Therneau, B.P. Yawn, and J.L. St Sauver. 2014. Prevalence of multimorbidity in a geographically defined American population: patterns by age, sex, and race/ethnicity. *Mayo Clinic proceedings*. 89:1336-1349.

Rock, K.L., and H. Kono. 2008. The inflammatory response to cell death. *Annu Rev Pathol-Mech*. 3:99-126.

Rodriguez-Bies, E., P. Navas, and G. Lopez-Lluch. 2015. Age-Dependent Effect of Every-Other-Day Feeding and Aerobic Exercise in Ubiquinone Levels and Related Antioxidant Activities in Mice Muscle. *J Gerontol a-Biol*. 70:33-43.

Roos, M.R., C.L. Rice, and A.A. Vandervoort. 1997. Age-related changes in motor unit function. *Muscle & Nerve*. 20:679-690.

Rooyackers, O.E., D.B. Adey, P.A. Ades, and K.S. Nair. 1996. Effect of age on in vivo rates of mitochondrial protein synthesis in human skeletal muscle. *Proceedings of the National Academy of Sciences of the United States of America*. 93:15364-15369.

Rosenberg, I.H. 1997. Sarcopenia: Origins and Clinical Relevance. *The Journal of Nutrition*. 127:990S-991S.

Rossier, M.F. 2006. T channels and steroid biosynthesis: in search of a link with mitochondria. *Cell Calcium*. 40:155-164.

Roth, G.S., L.H. Brennecke, A.W. French, N.G. Williams, K.S. Waggie, H.A. Spurgeon, and D.K. Ingram. 1993. Pathological Characterization of Male Wistar Rats from the Gerontology Research-Center. *J Gerontol*. 48:B213-B230.

Roth, G.S., M.A. Lane, D.K. Ingram, J.A. Mattison, D. Elahi, J.D. Tobin, D. Muller, and E.J. Metter. 2002. Biomarkers of Caloric Restriction May Predict Longevity in Humans. *Science*. 297:811-811.

Rousset, S., M.C. Alves-Guerra, J. Mozo, B. Miroux, A.M. Cassard-Doulcier, F. Bouillaud, and D. Ricquier. 2004. The biology of mitochondrial uncoupling proteins. *Diabetes*. 53:S130-S135.

Rule, A.D., H. Amer, L.D. Cornell, S.J. Taler, F.G. Cosio, W.K. Kremers, S.C. Textor, and M.D. Stegall. 2010. The Association Between Age and Nephrosclerosis on Renal Biopsy Among Healthy Adults. *Ann Intern Med*. 152:561-+.

Saraste, M. 1999. Oxidative phosphorylation at the fin de siecle. *Science*. 283:1488-1493.

Scaffidi, P., T. Misteli, and M.E. Bianchi. 2002. Release of chromatin protein HMGB1 by necrotic cells triggers inflammation. *Nature*. 418:191-195.

Schaap, L.A., S.M.F. Pluijm, D.J.H. Deeg, T.B. Harris, S.B. Kritchevsky, A.B. Newman, L.H. Colbert, M. Pahor, S.M. Rubin, F.A. Tylavsky, M. Visser, and H.A. Study. 2009. Higher Inflammatory Marker Levels in Older Persons: Associations With 5-Year Change in Muscle Mass and Muscle Strength. *J Gerontol a-Biol*. 64:1183-1189.

Schiaffino, S., and C. Reggiani. 2011. Fiber Types in Mammalian Skeletal Muscles. *Physiol. Rev.* 91:1447-1531.

Schmidt, A., B. Marescau, E.A. Boehm, W.K.J. Renema, R. Peco, A. Das, R. Steinfeld, S. Chan, J. Wallis, M. Davidoff, K. Ullrich, R. Waldschutz, A. Heerschap, P.P. De Deyn, S. Neubauer, and D. Isbrandt. 2004. Severely altered guanidino compound levels, disturbed body weight homeostasis and impaired fertility in a mouse model of guanidinoacetate N-methyltransferase (GAMT) deficiency. *Hum Mol Genet*. 13:905-921.

Schmidt, O., N. Pfanner, and C. Meisinger. 2010. Mitochondrial protein import: from proteomics to functional mechanisms. *Nat Rev Mol Cell Bio*. 11:655-667.

Schriner, S.E., N.J. Linford, G.M. Martin, P. Treuting, C.E. Ogburn, M. Emond, P.E. Coskun, W. Ladiges, N. Wolf, H. Van Remmen, D.C. Wallace, and P.S. Rabinovitch. 2005. Extension of Murine Life Span by Overexpression of Catalase Targeted to Mitochondria. *Science*. 308:1909-1911.

Schwarze, S.R., C.M. Lee, S.S. Chung, E.B. Roecker, R. Weindruch, and J.M. Aiken. 1995. High levels of mitochondrial DNA deletions in skeletal muscle of old rhesus monkeys. *Mechanisms of ageing and development*. 83:91-101.

Shah, V.O., J. Scariano, D. Waters, C. Qualls, M. Morgan, G. Pickett, C. Gasparovic, K. Dokladny, P. Moseley, and D.S.C. Raj. 2009. Mitochondrial DNA deletion and sarcopenia. *Genet Med*. 11:147-152.

Sharples, A.P., D.C. Hughes, C.S. Deane, A. Saini, C. Selman, and C.E. Stewart. 2015. Longevity and skeletal muscle mass: the role of IGF signalling, the sirtuins, dietary restriction and protein intake. *Aging Cell*. 14:511-523.

Sheydina, A., D.R. Riordon, and K.R. Boheler. 2011. Molecular mechanisms of cardiomyocyte aging. *Clin Sci*. 121:315-329.

Shin, M.G., S. Kajigaya, M. Tarnowka, J.P. McCoy, B.C. Levin, and N.S. Young. 2004. Mitochondrial DNA sequence heterogeneity in circulating normal human CD34 cells and granulocytes. *Blood*. 103:4466-4477.

Sies, H., E. Cadenas, M.C.R. Symons, and G. Scott. 1985. Oxidative Stress: Damage to Intact Cells and Organs [and Discussion]. *Philosophical Transactions of the Royal Society of London. B, Biological Sciences*. 311:617-631.

Simonetti, S., X. Chen, S. Dimauro, and E.A. Schon. 1992. Accumulation of Deletions in Human Mitochondrial-DNA during Normal Aging - Analysis by Quantitative Pcr. *Biochimica et biophysica acta*. 1180:113-122.

Siu, P.M., E.E. Pistilli, and S.E. Alway. 2008. Age-dependent increase in oxidative stress in gastrocnemius muscle with unloading. *Journal of Applied Physiology*. 105:1695-1705.

Siu, P.M., E.E. Pistilli, D.C. Butler, and S.E. Alway. 2005. Aging influences cellular and molecular responses of apoptosis to skeletal muscle unloading. C338-C349 pp.

Sohal, R.S., and W.C. Orr. 2012. The Redox Stress Hypothesis of Aging. *Free radical biology & medicine*. 52:539-555.

Soti, C., A.S. Sreedhar, and P. Csermely. 2003. Apoptosis, necrosis and cellular senescence: chaperone occupancy as a potential switch. *Aging Cell*. 2:39-45.

Strasser, H., M. Tiefenthaler, M. Steinlechner, G. Bartsch, and G. Konwalinka. 1999. Urinary incontinence in the elderly and age-dependent apoptosis of rhabdosphincter cells. *The Lancet*. 354:918-919.

Subrarnaniam, V., P. Golik, D.G. Murdock, S. Levy, K.W. Kerstann, P.E. Coskun, G.A. Melkonian, and D.C. Wallace. 2008. MITOCHIP assessment of differential gene expression in the skeletal muscle of Ant1 knockout mice: Coordinate regulation of OXPHOS, antioxidant, and apoptotic genes. *Bba-Bioenergetics*. 1777:666-675.

Suh, J.H., S.H. Heath, and T.M. Hagen. 2003. Two subpopulations of mitochondria in the aging rat heart display heterogenous levels of oxidative stress. *Free Radical Biology and Medicine*. 35:1064-1072.

Syntichaki, P., K. Xu, M. Driscoll, and N. Tavernarakis. 2002. Specific aspartyl and calpain proteases are required for neurodegeneration in C. elegans. *Nature*. 419:939-944.

Szulc, P., T.J. Beck, F. Marchand, and P.D. Delmas. 2005. Low skeletal muscle mass is associated with poor structural parameters of bone and impaired balance in elderly men - The MINOS study. *J Bone Miner Res*. 20:721-729.

Szulc, P., F. Munoz, F. Marchand, R. Chapurlat, and P.D. Delmas. 2010. Rapid loss of appendicular skeletal muscle mass is associated with higher all-cause mortality in older men: the prospective MINOS study. *Am J Clin Nutr*. 91:1227-1236.

Taanman, J.W. 1999. The mitochondrial genome: structure, transcription, translation and replication. *Bba-Bioenergetics*. 1410:103-123.

Tamaki, T., S. Uchiyama, and S. Nakano. 1992. A Weight-Lifting Exercise Model for Inducing Hypertrophy in the Hindlimb Muscles of Rats. *Med Sci Sport Exer*. 24:881-886.

Tarnawski, A.S., A. Ahluwalia, and M.K. Jones. 2014. Increased susceptibility of aging gastric mucosa to injury: The mechanisms and clinical implications. *World J Gastroentero*. 20:4467-4482.

Tavernarakis, N. 2007. Cardiomyocyte necrosis: Alternative mechanisms, effective interventions. *Bba-Mol Cell Res*. 1773:480-482.

Taylor, R.W., M.J. Barron, G.M. Borthwick, A. Gospel, P.F. Chinnery, D.C. Samuels, G.A. Taylor, S.M. Plusa, S.J. Needham, L.C. Greaves, T.B. Kirkwood, and D.M. Turnbull. 2003.

Mitochondrial DNA mutations in human colonic crypt stem cells. *J Clin Invest*. 112:1351-1360.

Taylor, S.D., N.G. Ericson, J.N. Burton, T.A. Prolla, J.R. Silber, J. Shendure, and J.H. Bielas. 2014. Targeted enrichment and high-resolution digital profiling of mitochondrial DNA deletions in human brain. *Aging Cell*. 13:29-38.

Terman, A., and U.T. Brunk. 2004. Myocyte aging and mitochondrial turnover. *Experimental Gerontology*. 39:701-705.

Testa, G., F. Biasi, G. Poli, and E. Chiarpotto. 2014. Calorie Restriction and Dietary Restriction Mimetics: A Strategy for Improving Healthy Aging and Longevity. *Curr Pharm Design*. 20:2950-2977.

Tonkonogi, M., M. Fernstrom, B. Walsh, L.L. Ji, O. Rooyackers, F. Hammarqvist, J. Wernerman, and K. Sahlin. 2003. Reduced oxidative power but unchanged antioxidative capacity in skeletal muscle from aged humans. *Pflug Arch Eur J Phy*. 446:261-269.

Trifunovic, A., A. Wredenberg, M. Falkenberg, J.N. Spelbrink, A.T. Rovio, C.E. Bruder, M. Bohlooly-Y, S. Gidlof, A. Oldfors, R. Wibom, J. Tornell, H.T. Jacobs, and N.G. Larsson. 2004. Premature ageing in mice expressing defective mitochondrial DNA polymerase. *Nature*. 429:417-423.

Tsukihara, T., H. Aoyama, E. Yamashita, T. Tomizaki, H. Yamaguchi, K. Shinzawa-Itoh, R. Nakashima, R. Yaono, and S. Yoshikawa. 1996. The Whole Structure of the 13-Subunit Oxidized Cytochrome c Oxidase at 2.8 Å. *Science*. 272:1136-1144.

Ungewitter, E., and H. Scrable. 2009. Antagonistic pleiotropy and p53. *Mechanisms of ageing and development*. 130:10-17.

van Heemst, D. 2010. Insulin, IGF-1 and longevity. *Aging Dis*. 1:147-157.

Vandeursen, J., P. Jap, A. Heerschap, H. Terlaak, W. Ruitenbeek, and B. Wieringa. 1994. Effects of the Creatine Analog Beta-Guanidinopropionic Acid on Skeletal-Muscles of Mice Deficient in Muscle Creatine-Kinase. *Bba-Bioenergetics*. 1185:327-335.

VanTuyle, G.C., J.P. Gudikote, V.R. Hurt, B.B. Miller, and C.A. Moore. 1996. Multiple, large deletions in rat mitochondrial DNA: Evidence for a major hot spot. *Mutat Res-Fund Mol M*. 349:95-107.

Visser, M., D. Deeg, and P. Lips. 2003. Low Vitamin D and High Parathyroid Hormone Levels as Determinants of Loss of Muscle Strength and Muscle Mass (Sarcopenia): The Longitudinal Aging Study Amsterdam. *The Journal of Clinical Endocrinology & Metabolism*. 88:5766-5772.

Walston, J., N. Fedarko, H. Yang, S. Leng, B. Beamer, S. Espinoza, A. Lipton, H. Zheng, and K. Becker. 2008. The Physical and Biological Characterization of a Frail Mouse Model. *The Journals of Gerontology Series A: Biological Sciences and Medical Sciences*. 63:391-398.

Wanagat, J., Z. Cao, P. Pathare, and J.M. Aiken. 2001. Mitochondrial DNA deletion mutations colocalize with segmental electron transport system abnormalities, muscle fiber atrophy, fiber splitting, and oxidative damage in sarcopenia. *The FASEB Journal*. 15:322-332.

Wanagat, J., M.R. Wolff, and J.M. Aiken. 2002. Age-associated changes in function, structure and mitochondrial genetic and enzymatic abnormalities in the Fischer 344 x Brown Norway F-1 hybrid rat heart. *J Mol Cell Cardiol*. 34:17-28.

Weindruch, R., and E.J. Masoro. 1991. Concerns About Rodent Models for Aging Research. *J Gerontol*. 46:B87-B88.

Weismann, A. 1889. Essays Upon Heredity and Kindred Biological Problems. Carlendon Press, Oxford.

Whitman, S., M. Wacker, S. Richmond, and M. Godard. 2005. Contributions of the ubiquitin–proteasome pathway and apoptosis to human skeletal muscle wasting with age. *Pflugers Arch - Eur J Physiol*. 450:437-446.

WHO. 2010. Global Health and Aging. World Health Organization (WHO).

Wiesner, R.J., T.V. Hornung, J.D. Garman, D.A. Clayton, E. O'Gorman, and T. Wallimann. 1999. Stimulation of mitochondrial gene expression and proliferation of mitochondria following impairment of cellular energy transfer by inhibition of the phosphocreatine circuit in rat hearts. *J Bioenerg Biomembr*. 31:559-567.

Williams, G.C. 1957. Pleiotropy, Natural-Selection, and the Evolution of Senescence. *Evolution*. 11:398-411.

Wood, L.K., E. Kayupov, J.P. Gumucio, C.L. Mendias, D.R. Claflin, and S.V. Brooks. 1985. Intrinsic stiffness of extracellular matrix increases with age in skeletal muscles of mice. *Journal of Applied Physiology*. 117:363-369.

Woodhouse, L.J., A. Mukherjee, S.M. Shalet, and S. Ezzat. 2006. The Influence of Growth Hormone Status on Physical Impairments, Functional Limitations, and Health-Related Quality of Life in Adults. *Endocrine Reviews*. 27:287-317.

Woodhouse, L.J., A. Mukherjee, S.M. Shalet, and S. Ezzat. 2006. The influence of growth hormone status on physical impairments, functional limitations, and health-related quality of life in adults. *Endocrine Reviews*. 27:287-317.

Yadav, V.K., J. DeGregori, and S. De. 2016. The landscape of somatic mutations in protein coding genes in apparently benign human tissues carries signatures of relaxed purifying selection. *Nucleic Acids Research*. 44:2075-2084.

Yan, L., S. Gao, D. Ho, M. Park, H. Ge, C. Wang, Y. Tian, L. Lai, M.S. De Lorenzo, D.E. Vatner, and S.F. Vatner. 2013. Calorie restriction can reverse, as well as prevent, aging cardiomyopathy. *AGE*. 35:2177-2182.

Yang, S., L.-H. Long, D. Li, J.-K. Zhang, S. Jin, F. Wang, and J.-G. Chen. 2015. β-Guanidinopropionic acid extends the lifespan of Drosophila melanogaster via an AMP-activated protein kinase-dependent increase in autophagy. *Aging Cell*. 14:1024-1033.

Yaniv, Y., M. Juhaszova, and S.J. Sollott. 2013. Age-related changes of myocardial ATP supply and demand mechanisms. *Trends Endocrin Met*. 24:495-505.

Yee, K., and K. Vousden. 2008. Contribution of membrane localization to the apoptotic activity of PUMA. *Apoptosis*. 13:87-95.

Young, A., M. Stokes, and M. Crowe. 1985. The Size and Strength of the Quadriceps Muscles of Old and Young Men. *Clin Physiol*. 5:145-154.

Yu, W., O. Gubkina, N. Mechawar, D. Elwell, R. Quirion, and S. Krantic. 2011. Expression of apoptosis-inducing factor (AIF) in the aged rat brain. *Neurobiology of Aging*. 32:179-180.

Zeiss, C.J. 2003. The apoptosis-necrosis continuum: Insights from genetically altered mice. *Vet Pathol*. 40:481-495.

Zhang, C., A. Baumer, R.J. Maxwell, A.W. Linnane, and P. Nagley. 1992. Multiple mitochondrial DNA deletions in an elderly human individual. *Febs Lett*. 297:34-38.

Zhang, D.W., J. Shao, J. Lin, N. Zhang, B.J. Lu, S.C. Lin, M.Q. Dong, and J.H. Han. 2009. RIP3, an Energy Metabolism Regulator That Switches TNF-Induced Cell Death from Apoptosis to Necrosis. *Science*. 325:332-336.

Zoico, E., and R. Roubenoff. 2002. The Role of Cytokines in Regulating Protein Metabolism and Muscle Function. *Nutrition Reviews*. 60:39-51.

Zong, H.H., J.M. Ren, L.H. Young, M. Pypaert, J. Mu, M.J. Birnbaum, and G.I. Shulman. 2002. AMP kinase is required for mitochondrial biogenesis in skeletal muscle in response to chronic energy deprivation. *Proceedings of the National Academy of Sciences of the United States of America*. 99:15983-15987.

Zong, W.X., and C.B. Thompson. 2006. Necrotic death as a cell fate. *Gene Dev*. 20:1-15.